NOVEL METHODS FOR THE SEPARATION AND INTERVENTION OF *SALMONELLA TYPHIMURIUM* FOR FOOD SAFETY APPLICATIONS

A Thesis
Presented to
The Academic Faculty

by

Amber Pizzo

In Partial Fulfillment
of the Requirements for the Degree
Master of Science in the
School of Mechanical Engineering

Georgia Institute of Technology
August 2013

NOVEL METHODS FOR THE SEPARATION AND INTERVENTION OF *SALMONELLA TYPHIMURIUM* FOR FOOD SAFETY APPLICATIONS

Approved by:

Dr. Peter Hesketh, Advisor
School of Mechanical Engineering
Georgia Institute of Technology

Dr. Jie Xu
Georgia Tech Research Institute
Georgia Institute of Technology

Dr. Todd Sulchek
School of Mechanical Engineering
Georgia Institute of Technology

Date Approved: June 17, 2013

ACKNOWLEDGEMENTS

I would like to thank several people who have helped me to succeed not only in this project, but in my graduate career.

I would first like to thank Dr. Peter Hesketh. Not only is he currently my research advisor, but he also opened the door to Georgia Tech for me when he offered me a position as an undergraduate research assistant in his group in 2009. When I decided to come to Georgia Tech for my graduate studies, he again welcomed me into his research group, and for that I am truly thankful. He has given me many extraordinary opportunities over the last four years, and I know that without him I would not have come as far as I have today. I have learned a great deal from him, and I am very proud to call him my advisor.

I would also like to thank Dr. Jie Xu, who has acted as my co-advisor. She has truly been the driving force in my research. Her guidance has helped to shape the researcher I am today, teaching me to appreciate unexpected results as well as pushing me to learn as much as possible. I'd especially like to thank her for giving me a crash course in microbiology over the last year and a half.

I want to thank my research group peers for helping me to survive graduate school. I really appreciate their willingness to help me further my project by letting me pester them with questions and bounce ideas off of them. They have helped keep my spirits up and allowed me to stay focused in my research.

I'd like to thank Dr. Mikkel Thomas for reminding me not to be a perfectionist, both inside and outside the cleanroom. His advice has helped to keep me sane during my

graduate career. He has not only become a mentor to me, but a good friend, and I am very thankful for that.

I am very grateful to my parents and my brother for always encouraging me in my studies. It has been difficult being so far from my family, but it is very comforting to know they are there for me when I need them. I am truly blessed to have such a loving family. Without their support, I wouldn't be where I am today.

I'd like to give a very special thanks to my best friend, Kayla, who has been by my side through everything since we were just little ones in elementary school. She has always been the one to listen when I need to vent, and the one I go to when I need a silly laugh. I thank her for always being there for me, and knowing when to send her amazing care packages to cheer me up.

Lastly I would like to thank Ricardo Aguilar, who has been everything I've needed whenever I needed it. I am truly thankful to have him in my life. He has always been there for me, celebrating with me during the good times and being my support system during the hard times. I want to thank him for his patience and understanding during the times I was the most stressed. I couldn't have done this without him.

TABLE OF CONTENTS

LIST OF TABLES

LIST OF FIGURES

LIST OF SYMBOLS AND ABBREVIATIONS

σ	Standard Deviation
μm	Micrometer (1×10^{-6} m)
nm	Nanometer (1×10^{-9} m)
μL	Microliter (1×10^{-6} L)
CFU	Colony Forming Unit
DI	Deionized
g	Gram
ICP-OES	Inductively Coupled Plasma Optical Emission Spectrometry
L	Liter
m	Meter
mL	Milliliter
MNP	Magnetic Nanoparticle
NP	Nanoparticle
PBS	Phosphate Buffer Solution
Ppb	parts per billion
Ppm	parts per million
SEM	Scanning Electron Microscope
TSA	Trytpicase Soy Agar
TSB	Tryptic Soy Broth

SUMMARY

This work begins with chemotaxis studies involving *Salmonella typhimurium*. Known chemical attractants (ribose, aspartic acid, etc.) and repellents (nickel chloride, sodium acetate, etc.) were tested to direct bacteria swimming patterns. It was found that high concentrations of both attractant and repellent, approximately 10% chemical in deionized (DI) water, yielded better separation results than lower concentrations, such as 1% and .1% chemical in DI water. Utilizing these attractants or repellents appropriately can allow live bacteria to be directed in a desired manner in a microfluidic device, while dead bacteria, which yield no response, can be separated into a waste reservoir.

Another important aspect of bacteria separation is preconcentration, or the process of concentrating bacteria in a usable amount of liquid for further analysis in a microfluidic device. This study introduces a method of capturing *Salmonella typhimurium* through the use of magnetic nanoparticles (MNPs) without functionalizing them with antibody or amine coatings. Based on the work by Deng et al., MNPs were prepared in various ways to alter their diameter and surface characteristics to achieve optimal bacteria capture efficiency. A capture efficiency of approximately 94% has been achieved by altering chemical quantities in the MNP fabrication process. A macro-scale flow cell prototype was designed and characterized in order to 'clean' large volumes of buffer and separate the bacteria-MNP aggregates through the use of a magnetic field.

Finally, intervention of bacteria is a significant topic in food safety applications. This study utilizes Fe (III) to inhibit bacteria growth. This chemical was used in the presence of *Salmonella*, *E. coli*, *Staphylococcus*, and *Pseudomonas*. Further experiments were conducted with raw chicken and lettuce contaminated with *Salmonella typhimurium*. Using as little as .005M Fe III in DI water, up to 5 orders of magnitude reduction in bacteria growth was seen on test plates as compared to control plates.

CHAPTER 1

INTRODUCTION

This chapter gives a short background for the bacteria primarily used in this work, *Salmonella typhimurium*, as well as reasons for food safety concerns due to the prevalence of illness caused by this type of bacteria. This chapter also briefly details some existing technologies used for chemotaxis, separation of bacteria, and intervention of bacteria. Finally, a description of how the bacteria was diluted and quantified throughout the experiments in this work is given.

1.1 Salmonella Background

Salmonella typhimurium is classified as a Gram-negative bacterium, meaning that it has an outer membrane that protects the cell from penetration of materials from its environment [1]. A typical *Salmonella* cell can be seen in Figure 1.1.
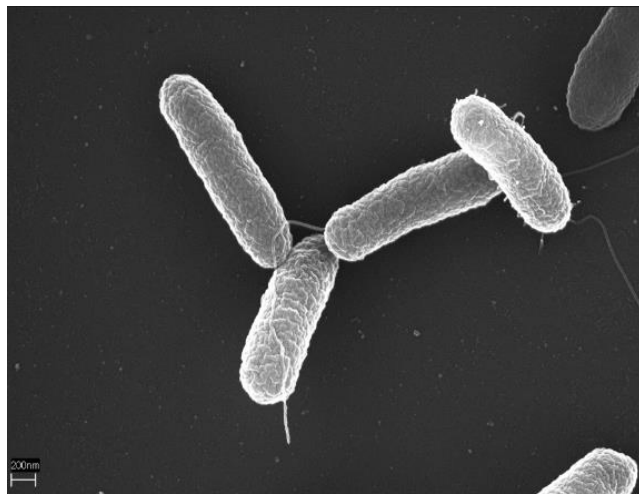
Figure 1.1 A typical *Salmonella* cell [2]

This rod-shaped bacterium is approximately .5µm to 1.5µm in width and approximately 2µm to 5µm in length. The zeta potential of this bacterium is approximately -17mV at a neutral pH, meaning that it has a negative surface charge [3].

It has many hair-like structures known as flagella, which enable movement of approximately 30µm/s by rotating these structures. Speeds as high as 55µm/s have also been demonstrated [4].

This type of bacteria is pathogenic, and is known to cause illness in humans and mammals. Typically this illness is due to ingestion of raw meats, contaminated dairy products, or contaminated vegetables [5]. These infections are the result of live bacteria cells. Consumption of dead cells on foods will not result in sickness, as the cells are unable to attach to the intestines. Most people will experience abdominal pain and diarrhea for approximately one week, before the infection clears up on its own. However, those with poor immune systems, such as children and the elderly, can experience severe symptoms and even death if not treated with antibiotics [5].

According to the Center for Disease Control and Prevention, over 1.2 million cases of salmonellosis occur each year in the United States, with approximately 400 fatal cases [6]. Therefore, research into methods of separating live and dead cells, as well as inhibiting bacteria growth on food is in high demand.

1.2 Bacteria Separation Background

Bacteria separation is a very important field not only for improving food safety for public health, but also for bacteria analysis (such as determining if cells are pathogenic, where they originated from, etcetera). Therefore, preconcentration methods must be employed. Preconcentration is defined as the concentration of a trace element prior to analysis [7]. In this study, this trace material is bacteria. Preconcentration aims to not only remove bacteria from food and water sources, but to concentrate the bacteria into small volumes so that the sample can be further analyzed in a microfluidic device. Typically, for drinking water applications, volumes of water to be cleaned are several hundreds of gallons. It is impossible to use microfluidic devices to separate and analyze bacteria from this volume. Therefore, preconcentration techniques can be implemented to

cleanse the volume of bacteria, as well as concentrate that bacteria into a small volume for further testing.

1.2.1 Filtration

Currently, there are many methods available for the removal of bacteria from food and water applications. One of the most popular and effective methods of bacteria removal is filtration [8]. Water treatment utilizes a very complicated process to ensure safe drinking water to the public. Filtration is one step of many involved in the water treatment process. Filtration involves forcing contaminated media to pass through several porous membranes of varying pore size. As the pore size decreases, the number of particulates that can pass through the filter decreases, effectively removing a bulk of unwanted material from the media. Common large-scale filtration processes use sand filtration to remove particulates from drinking water [9]. Slow sand filtration utilizes a biofilm of bacteria to cleanse water. It is a very slow process and requires a large area of land, due to the low flow rate. Even though this process is not time-efficient, it is effective at removing bacteria and viruses from the water. Rapid sand filtration, on the other hand, is much faster because it is a physical process. However, rapid sand filtration is not able to effectively remove bacteria. It is able to remove large particulates, where bacteria might be attached. Then, a chemical disinfection step, such as the introduction of chlorine, can be employed. Since rapid sand filtration does remove some bacteria attached to larger particulates, the amount of chlorine needed for disinfection is lessened, making this filtration step important.

Sometimes, this method of water treatment is not effective enough to treat extremely contaminated water. Therefore, smaller filters can be utilized, such as ultra- and nano-filters [10]. These filter membranes have extremely small pore sizes, .01µm and .001µm respectively. These methods are effective in separating bacteria and viruses from water, but are unable to separate dissolved substances. For instances where this is

necessary, reverse osmosis can be used. Figure 1.2 shows many filtration methods and the particle size they are capable of removing.
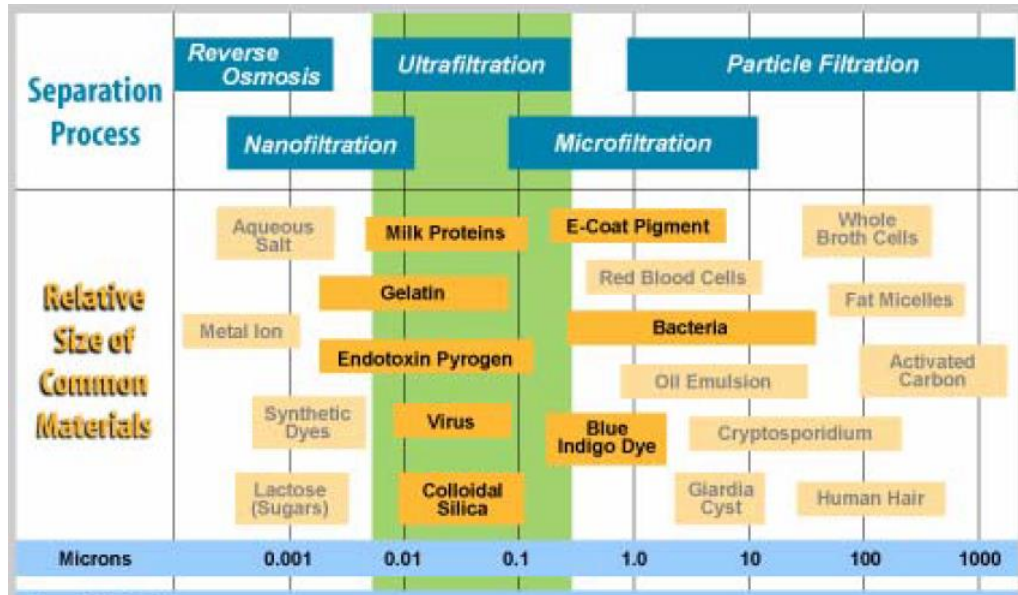
Figure 1.2 Chart describing different filtration methods and their capabilities [10]

These methods of filtration are effective at removing bacteria for water treatment purposes. However, the filtered bacteria cells are not intended to be studied, and therefore filtration at this scale is not a useful preconcentration method. If the cells are to be analyzed after separation, other methods can be used.

1.2.2 Chemotaxis Background

One process through which bacteria separation can take place is known as chemotaxis. Chemotaxis is the process by which bacteria direct their movement based on their environment. Bacteria sense chemical composition changes in their surroundings, and adjust their movement accordingly, swimming toward food sources and away from potentially hazardous or unfavorable chemicals [11]. Sensing of these chemicals is done through proteins on the bacterium's surface, known as chemoreceptors. This movement is modulated by the bacterium's flagella, which rotate in a specific direction based on the bacterium's surroundings. There are two distinctive swimming methods for bacteria: the

4

run and the tumble. When the flagella are rotated counterclockwise, the cell is propelled forward in a linear, stable motion, known as a run [12]. When the flagella are rotated clockwise, the bacterium's swimming is randomized, resulting in a tumble. These two mechanisms can be seen in Figure 1.3.
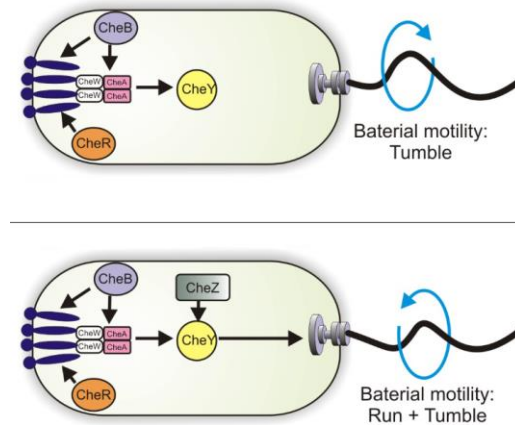
Figure 1.3 Schematic of flagella rotation and resulting movement [13]

If the bacterium is moving in a favorable direction, more runs than tumbles will be observed. However, if the bacterium senses that it is moving in an unfavorable direction, more tumbling will be observed, in an attempt to change its movement to a more favorable direction.

In this work, chemotaxis is studied through the use of capillary tubes filled with known attractant and repellent chemicals. This is described in Chapter 2. The use of capillary tubes to determine bacterial response to chemicals has been very well studied. One of the world's foremost contributors to the study of bacterial chemotaxis is Julius Adler. Adler adapted a method of Wilhelm Pfeffer, who had previously used chemicals to attract and repel bacteria [14]. Adler wanted to quantify this attraction and repulsion response, so he utilized capillary tubes. These tubes could be quantified using a conventional bacterial quantification method of agar plates, discussed in Section 1.4.3. One such paper which describes this capillary tube characterization is entitled "A Method for Measuring Chemotaxis and Use of the Method to Determine Optimum Conditions for

Chemotaxis by *Escherichia coli*" [15]. However there are many more published works on this method.

This method was studied because it allows bacteria separation and it does not kill the cells. Therefore, these separated cells can be further studied. A discussion of how this separation can be implemented in a real-life setting is described in Section 2.5.

1.2.3 Nanoparticle Background

Another method of bacteria separation that has become increasingly popular is the use of magnetic nanoparticles. Nanoparticles are spherical structures less than 1 micron in diameter and have become increasingly popular in biomedical applications, such as drug delivery [16]. Magnetic nanoparticles have the added benefit of possessing magnetic properties; that is, these particles can be separated from a fluid by a magnetic field. This property is extremely important in this work, as it will be the method of separating bacteria from contaminated water samples. This method is described in detail in Section 3.2.1. Essentially, bacteria cells attach to the nanoparticles in some way, and then can be separated by the nanoparticles in a magnetic field.

The nanoparticles used in this work were fabricated based on a published method. This fabrication method is described and modified in Section 3.1. Although there are many techniques for formation of nanoparticles described in the literature, comparison of fabrication techniques is not the focus of this study, and therefore, will not be discussed.

Currently there are many approaches to using nanoparticles for bacteria capture, typically through coating the nanoparticles with a material that will promote bacterial attachment. Some methods that will be discussed in this section are antibody coatings, antibiotic functionalization, and amine-functionalization.

<u>1.2.3.1 Antibody Coating</u>

Recently, the use of antibody coatings on nanoparticles has become a popular method of attaching a bacteria specimen to their surfaces. An antibody is a Y-shaped protein, and is able to attach to a structure on a bacterium's or virus's surface, known as an antigen. This method is often referred to as a 'lock and key' attachment [17]. It is a selective method of attachment, meaning that the antibody only recognizes the specific antigen that it can bind with. All other specimens with different antigens will remain unattached to this structure. This type of attachment can be seen in Figure 1.4.
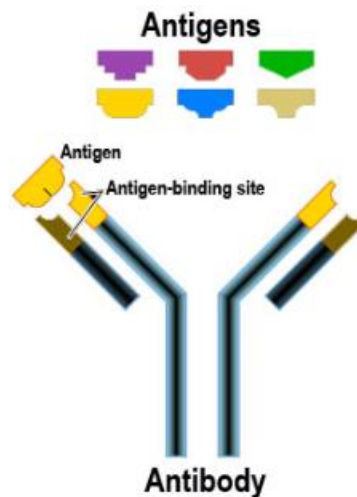
Figure 1.4 Antibody-antigen interaction [18]

Typically, these antibodies are able to tag the specimen they attach to so the body's immune system can neutralize it. In one work, 13 nm gold nanoparticles were used with an antibody coating to detect *Aeromonas salmonicida* [19]. In the presence of this type of bacteria, the nanoparticles would agglutinate with a reddish purple color, and this could be seen without the use of a microscope. This agglutination was not seen, however, if other types of bacteria were tested, proving this method's selectivity. Detection of this bacteria occurred in under an hour. In another work by Varshney et al., magnetic nanoparticles were utilized with *E. coli* antibodies attached to their surface [20]. The nanoparticles were mixed with contaminated beef samples, and then separated from

7

the sample using a magnet. Bacteria capture efficiency was 94% in approximately 15 minutes.

The use of a magnet by Varshney et al. closely matches the method of bacteria separation used in this work, discussed in Chapter 3. However, this study does not functionalize the nanoparticle surfaces with antibodies. Antibody functionalization allows selective bacteria capture. This work aimed to expand *Salmonella* capture to other types of bacteria, without coating the nanoparticles with several different antibody coatings.

1.2.3.2 Antibiotic Coating

Another method of bacteria capture uses antibiotic attachment to the surface of magnetic nanoparticles. This method is not as selective as the antibody-functionalized nanoparticles, because antibiotics are capable of interacting with many types of specimens. One work by Kell et al. utilized vancomycin to functionalize magnetic nanoparticle surfaces, which can be seen in Figure 1.5 [21].
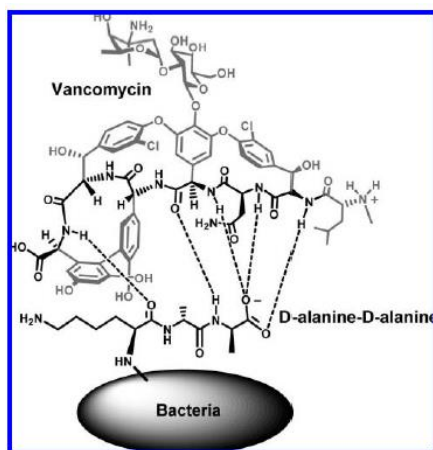
Figure 1.5 Schematic of vancomycin-coated nanoparticle-bacteria interaction [21]

As can be from Figure 1.5, the interaction of the bacteria and vancomycin coating is through five hydrogen bonds. By increasing the amount of antibiotic attached to the surface of the nanoparticle, bacteria capture time was significantly reduced in this work. Kell et al. tested many different types of bacteria, and were able to achieve capture efficiencies over 60% for several of these strains.

Again, Kell et al. utilized a magnetic field to separate bacteria attached to these nanoparticles, which is the method used in this work as well. However antibiotic coatings were not employed in this study.

1.2.3.3 Amino Group Coating

The method of coating nanoparticles for bacteria capture that is most similar to what was used in this work is amine-functionalization. This method requires a monolayer of amine groups to attach to the nanoparticles. These amine groups alter the surface charge of the nanoparticle from negative to positive. The method of capturing bacteria is a purely electrostatic interaction, rather than a binding mechanism as seen in Sections 1.2.3.1 and 1.2.3.2. Like antibiotic coatings, this method is not selective, but instead allows capture of many types of bacteria.

An example of a work that utilizes this method of bacteria capture is "Amine-Functionalized Magnetic Nanoparticles for Rapid Capture and Removal of Bacterial Pathogens" by Huang et al.[22]. The nanoparticles were coated with silica and then γ-aminopropyltriethoxysilane (APTES) was used to alter the surface chemistry of the particles to achieve a positive surface charge. The method of coating these nanoparticles can be seen in Figure 1.6.
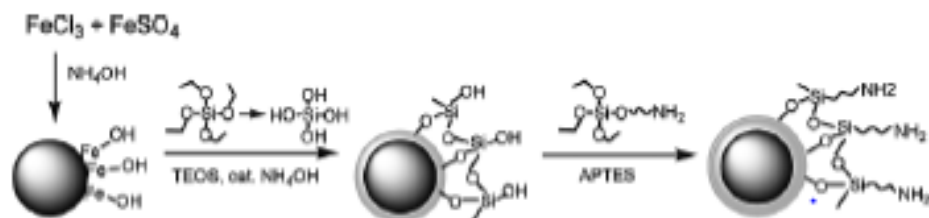
Figure 1.6 Schematic for coating nanoparticles with amine groups [22]

Once the nanoparticles were coated, bacteria and nanoparticles were placed on a rotary shaker in an incubator for approximately 15 minutes. Magnets were used to separate the bacteria-nanoparticle aggregates from the supernatant. Huang et al. reported capture efficiencies of approximately 97% for *E.coli*. However, the capture efficiency for

Salmonella was much lower, approximately 55%. It is possible that *E.coli* yielded a better capture efficiency since they are more negatively charged than *Salmonella* (*E. coli* has a zeta potential of approximately -47mV) [3].

Amine-functionalization in the work by Huang et al. utilized an electrostatic interaction for bacteria capture. However, this method used a monolayer coating of positively charged amine groups in order to attract negatively charged bacteria.

In this work, polymers with positive zeta potentials were used to coat the nanoparticles. Polymers are essentially long chains comprised of many layers of amino groups, rather than a monolayer as seen with amine-functionalization. This will allow an increased charge density on the nanoparticle surface. Theoretically, this should increase the probability of attraction between the nanoparticles and bacteria, yielding a better capture efficiency. Discussion of polymers and coating methods used in this work can be found in Section 3.1.

1.3 Bacteria Intervention Background

For water applications, as well as meat processing, chlorination is the most common method of bacterial disinfection [23]. Disinfection with chlorine is facilitated by breaking the bonds of molecules in microorganisms, resulting in their death. Chlorine is an inexpensive, reliable method to kill microorganisms in water treatment facilities, as well as chillers at poultry processing facilities. The level of chlorine can be easily monitored and controlled [24].

For applications involving disinfection of water with organic materials, it is extremely important to carefully monitor the chlorine level being used. This is because chlorine reacts with organic material and loses its disinfection capabilities [23]. If chlorine loses its efficacy due to an excess of organic material, no disinfection will occur, and public health could be at risk.

Other methods of water disinfection are ozone and ultraviolent radiation. Ozone water treatment involves oxidizing bacteria, which is the same method of killing as chlorine. Its advantages include being usable at many pH values and not having a residual taste, as is seen with chlorine [25].However, the disadvantages of this method are that it requires expensive equipment which must be maintained, and its residual time is measured in minutes, rather than hours as is the case with chlorine [25]. This means that its disinfection does not continue after the fluid has left the equipment, while residual chlorine continues to disinfect for a long period of time. In this work, intervention methods were compared to the efficiency of chlorination, as that is the current standard.

Ferric chloride was tested in this work to ascertain its antibacterial properties. However, this compound has also been used for water treatment [26]. Ferric chloride is known to provide good turbidity removal because it acts as a flocculant. Turbidity is the cloudiness of a fluid due to suspended particulates. Ferric chloride hydrolyzes in water and forms ferric hydroxide. This product is able to bind with colloidal particles in the water to be treated, as well as to itself. This causes the formation of floc, or the aggregation of these suspended colloidal particles [26]. This floc can then be collected through sediment removal.

Although ferric chloride has been used to treat water for turbidity, its antibacterial capabilities are far from well-researched. Therefore, this study delves into its efficacy at killing different types of bacteria in different food matrices.

1.4 Bacteria Preparation, Quantification, and Disposal

1.4.1 Bacteria Growth

For all experiments in this work, bacteria samples were grown at 37°C for approximately 18 hours in Tryptic Soy Broth (TSB), a conventional, nutrient-rich medium used for bacteria growth. After 18 hours of growth, the bacteria sample has

reached its maximum concentration, on the order of 10^9 cell forming units per milliliter, or CFU/mL. The term 'cell forming unit' will be discussed further in Section 1.4.3.

A growth curve for bacteria can be seen in Figure 1.7.
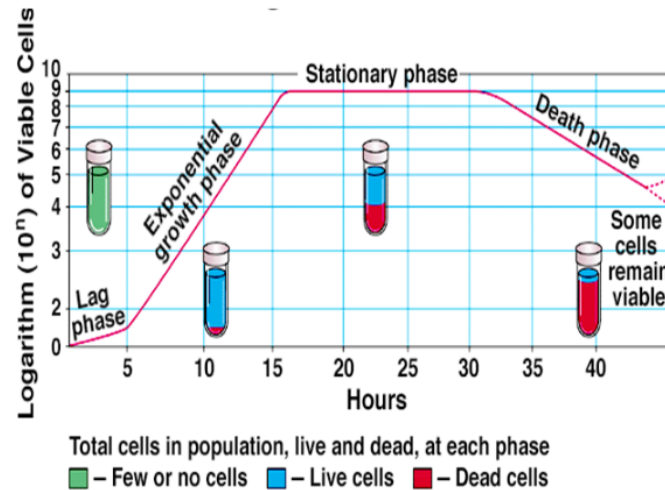
Figure 1.7 Growth curve for bacteria [27]

From this figure, it can be seen that bacteria growth occurs in four phases [28]. For the first several hours, very little bacterial reproduction occurs. This is known as the lag phase. During this time, there is an excess of nutrients in the growth medium and very few cells. After this time, there is a phase of exponential growth. During this period, the nutrients are being consumed rapidly and cells are dividing to exponentially increase the bacteria concentration of the sample. This continues until the stationary phase is reached, during which nutrients have become depleted, and the growth rate is relatively equal to the death rate of the sample. Finally, the sample reaches the last stage of growth, where the cell death rate is high, due to lack of nutrients in the environment. During this time, the sample becomes increasingly concentrated with dead cells.

1.4.2 Bacteria Concentration Counting

To utilize the bacteria sample with a high concentration of viable cells, the sample is removed from the incubator after approximately 18 to 20 hours and testing is begun.

To determine the bacteria sample's initial concentration, a series dilution method is employed. This method requires that the sample is diluted repeatedly in a systematic method until a quantifiable number of cells can be reached. To begin this dilution method, the grown culture is mixed using a vortexer, to ensure the sample's bacteria concentration is uniform. Next, 100 μL of this grown culture is diluted in 1mL of TSB. This corresponds to a tenfold dilution of the grown culture. Then, this 10x dilution is vortexed, and 100μL of it is diluted in 1mL of TSB. This new dilution corresponds to a hundredfold dilution of the grown culture. This method is continued until the grown culture has been diluted 10^7x. The expected concentration of bacteria in this 10^7x dilution is on the order of 10^2 CFU/mL.

1.4.3 Bacteria Quantification

The last step of this concentration testing process is to be able to quantify the bacteria in the sample. To do this, Trypticase Soy Agar (TSA) is utilized. This medium allows the growth of bacteria colonies. A sample of bacteria is spread on the agar plate and incubated for several hours at 37°C. During this incubation time, the viable bacteria spread on the plate will reproduce and form macroscopic, circular clusters that can be quantified without the use of a microscope. Each cluster represents one colony forming unit (CFU). These CFUs can be counted, and based on the dilution plated, the starting concentration of the sample can be calculated. It is not possible to determine if each colony was formed from a single bacterium or several hundred. Therefore, the concentration determined from this quantification is given as CFU/mL rather than cells/mL.

TSA is a nonselective growth medium, meaning that many types of bacteria will be able to give rise to colonies when plated on this medium. However, it is sometimes possible to determine if different bacteria than the desired specimen has grown on the plate, due to its colony size. There are also selective growth mediums available for

Salmonella, which allow colonies formed by *Salmonella* to display a specific color on the plate. For this work, TSA was utilized for all plating procedures. All numbers listed in tabulated results are average counts of the number of CFUs on the agar plates from each experiment.

1.4.4 Bacteria Sample Dilution

For testing, samples of bacteria were diluted in different buffers based on each experiment. To dilute the bacteria sample as accurately as possible, a series dilution method similar to the concentration counting method was utilized. To begin dilution of the grown culture, one milliliter of the culture is diluted in 10mL of the desired buffer. This 10x dilution is vortexed, and 1mL of this sample is diluted again in 10mL of the desired buffer. This method continues until the desired concentration is achieved. Utilizing this method is reliable because it not only allows the bacteria to be suspended in the buffer of choice for the experiment, but it allows accurate dilution of the sample. If a smaller sample from the grown culture were used, such as 100μL, it would be more difficult to ensure that the culture is so uniformly mixed that a representative concentration can be found in such a small volume.

1.4.5 Bacteria Disposal

It is extremely important to properly dispose of all contaminated waste for the safety of people and the environment. After all experiments were completed, all waste, including centrifuge tubes, pipette tips, plate spreaders, and agar plates, were autoclaved. This autoclave process keeps the waste at 121ºC under high pressure for 15 minutes. This exposure to heat and pressure kills the bacteria on contaminated waste, and it can then be disposed of safely.

CHAPTER 2

CHEMOTAXIS

This chapter focuses on the use of chemicals to attract and repel bacteria in efforts of separating live and dead cells. This process of directing bacteria movement is known as chemotaxis. All experiments in this chapter were performed using *Salmonella typhimurium*.

2.1 Initial Setups

2.1.1 Attractant Chemical Testing

Testing began by comparing the efficiency of three known chemical attractants: ribose, serine, and aspartic acid [29]. The first setup to be used for testing can be seen in Figure 2.1.
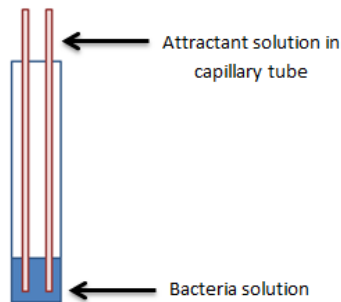
Figure 2.1 Initial setup with capillary tubes used to test attract chemicals

This setup involved two capillary tubes partially submerged in a solution of bacteria. These capillary tubes were filled with approximately 50 μL of a chemical attractant solution. Control tests were performed using capillary tubes filled with DI water. This experiment's purpose was to determine which attractant was most effective at attracting bacteria into the capillary tube in ten minutes. After the experiment was over, each capillary tube was emptied onto an agar plate and incubated at 37°C for approximately 18 hours. The first chemical attractant concentration tested was 1% chemical in DI water. A

sample of *Salmonella typhimurium* was grown in TSB at 37°C for approximately 18 hours. Different dilutions of this grown culture were used in the experiment to determine which was best for quantification purposes. These dilutions were performed using PBS. Each capillary tube represented one test. Average counts of CFUs on the agar plates from this initial testing can be seen in Table 2.1.

Table 2.1 Results of initial chemical testing using 1% attractant solution

Dilution	Quantification	Aspartic Acid	Serine	Ribose	DI water
10x	Average	Thousands	Thousands	Thousands	Thousands
100x	Average	Thousands	Thousands	Thousands	Thousands
10^3x	Average	66	55	58	80
10^3x	σ	62.2	64.3	45.3	43.1
10^4x	Average	15	43	34	32
10^4x	σ	19.8	32.5	5.7	13.4

From this testing, no conclusive results were seen, since the DI water control tests collected the same amount of bacteria as the chemical attractants. However, the test was able to conclude that a 10^4 x dilution of *Salmonella* was best for future tests.

To continue testing, a new setup was used to better control the volume of attractant solution. This new setup can be seen in Figure 2.2.
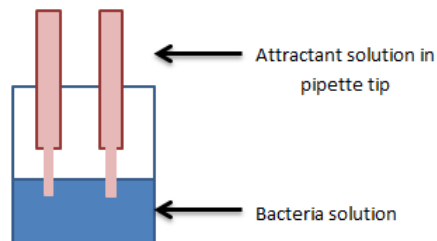
Figure 2.2 Second test setup for attractant testing

This new setup featured two pipette tips filled with approximately 10μL of an attractant solution suspended in a solution of bacteria. It was chosen over the setup in Figure 2.1 because it was a more accurate way to measure the initial volume. The first test conducted with this new setup was to determine what concentration of chemical was best for attracting bacteria. Solutions of .1%, 1%, and 10% chemical in DI water were tested. The tips were filled with the proper concentration of each chemical and submerged in a 10^4x dilution of *Salmonella* for ten minutes. As a control test, tips were filled with DI water and submerged in the bacteria solution for comparison purposes. The tips were then emptied onto agar plates and incubated at 37ºC for approximately 18 hours. The results of this testing can be seen in Table 2.2.1 and Table 2.2.2. Each pipette tip represented one test, and the average of the two tests is represented in the table.

Table 2.2.1 Results of chemical concentration variations with setup from Figure 2.2

Chemical	Quantification	.1 %	1%	10%
Aspartic Acid	Average	0	1	14
	σ	0	0.7	4.2
Serine	Average	1	1	15
	σ	1.4	0.7	6.4
Ribose	Average	1	2	11
	σ	1.4	0.7	0

Table 2.2.2 Results of DI water control test with setup in Figure 2.2

	Average	σ
DI water	0	0

From the results in Table 2.2.1, it is obvious that the highest concentration used was best for attracting bacteria. The control tests revealed that the bacteria were attracted to the chemical solutions, and were not simply swimming into the tips arbitrarily.

2.1.2 Repellent Chemical Testing

The next experiment used the setup in Figure 2.2 to determine if adding a repellent to the *Salmonella* solution could force the bacteria to swim into the tips containing chemical attractants. The hypothesis was that the bacteria would swim away from the repellent and into the tips in higher numbers than the previous experiment, where no repellent was introduced.

The setup for this experiment can be seen in Figure 2.3.
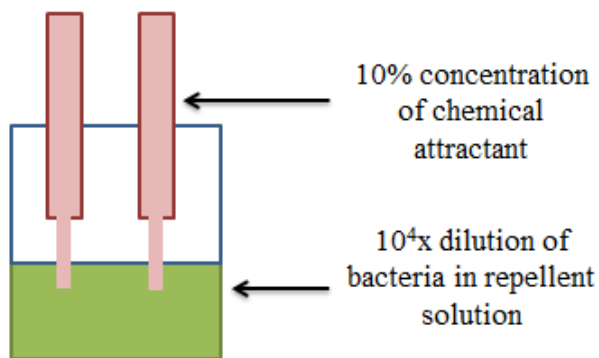
Figure 2.3 Setup for testing repellents and attractants together

The first repellent to be tested was sodium acetate [30]. The concentrations of sodium acetate tested were 0M (control experiment), 5×10^{-3}M, 5×10^{-2}M, and 5×10^{-1}M. The 10^4x dilution of bacteria was prepared in PBS and then this repellent was added until the desired concentration was reached. The tips filled with 10μL of 10% chemical attractant in DI water were exposed to the bacteria solution for ten minutes, and then the contents of the tips were plated. Again, tips filled with DI water were used as control samples. The results of this testing can be seen in Table 2.3.

Table 2.3 Results of sodium acetate testing using setup in Figure 2.3

Concentration of sodium acetate	Quantification	Aspartic Acid	Serine	Ribose	DI water
0M	Average	18	12	13	1
	σ	2.1	15.6	2.1	0
5×10^{-3}M	Average	18	7	8	1
	σ	2.1	2.1	2.1	0.7
5×10^{-2}M	Average	13	4	15	0
	σ	1.4	3.5	2.1	0
5×10^{-1}M	Average	7	5	6	1
	σ	5.7	2.8	2.8	0.7

As can be seen by Table 2.3, there is no appreciable difference between the results of this test and the results of Table 2.2.1, where no repellent was used. Therefore, it was decided to repeat this test using phenol, which is a more aggressive repellent [31]. The concentrations used for phenol were 1×10^{-1}M, 1×10^{-2}M, and 1×10^{-3}M. This test also included tips filled with all three chemical attractants mixed together at a concentration of 10% of each chemical in DI water (100mg of each chemical in 1mL of DI water). This solution was referred to as 'All Solution'. The results of this phenol testing can be seen in Table 2.4.

Table 2.4 Results of phenol testing using setup in Figure 2.3

Concentration of phenol	Quantity	Aspartic Acid	Serine	Ribose	DI water	All solution
1×10^{-3}M	Average	12	2	9	2	49
	σ	2.8	0	5.7	2.1	43.8
1×10^{-2}M	Average	10	9	6	1	67
	σ	0.7	11.3	1.4	0.7	33.2
1×10^{-1}M	Average	5	10	9	0	28
	σ	4.2	7.8	7.8	0	2.1

Again, this test did not show a noticeable difference between the results with a repellent and the results from Table 2.2.1, where no repellent was added. Since phenol is a more aggressive chemical repellent than sodium acetate, it was hypothesized that the bacteria concentration in the tips at the end of the experiment would be much greater. It is interesting to note that the results for the 'All Solution' are much greater than the results of any of the individual chemical attractants for all concentrations of phenol. Therefore, for further testing, this solution was used instead of the individual chemical attractant solutions.

2.2 Time Variation Testing and Introduction of Final Setup

The next testing performed was varying the time that the bacteria solution was exposed to the 'All Solution'. Ten minutes had been used in previous testing. The experiment was performed for two minutes, five minutes, ten minutes, and 30 minutes to deduce which time would result in the highest number of bacteria in the tips. The setup in Figure 2.2 was used. The bacteria solution concentration remained at 10^4x dilution of the grown culture. The results of this initial time variation test can be seen in Table 2.5. Again, each pipette tip represented one test and the average of the two tests is represented in the table. Two trials were performed for each test time.

Table 2.5 Results of initial time variation test using setup in Figure 2.2

Time	Average	σ
2 minutes	16	19.1
5 minutes	81	1.4
10 minutes	13	16.3
30 minutes	33	3.5

Based on this test, it appears that five minutes yielded the highest amount of bacteria. However, after many tests were performed using the setup in Figure 2.2, it was

noticed that the level in the pipette tips decreased when placed in the bacteria solution. This meant that the attractant solution was draining slightly into the bacteria solution because the top of the tips were not sealed before testing. This was not an accurate way to determine how much bacteria was attracted to the chemical solution because a portion of it was introduced to the bacteria without the cells swimming into the tip. Therefore, the setup had to be changed. The new setup can be seen in Figure 2.4.
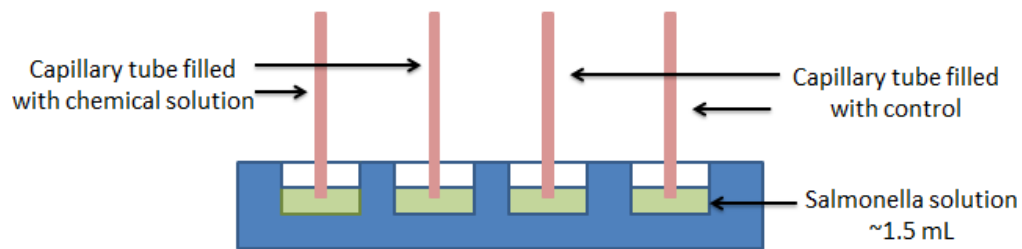
Figure 2.4 Chemotaxis setup using vacuum grease to seal capillary tubes

The setup consists of four wells filled with approximately 1.5mL of the bacteria solution (10^4x dilution of bacteria in PBS). A capillary tube was suspended in each of the wells. The top of each capillary tube was sealed with vacuum grease to ensure that the chemical solutions did not drain into the bacteria solutions. Two of the capillary tubes were filled with 5µL of the 'All Solution' and the other two capillary tubes were filled with 5µL of DI water, as a control test. All of these tests were performed simultaneously. After the test, each capillary tube was emptied onto an agar plate and incubated at 37°C for approximately 18 hours.

It was also decided to test the bulk bacteria concentration that was placed in the wells of the setup before each experiment. This would allow the final concentration inside the capillary tube to be compared to the bulk solution of bacteria in the wells. This would also allow verification of the starting concentration of bacteria in the wells. To test this concentration, the 10^4x dilution of the grown bacteria sample was prepared. A 10µL sample was taken from this bulk bacteria solution and diluted in 1mL of TSB. A 100µL sample was taken and plated.

Using this new setup in Figure 2.4, the time variation test was repeated. This time, the test durations were two minutes, five minutes, 15 minutes, and 30 minutes. The results of this testing can be seen in Table 2.6.1 and Table 2.6.2.

Table 2.6.1 Results of time variation test using setup in Figure 2.4

	All Solution Average	All Solution σ	DI water Average	DI water σ
2 minutes	14	0	1	1.4
5 minutes	4	5.7	1	0.7
15 minutes	11	11.3	2	2.1
30 minutes	18	1.4	1	1.4

Table 2.6.2 Results of concentration testing of bulk bacteria solution for time variation experiment 1

	1st Dilution	Corresponding Starting Concentration in Wells
Bulk Bacteria Solution	76	7.6×10^4 CFU/mL

From Table 2.6.1, it appeared the average from each of these tests was very similar. There does not seem to be any significant difference between test durations. It was decided to begin using PBS for testing. Thus far, only the bacteria solution was diluted with PBS, and the attractant solution and control tests used DI water. The next set of tests used PBS to dilute the attractant solution (100mg of each attractant in 1 mL of PBS). PBS was also used as the control sample, in place of DI water. Test durations were also changed to see if longer times would result in higher amounts of bacteria. Test times were changed to two minutes, ten minutes, 30 minutes, and 60 minutes. The results of this testing can be seen in Tables 2.7.1 and 2.7.2.

Table 2.7.1 Results of time variation testing with PBS

	All Solution Average	All Solution σ	PBS 1 Average	PBS 2 σ
2 minutes	34	21.2	8	9.2
10 minutes	31	3.5	1	0.7
30 minutes	16	21.2	2	1.4
60 minutes	45	4.9	4	3.5

Table 2.7.2 Results of concentration testing of bulk bacteria solution for time variation experiment 2

	1st dilution	Corresponding starting Concentration in Wells
Bulk Bacteria Solution	119	1.19×10^5 CFU/mL

From Table 2.7.1 it can be seen that the averages from the 'All Solution' are higher than previous testing results seen in Table 2.6.1. However, it was also noted that the starting concentration in the wells from the first time variation test (Table 2.6.2) was less than the starting concentration in the second time variation test (Table 2.7.2). The second test utilized a freshly grown sample of bacteria for testing. The previous tests used a grown sample of bacteria that had been refrigerated. This refrigeration could have been affecting the mobility of the bacteria over time. It was decided that a freshly grown sample of bacteria was to be used for all future testing.

From Table 2.7.1, two minutes and ten minutes showed comparable results to the 60 minute test. Therefore these two time durations were used for further testing.

2.3 Low Concentration Testing using Final Setup

Now that PBS was being used to dilute the chemical attractant solution, it was decided to test lower concentrations of this 'All Solution.' Concentrations of .1%, 1%, and 10% of each chemical in 1mL of PBS were tested using the setup in Figure 2.4. A

10^4x dilution of the grown bacteria culture was used in the wells. PBS control tests were performed one time for each test length. The results of this testing can be seen in Table 2.8.

Table 2.8 Results of varying chemical concentration testing using setup in Figure 2.4

Concentration	Test Length	All Solution Average	All Solution σ	PBS 1 Average	PBS 2 σ
.1%	2 minutes	2	0.7	-	-
	10 minutes	1	0	-	-
1%	2 minutes	3	0.7	1	0.7
	10 minutes	6	3.5	1	0.7
10%	2 minutes	15	16.9	-	-
	10 minutes	40	4.9	-	-

Based on these test results, it can be seen that 10% of each chemical in 1mL PBS yielded significantly higher results than any of the other concentrations tested.

Another known chemical attractant of bacteria is glucose [32]. The next experiment performed was to add 10% glucose to the 'All Solution' currently being used to deduce if better results could be demonstrated. This test length was ten minutes. All other aspects of the previous experiment were kept the same, including the bacteria concentration and the use of PBS as the control sample. The results of this glucose testing can be seen in Table 2.9.

Table 2.9 Results of varying chemical concentration testing with glucose in 'All Solution'

Concentration	All Solution w/ Glucose Average	All Solution w/ Glucose σ	PBS 1 Average	PBS 2 σ
.1%	9	3.5	1	0.7
1%	5	3.5	2	2.1
10%	30	3.5	0	0

The addition of glucose did not appear to have a significant effect on bacteria movement into the capillary tubes. It was proposed that this was due to the fact that the 'All Solution' already contained a very high concentration of attractant chemicals and the addition of the glucose was unnecessary.

2.4 Repellent Chemical Testing using Final Setup

The next experiment utilized sodium acetate and nickel chloride as repellents. The setup of the experiments involving these repellents is shown in Figure 2.5.
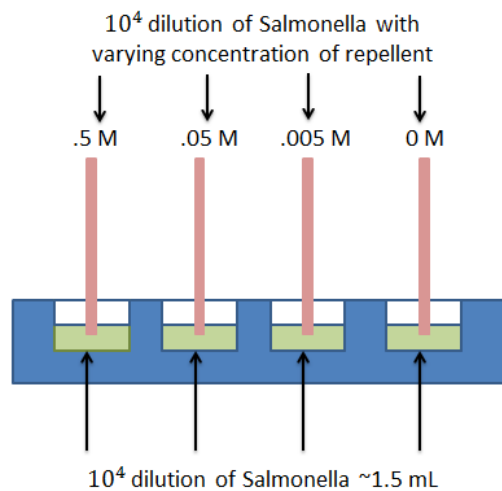
Figure 2.5 Updated setup for testing of repellents

This setup involved preparing a 10^4x dilution of bacteria in PBS. 1.5mL of this solution was placed in each of the wells in Figure 2.5. 1mL of this solution was also placed in eight 2mL centrifuge tubes. Sodium acetate was added to four of these tubes to achieve the desired concentration of repellent: $5\text{x}10^{-1}$M, $5\text{x}10^{-2}$M, $5\text{x}10^{-3}$M, and 0M. Nickel chloride was added to the other four tubes to achieve the same concentrations of this repellent. A capillary tube filled with each of these concentrations was then partially submerged in one of the wells in Figure 2.5 for ten minutes. After ten minutes, the contents of the capillary tube would be emptied on an agar plate and incubated at 37°C for approximately 18 hours. Each concentration of both repellents was tested twice for consistency purposes. The bulk bacteria concentration from the wells was tested and the

results can be seen in Table 2.10. The results of the sodium acetate testing can be seen in Table 2.11 and the results of the nickel chloride testing can be seen in Table 2.12.

Table 2.10 Results of concentration testing of bulk bacteria solution for repellent testing using Figure 2.5

	1st dilution	Corresponding starting Concentration in Wells
Bulk Bacteria Solution	151	1.51×10^5 CFU/mL

Table 2.11 Results of sodium acetate testing using setup in Figure 2.5

Sodium Acetate	0M	5×10^{-3}M	5×10^{-2}M	5×10^{-1}M
Average	86	93	78	52
σ	45.3	6.4	4.9	28.3

Table 2.12 Results of nickel chloride testing using setup in Figure 2.5

Nickel Chloride	0M	5×10^{-3}M	5×10^{-2}M	5×10^{-1}M
Average	70	14	8	9
σ	9.2	12.0	2.8	3.5

It can be seen from Table 2.11 that, as the concentration of sodium acetate increases, the number of bacteria in the capillary tube decreases. This was the expected outcome of the experiment. It was hypothesized that, if repellent was introduced to the bacteria in the capillary tube, the bacteria would try to swim away from this chemical into the wells. Therefore, the concentration of bacteria in the capillary tubes containing repellent was expected to be lower than the concentration of bacteria in the capillary tube with no repellent (0M).

Based on the results in Table 2.12, there was a lower bacteria concentration in all capillary tubes after ten minutes compared to the results in Table 2.11. This may suggest

that nickel chloride is a stronger repellent and was able to force the bacteria out of the capillary tube more effectively.

The setup in Figure 2.5 was utilized again to test another possible repellent: ferric nitrate. The results of this testing can be seen in Tables 2.13.1 and 2.13.2.

Table 2.13.1 Results of concentration testing of bulk bacteria solution for repellent testing using Figure 2.5

	1st dilution	Corresponding starting Concentration in Wells
Bulk Bacteria Solution	137	1.37x10^5 CFU/mL

Table 2.13.2 Results of ferric nitrate testing using setup in Figure 2.5

Ferric Nitrate	0M	5x10^{-3}M	5x10^{-2}M	5x10^{-1}M
Average	44	0	0	0
σ	10.6	0	0	0

There appeared to be no bacteria growth from any of the capillary tubes exposed to ferric nitrate. This prompted further testing of this chemical for its bacteria inhibition characteristics. This is discussed in Chapter 5.

The last setup to be tested utilized both attractants and repellents. This setup can be seen in Figure 2.6.
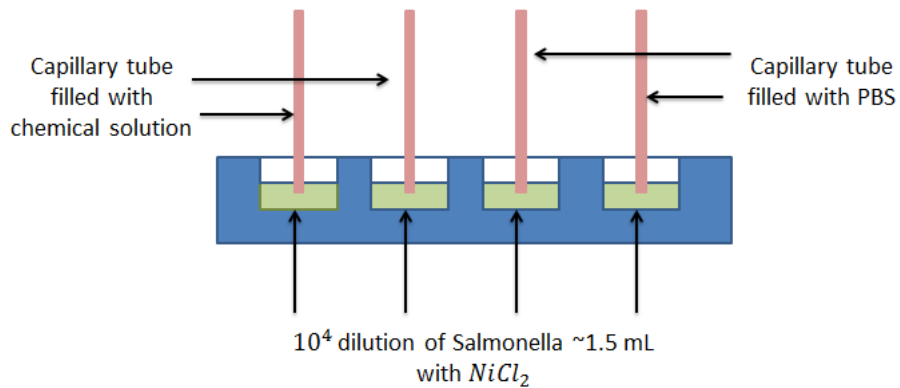
Figure 2.6 Updated setup for testing of repellents and attractants

In this setup, repellent is introduced to the bacteria solution in the wells. The capillary tubes in each of the wells are filled with the 'All Solution' of chemical attractants. The idea behind this setup was that the repellent in the wells would force the bacteria to swim into the capillary tubes, toward a more preferable environment. The repellent used in this experiment was nickel chloride, since it seemed to provide better results than sodium acetate.

To begin the experiment, a bacteria solution (grown sample diluted 10^4x in PBS) was prepared. Nickel chloride was added to this solution to achieve a concentration of 5×10^{-2}M. This solution was placed in each of the wells. A capillary tube filled with 5µL of the 'All Solution' of chemical attractants was partially submerged in two wells for ten minutes. A capillary tube filled with 5µL of PBS was partially submerged in the other two wells for ten minutes as a control sample. After ten minutes, the contents of the capillary tubes were emptied on agar plates and incubated at 37°C for approximately 18 hours.

As a control test, the setup in Figure 2.4 was used. Each well contained a bacteria solution that was diluted 10^4x in PBS. However, no repellent was introduced. The capillary tubes containing the attractant solution or PBS were introduced to the wells for ten minutes, and then plated.

A sample from each bacteria solution (with and without repellent) was plated for quantification purposes to ensure the two concentrations were equal. The results of this concentration testing can be seen in Table 2.14.1 and 2.14.2.

Table 2.14.1 Results of concentration testing of bulk bacteria solution with NiCl$_2$

	1st dilution	Corresponding starting Concentration in Wells
Bulk Bacteria Solution with NiCl$_2$	127	1.27×10^5 CFU/mL

Table 2.14.2 Results of concentration testing of bulk bacteria solution with no $NiCl_2$

	1st dilution	Corresponding starting Concentration in Wells
Bulk Bacteria Solution with $NiCl_2$	128	1.28×10^5 CFU/mL

As can be seen from the bulk concentration testing, the two starting concentrations were very similar. The results of the tests with and without nickel chloride can be seen in Table 2.15.

Table 2.15 Results of nickel chloride testing using setup in Figure 2.6

	Test	All Solution Average	All Solution σ	PBS Average	PBS σ
0 $NiCl_2$	Test 1	109	152.7	2	1.4
	Test 2	176	10.6	1	0
$NiCl_2$	Test 1	14	19.8	2	0.7
	Test 2	32	45.3	1	1.4

From the results in Table 2.15 it can be seen that the averages from the attractant-filled capillary tubes are much higher for the bacteria solution with no nickel chloride introduced. This was unexpected due to the fact that it was thought the bacteria would have more motivation to swim away from the repellent and into the attractant environment. However, these results could be due in part to the nickel chloride negatively affecting the swimming patterns of the bacteria, thereby inhibiting them from swimming into the capillary tubes.

2.5 Discussion

From the chemotaxis experiments in this chapter, it seems obvious that the bacteria could be drawn into the capillary tubes simply by introducing an attractant chemical. The use of control tubes filled with either PBS or DI water serves as a good comparison to this attraction, since very low concentrations of bacteria were found in

these tubes at the completion of each experiment. Even when a chemical repellent was introduced to the wells as seen in Figure 2.6, very low concentrations of bacteria were found in the control tubes. It was hypothesized that the bacteria would try to escape the repellent environment and swim into the attractant tubes. However, this did not occur. This can be explained because, with the attractant tubes, there's a small chemical gradient that is created in the well at the opening of the capillary tube. The cells are able to swim toward this gradient and thus into the capillary tube. However, the control tubes are only filled with the buffer that they are already dispersed in, either DI water or PBS. There is no real chemical gradient that they can detect and swim towards. As such, there is a very small probability that the bacteria will swim into the tube arbitrarily, since the opening of the capillary tubes is extremely small, approximately 150µm. Therefore, the attractant alone is responsible for drawing bacteria into the capillary tube.

The amount of attractant in the capillary tubes makes a significant difference, as was seen when determining the optimal concentration of attractant in Table 2.2.1 and Table 2.8. It seems that the amount of attractant in the 'All solution' was optimal, due to the fact that when glucose was added, no significant increase in bacteria concentration in the capillary tubes was seen (Table 2.9). The 'All solution' contains a very concentrated amount of chemicals and therefore appeared to produce a stronger chemical gradient at the opening of the capillary tubes, which the bacteria could detect more easily.

Using the final setup, as seen in Figure 2.4, was able to produce reliable, consistent results through the use of the vacuum grease to seal the capillary tubes. In some chemotaxis studies, capillary tubes are utilized, and they are sealed by melting the end of each tube closed [15]. Using vacuum grease was a simple, inexpensive, and safe way to ensure that the chemical was not diffusing uncontrollably into the wells containing bacteria, as was the case with the setup shown in Figure 2.2.

It is important to note that a fresh growth of bacteria is needed to demonstrate successful results. This is due to the fact that, when viewing the bacteria under a

microscope, a noticeable change in their motility is obvious when the bacteria sample is stored in a refrigerator versus freshly grown. The bacteria are not killed when kept in lower temperatures. Their motility decreases drastically, until the sample is brought to room temperature. Typically a *Salmonella* bacterium can move up to 20μm/s [33]. However, even at room temperature, these older samples do not exhibit the same motility as a freshly grown sample. This could be due to the fact that some of the bacteria in the stored sample are dead, and the rest have aged. On the other hand, freshly grown bacteria exhibit quick motility since they were recently grown and have never been stored at a low temperature.

Currently, this technique of directing bacteria movement through the use of chemical attractants and repellents is being used in a microfluidic device to separate live and dead cells, as seen in Figure 2.7.
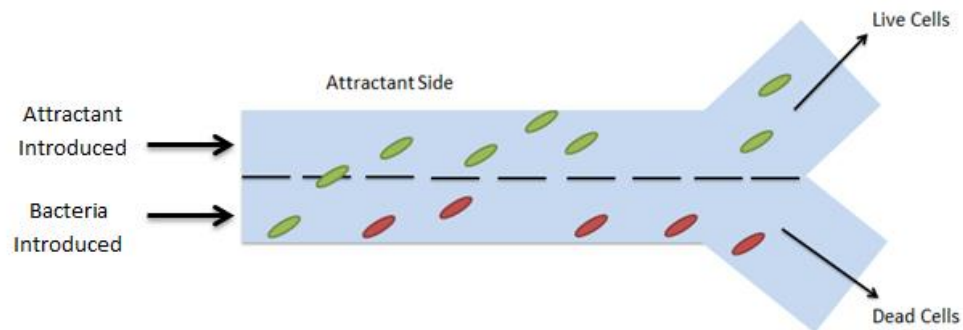
Figure 2.7 Schematic of microfluidic device used to separate live and dead cells

This device utilizes laminar flow. A bacteria sample is introduced on one side of a straight channel, and a chemical attractant is introduced on the other side of the channel. The use of laminar flow ensures that the bacteria flow and attractant flow will not mix. The objective of this device is that the live bacteria cells will sense the chemical attractant and swim towards it, to the other side of the channel. The dead cells will continue to flow on the original side of the channel, since a dead cell is incapable of movement other than Brownian motion. After a sufficient channel length, when it is

expected that most of the live cells have had enough time to swim to the attractant side of the channel, the two flows separate. This separation will send live cells to a different well than dead cells. This type of device can be used to determine if bacteria that is found on food products or other material is infectious (live) or benign (dead).

For this device, it is extremely important that the bacteria are very motile. If the cells are live but do not swim toward the attractant side, the device will not separate the bacteria. This type of method must also account for cells that swim toward the attractant and then back to their original side of the channel. To prevent this action, a chemical repellent could be introduced on the opposing side of the attractant, and therefore force live cells away from the dead bacteria well and into the live bacteria well. Alternative designs to make this device more efficient and reliable are currently being researched.

Since it is obvious that this type of device will be most useful on a microfluidic level, it is possible that this type of separation technique can be paired with another technique that is more easily maintained on a large scale. It will be useful to first preconcentrate cells using a technique that can process large sample volumes quickly. Then, once the cells are already preconcentrated, this microfluidic device can be used to separate live cells from dead cells. This will be further discussed in Section 4.5.

CHAPTER 3

FABRICATION AND CHARACTERIZATION OF MAGNETIC

NANOPARTICLES

This chapter details the fabrication process for the magnetic nanoparticles used to separate bacteria from solutions. Experiments employing these fabricated nanoparticles are also described.

3.1 Fabrication of Magnetic Nanoparticles

To prepare magnetic nanoparticles in this study, the solvothermal reduction method published by Deng et al. in "Monodisperse Magnetic Single-Crystal Ferrite Monospheres" was utilized [34]. This method requires $FeCl_3$ to be reduced in the presence of ethylene glycol to Fe_3O_4 with the addition of heat and pressure. Sodium acetate is also required to stabilize the formed nanoparticles and to aid in the reduction process. Finally polyethylene glycol is used as a surfactant to reduce particle agglomeration. By modifying the quantities of reactants, changes in the size and surface characteristics of the nanoparticles were observed.

3.1.1 Altering Nanoparticle Size

3.1.1.1 Chitosan Coating

Fabrication of nanoparticles began by modifying the recipe set forth by Deng et al. through the addition of 1g of chitosan rather than 1g of polyethylene glycol. This polyethylene glycol was used primarily to keep the nanoparticles from agglomerating. However, it was decided to add chitosan instead due to the fact that this polymer typically yields a positive charge on the nanoparticle surface at certain pH values [35]. The

necessity of this positive charge is discussed in Section 3.2.1. The recipe for this mixture can be seen in Table 3.1.

Table 3.1 Nanoparticle recipe with 1g chitosan

	Amount
$FeCl_3 \cdot 6H_2O$	1.35g
Ethylene Glycol	40mL
Sodium Acetate	3.6g
Chitosan	1g

The entire mixture was stirred using a stir bar and stir plate for 30 minutes. Ten milliliters of the solution were autoclaved in a metal drum at 200℃ for approximately 15 hours.

After allowing the metal drum to reach room temperature, the black contents, formed nanoparticles, were washed with methanol several times. This was done using a magnetic separator from Invitrogen, as seen in Figure 3.1.

Figure 3.1 Magnetic separator [36]

The process of washing the nanoparticles can be seen in the diagram in Figure 3.2.
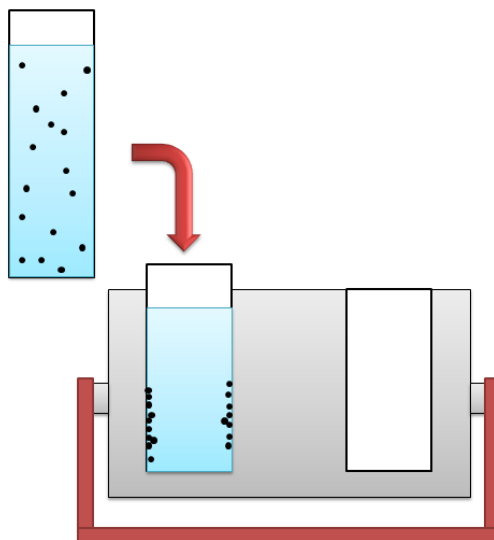
Figure 3.2 Magnetic nanoparticles being separated in magnetic separator

The magnetic separator employs extremely strong neodymium permanent magnets in its walls, with a magnetic field strength of approximately 4500 Gauss. As seen in Figure 3.2, the nanoparticles are dispersed in methanol. However, once they are placed in the magnetic separator, the nanoparticles separate from the carrier fluid and collect on the walls of the tube. Once the nanoparticles are collected on the sides of the tube, the supernatant can be carefully pipetted out of the tube, and the nanoparticles can be re-dispersed in fresh methanol. This process was repeated until the excess reactants were washed away from the nanoparticle solution.

Once the nanoparticle solution had been washed thoroughly, a sample could be viewed using a scanning electron microscope (SEM). A Hitachi 4700 SEM was employed to view all fabricated nanoparticles in this work. Approximately 3μL of the cleaned nanoparticle dispersion was placed on a TEM copper grid and allowed to dry in order to view the particles in the SEM.

The first set of nanoparticles prepared, with 1g of chitosan, can be seen in Figure 3.3.
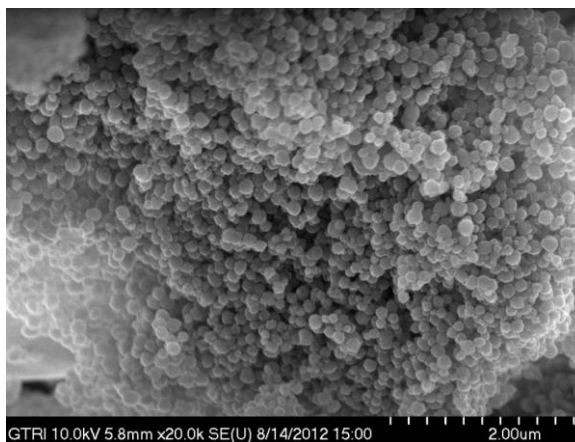
Figure 3.3 SEM image of magnetic nanoparticles with 1g chitosan

These nanoparticles appeared to be approximately 120-150nm in diameter. The particles were very uniform in size and shape. One noted characteristic of these nanoparticles was their adherence to the tube in which they were kept. Some of the nanoparticle solution would adhere to the tube, leaving what looked like a residue.

For this study, it was believed that larger particles would provide better bacteria capture efficiency because they would exert a larger force on the bacteria in the magnetic field. A typical *Salmonella* bacterium is approximately 2-5μm in length, and therefore, having larger particles attach to the cell should allow them to more easily drag it in a magnetic field.

The work by Deng et al. explained that their nanoparticle preparation would yield nanoparticles that were approximately 200nm in diameter after 8 hours, but if the mixture was kept in the oven at 200ºC for approximately 72 hours, they could achieve a particle diameter of 800nm. To test this assertion, 10 mL of the previous nanoparticle mixture was placed in the oven at 200ºC for approximately 63 hours. These nanoparticles can be seen in Figure 3.4.
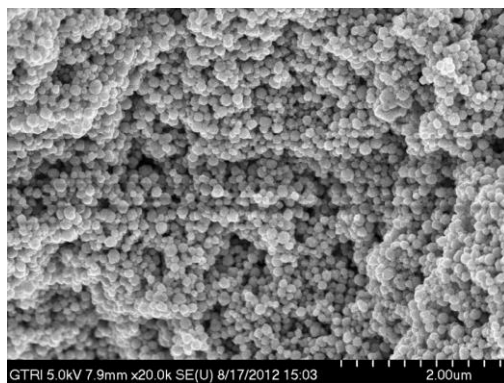
Figure 3.4 SEM image of magnetic nanoparticles with 1 g chitosan kept in oven for 63 hours

As can be seen from Figure 3.4, the nanoparticle diameter after almost three days in the oven is extremely similar to the nanoparticle diameter after only 15 hours in the oven, approximately 150nm.

3.1.1.2 Poly-L-Lysine Coating

The next coating to be added to the nanoparticle mixture was poly-l-lysine. This polymer was also chosen because it was thought to yield a positive zeta potential in neutral buffers [37]. The recipe for this mixture can be seen in Table 3.2.

Table 3.2 Nanoparticle recipe with 1mL poly-l-lysine

	Amount
$FeCl_3 \cdot 6H_2O$	1.35g
Ethylene Glycol	40mL
Sodium Acetate	3.6g
Poly-L-Lysine	1mL

This mixture was placed in an oven at 200ºC for approximately 20 hours. The resulting nanoparticles can be seen in Figure 3.5.
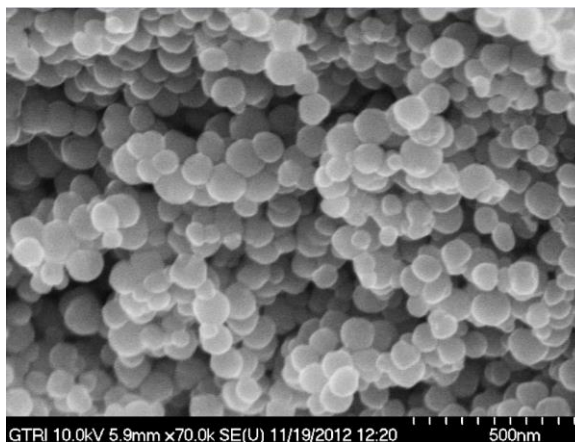
Figure 3.5 SEM image of magnetic nanoparticles with 1mL poly-l-lysine

As can be seen in Figure 3.5, these nanoparticles appear to have good uniformity and are between 110-150nm in diameter. The main attribute that was noticed from the addition of poly-l-lysine was that the nanoparticles separated much more quickly in the magnetic field than any other fabricated nanoparticles. Also, these particles did not adhere to the centrifuge tubes they were stored in.

3.1.1.3 No Coating

Since the nanoparticle diameter was unchanged by increasing its time in the oven, it was decided to prepare nanoparticles with no polymer coating, to see what type of size difference could be observed with the removal of polymer from the recipe. Therefore, nanoparticles were prepared using the recipe in Table 3.3.

Table 3.3 Nanoparticle recipe with no addition of polymer coating

	Amount
$FeCl_3 \cdot 6H_2O$	1.35g
Ethylene Glycol	40mL
Sodium Acetate	3.6g

Ten milliliters of this mixture were autoclaved in an oven at 200ºC for approximately 16 hours. The resulting nanoparticles can be seen in Figure 3.6.
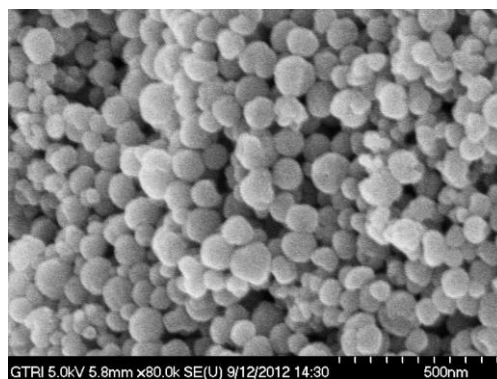
Figure 3.6 SEM image of magnetic nanoparticles with no polymer coating

From Figure 3.6, it can be seen that the nanoparticles still appear to be approximately 110nm in diameter. The uniformity of these nanoparticles is poor, compared to the chitosan-coated and poly-l-lysine-coated nanoparticles. It is obvious that the polymer coating had no effect on the nanoparticle size.

3.1.1.4 Changing Iron Content

Next, it was decided to continue fabricating uncoated nanoparticles, but change the quantity of the necessary chemicals. First, nanoparticles were fabricated with double the normal amount of $FeCl_3 \cdot 6H_2O$, in the hopes that adding more precursor material would allow more growth. The recipe for these nanoparticles can be seen in Table 3.4.

Table 3.4 Nanoparticle recipe with 2x Fe content

	Amount
$FeCl_3 \cdot 6H_2O$	2.7g
Ethylene Glycol	40mL
Sodium Acetate	3.6g

These nanoparticles were placed in an oven at 200ºC for approximately 20 hours. An image of the nanoparticles formed from this recipe can be seen in Figure 3.7.
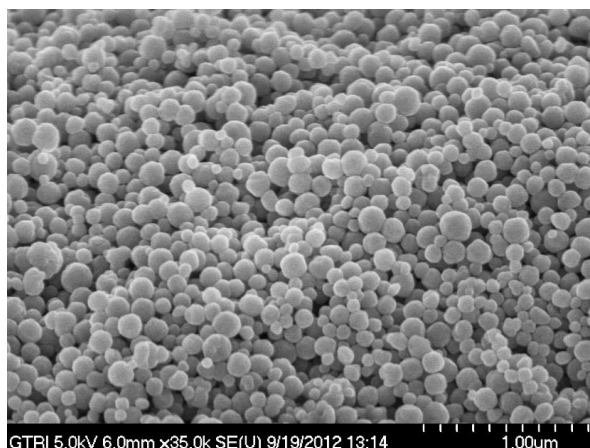
Figure 3.7 SEM image of magnetic nanoparticles with 2x Fe content

The uniformity of these nanoparticles is very poor. There are some particles that are close to 200nm and others that are less than 100nm. However, there is no appreciable difference in diameter from the nanoparticles prepared with the normal amount of Fe.

3.1.1.5 Changing Sodium Acetate Content

The next attempt to produce larger nanoparticles was to alter the amount of sodium acetate. Tables 3.5 and 3.6 show the next recipes that were used in the hopes of fabricating larger nanoparticles.

Table 3.5 Nanoparticle recipe with .5x sodium acetate content

	Amount
$FeCl_3 \cdot 6H_2O$	1.35g
Ethylene Glycol	40mL
Sodium Acetate	1.8g

Table 3.6 Nanoparticle recipe with 2x sodium acetate content

	Amount
$FeCl_3 \cdot 6H_2O$	1.35g
Ethylene Glycol	40mL
Sodium Acetate	7.2g

Both mixtures were placed in an oven at 200ºC for approximately 18 hours. Figure 3.8 shows the nanoparticles with half the normal amount of sodium acetate and Figure 3.9 shows the nanoparticles with double the normal amount of sodium acetate.
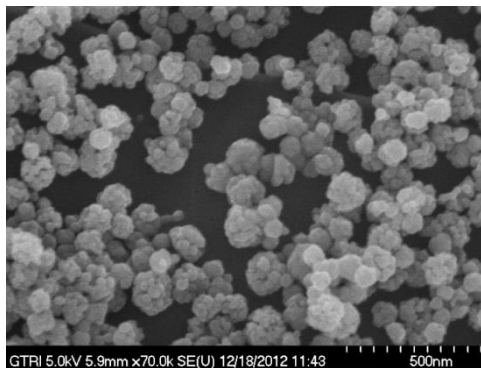
Figure 3.8 SEM image of magnetic nanoparticles with .5x sodium acetate content
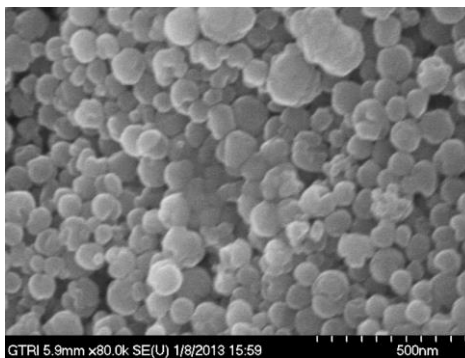
Figure 3.9 SEM image of magnetic nanoparticles with 2x sodium acetate content

As can be seen in Figure 3.8, the particles have a very rough surface, compared to all previously fabricated nanoparticles. It appears that reducing the sodium acetate content has a drastic effect on the surface characteristics of the particles, as well as particle uniformity. However, changing this chemical quantity did not affect the nanoparticle diameter. The particles still appear to be approximately 150 nm in average diameter.

On the other hand, doubling the amount of sodium acetate, as seen in Figure 3.9, yields particles with smooth surfaces and slightly better uniformity. The nanoparticles appear to be approximately 130nm in diameter on average.

Finally it was decided to determine nanoparticle characteristics if the recipe was modified to use only 10% of the normal amount of sodium acetate. This recipe can be seen in Table 3.7.

Table 3.7 Nanoparticle recipe with 10% sodium acetate content

	Amount
$FeCl_3 \cdot 6H_2O$	1.35g
Ethylene Glycol	40mL
Sodium Acetate	.36g

This mixture was placed in an oven at 200ºC for approximately 18 hours. However, no nanoparticles formed from this mixture after 18 hours. Therefore, it is obvious that the sodium acetate content is not only an essential part of controlling the surface characteristics of the particles, but also an integral ingredient for their formation. As the work by Deng et al. states, the sodium acetate is very important, along with the ethylene glycol, in the reduction of $FeCl_3$ to Fe_3O_4.

3.1.1.6 Adding Water to Nanoparticle Mixture

It was decided to add DI water to the nanoparticle mixture in place of half of the ethylene glycol to see what type of results would be seen. The altered nanoparticle recipe can be seen in Table 3.8.

Table 3.8 Nanoparticle recipe with addition of 50% DI water

	Amount
$FeCl_3 \cdot 6H_2O$	1.35g
Ethylene Glycol	20mL
DI water	20mL
Sodium Acetate	3.6g

This mixture was placed in an oven at 200℃ for approximately 20 hours. After the nanoparticle mixture was removed from the oven and allowed to cool to room temperature, it was discovered that the resulting nanoparticles were red in color. Up until this point, all fabricated nanoparticles had been black. These nanoparticles still exhibited magnetic properties. However, as time continued, the magnetic properties of the nanoparticles varied. At times, the particles separated very quickly in the magnetic field, and at other times, no separation could be seen. After washing the nanoparticles in methanol, a sample was viewed in the SEM. This sample can be seen in Figure 3.10.
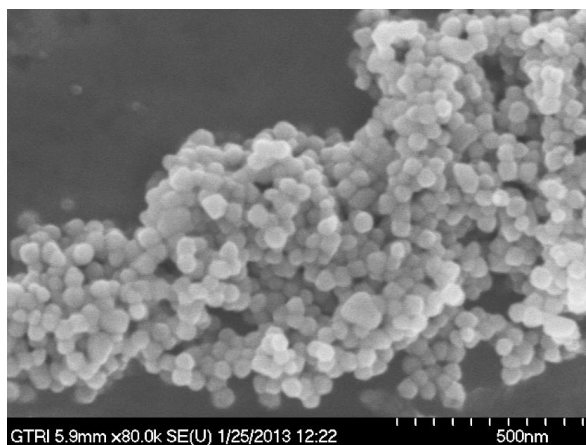
Figure 3.10 SEM image of magnetic nanoparticles with 50% DI water

As seen in Figure 3.10, these nanoparticles are smaller in diameter than all other nanoparticles fabricated thus far. They appear to be approximately 50-80nm in diameter. It can be seen that the nanoparticles appear to have smooth surfaces and decent uniformity.

It is possible that these nanoparticles are smaller because half of the reducing agent in the mixture, the ethylene glycol, was replaced with water. Therefore, the remaining ethylene glycol in the mixture was not able to reduce the $FeCl_3$ to Fe_3O_4 as effectively as with the normal amount, resulting in smaller nanoparticles.

3.1.1.7 Changing pH of Nanoparticle Mixture

The next step in modifying the nanoparticle recipe to achieve different size nanoparticles was to change the pH of the mixture. The pH of the mixture from Table 3.2 (the unaltered recipe by Deng et al.[34]) measured approximately 5.9. First the pH was changed to be more basic by introducing sodium hydroxide. NaOH was added to the mixture until a pH of approximately 8.5 was reached. Then, 10mL of the mixture were autoclaved at 200ºC for approximately 20 hours. The resulting nanoparticles can be seen in Figure 3.11.
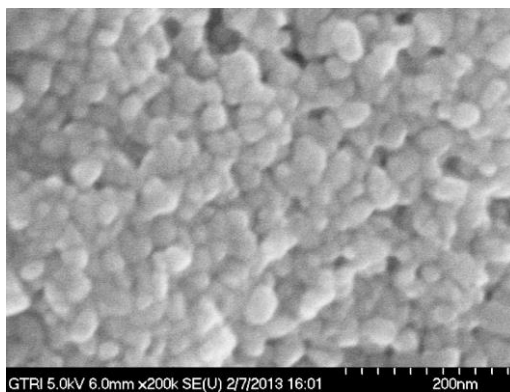
Figure 3.11 SEM image of magnetic nanoparticles with pH 8.5

The resulting nanoparticles were approximately 30-40nm in diameter. It was difficult to determine their size or even focus on them using the SEM because it appeared the electron beam was 'burning' the sample, as can be seen in Figure 3.12.
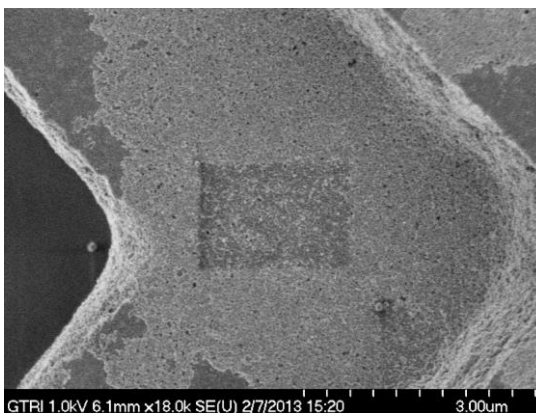
Figure 3.12 SEM image of magnetic nanoparticles with pH 8.5 changing color due to electron beam

As can be seen in Figure 3.12, there appears to be a darkened rectangle of nanoparticles in the sample. This appeared after focusing on this area for only a few seconds. It appeared as if the nanoparticles surface characteristics were changing under the beam. When inspecting this area of the film after it had darkened in color it almost seemed as if the particles were melting together. Even when reducing the voltage from 5kV down to 1kV, this problem was evident, as seen in Figure 3.12. This problem was only encountered with these nanoparticles. It is possible that these nanoparticles have a less stable structure than the previously fabricated batches of nanoparticles, and are more susceptible to the heat from the electron beam.

3.1.2 Changing Nanoparticle Shape and Magnetic Properties

An interesting discovery was made when lowering the mixture's pH. Acetic acid was added to the mixture recipe seen in Table 3.2 until a pH of approximately 3.8 was reached. Ten milliliters of this mixture were placed in an oven at 200°C for approximately 20 hours.

After removing this mixture from the oven and allowing it to cool to room temperature, it was discovered that the resulting particles were light yellow in color. Not only that, but these particles did not appear to exhibit any magnetic qualities when placed in the magnetic separator seen in Figure 3.1. In order to wash the sample of precursor materials, a centrifuge was utilized since the method in Figure 3.2 could not be used. After washing the sample, it was viewed using the SEM. The resulting particles can be seen in Figure 3.13.
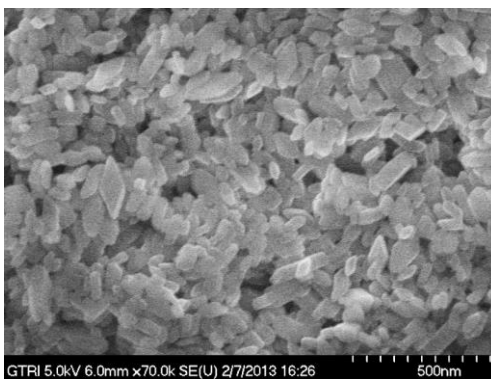
Figure 3.13 SEM image of particles with pH 3.8

As can be seen in Figure 3.13, the particles are no longer spherical, but instead appear rectangular and diamond-shaped. This change in shape simply by changing the pH of the mixture has been previously reported in the literature [38] [39]. It is possible that the structure of this iron oxide is different from previously fabricated nanoparticles. However, this would have to be verified using X-ray diffraction (XRD). Since these nanoparticles appeared to be only weakly magnetic, if magnetic at all, they were not used in any testing.

3.1.3 Polymer Coatings

The polymers to be tested on the nanoparticles were chitosan, poly-l-lysine and polyethyleneimine (PEI). PEI was not discussed due to the fact that it was only used in preliminary time experiments and discontinued. These coatings were chosen to change the surface charge of the nanoparticles from negative to positive. As can be seen in Tables 3.1 and 3.2, chitosan and poly-l-lysine were added to the initial mixture of nanoparticles before the mixture was placed into the oven in an attempt to coat them. However, another method of coating the nanoparticles with polymer was also attempted after the nanoparticles were formed. This was done by fabricating uncoated nanoparticles (Table 3.3) and then dispersing the nanoparticles in the desired polymer for a specific amount of time. The nanoparticles, in the polymer solution, were either placed in a sonication bath or vertical shaker for several hours to achieve a polymer coating.

46

3.2 Experimentation with Nanoparticles and Bacteria

3.2.1 Experimental Setup and Procedure

The bacteria types used, *Salmonella* specifically, have a negative zeta potential of approximately -17mV at pH 7 [3]. The nanoparticles were to be coated with polymers exhibiting positive zeta potentials at this pH, thereby creating an electrostatic attraction between the bacteria and the particles. For proper attachment of the nanoparticles and bacteria, they needed to be in contact for a certain period of time. In order to attach the nanoparticles to the bacteria sample, it was decided to place the nanoparticles and bacteria in a centrifuge tube and lay the tube on a horizontal shaker. By shaking the sample with the nanoparticles for a certain period of time, the nanoparticles were expected to attach to the bacteria due to electrostatic forces. The diagram in Figure 3.14 shows the expected outcome of shaking the nanoparticles and bacteria for a certain amount of time.
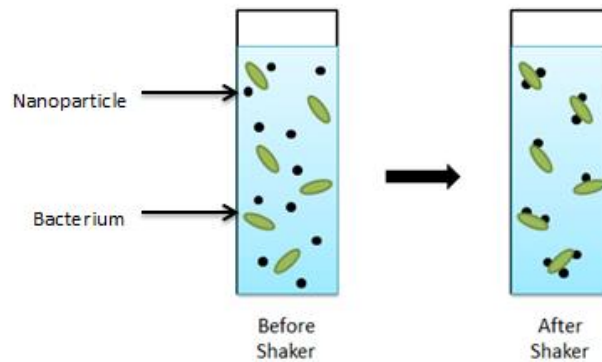
Figure 3.14 Nanoparticle and bacteria interaction before and after shaking sample

As can be seen from Figure 3.14, before shaking the sample, the nanoparticles and bacteria are separate and have not had the chance to interact and attach to one another. After a suitable amount of contact time on the shaker, however, the bacteria and nanoparticles have attached and therefore can be separated from the supernatant using the magnetic separator in Figure 3.2.

To perform a separation experiment, a specific dilution of magnetic nanoparticles and bacteria are placed in a centrifuge tube. A second centrifuge tube will be filled only with the specific dilution of bacteria. This tube will serve as a control experiment. Both centrifuge tubes are laid on the horizontal shaker for a certain period of time. After that time, both tubes will be placed in the magnetic separator as seen in Figure 3.2. After approximately 45 seconds, to allow the bacteria-nanoparticle aggregates in the experimental tube to separate, 100µL samples are pipetted from the center of each tube and plated. 100µL samples are also diluted appropriately and plated for quantification purposes. The control tube yields the starting concentration of bacteria in the two tubes and serves as a comparison for the tube with nanoparticles. This process can be seen in Figure 3.15.
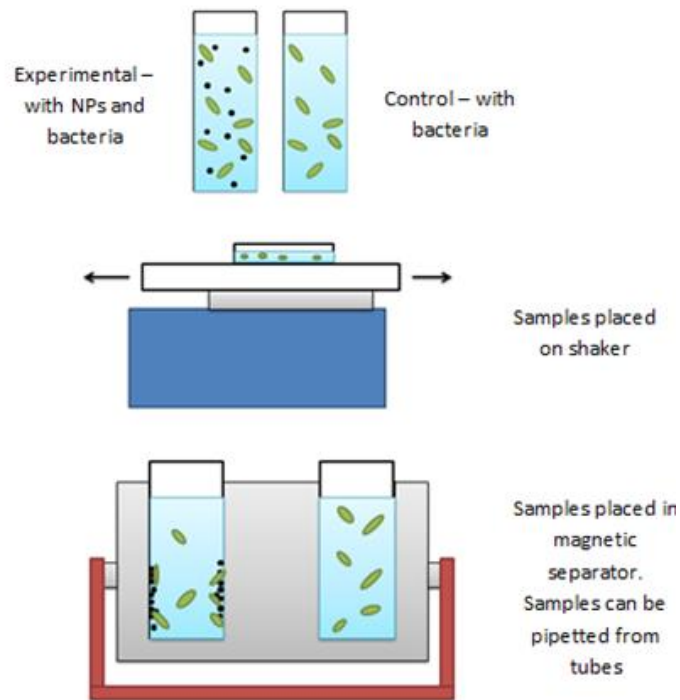
Figure 3.15 Diagram of experimental procedure using shaker

3.2.2 Preliminary Experiments

Preliminary experiments did not use calculated concentrations of nanoparticles. Instead, a tube with an unknown concentration of nanoparticles in a known volume of

buffer was used. These preliminary experiments mainly focused on determining the optimal contact time needed between the nanoparticles and the bacteria to yield the best capture efficiency. Therefore, nanoparticle concentrations were determined by comparing the volume of the nanoparticle dispersion used in each experiment. As long as this particular dispersion of nanoparticles was used, the experiments could be directly compared to each other. The experiment in Figure 3.15 was used, varying the time on the shaker. Experimental contact times were 10 minutes, 30 minutes, 60 minutes, and 120 minutes. The results of this testing with PEI-coated nanoparticles can be seen in Figure 3.16.
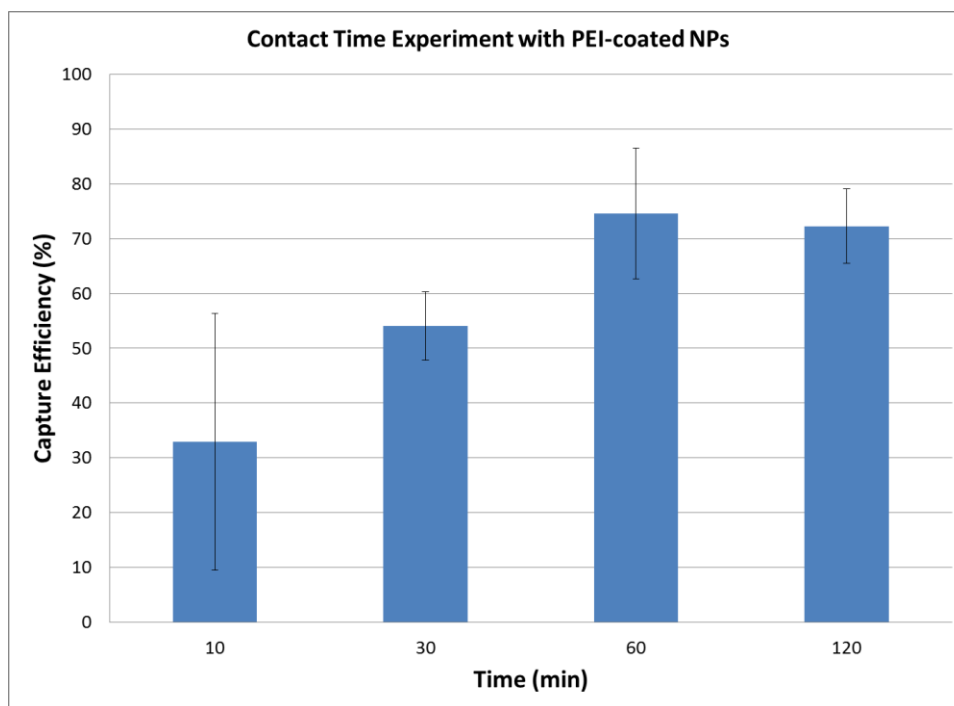
Figure 3.16 Results of contact time variation test with PEI-coated NPs

From Figure 3.16, it can be seen that one hour on the shaker yields a significantly better capture efficiency than 30 minutes. However, after one hour, the capture efficiency actually decreases. This trend was also seen using poly-l-lysine-coated nanoparticles, as can be seen in Figure 3.17.
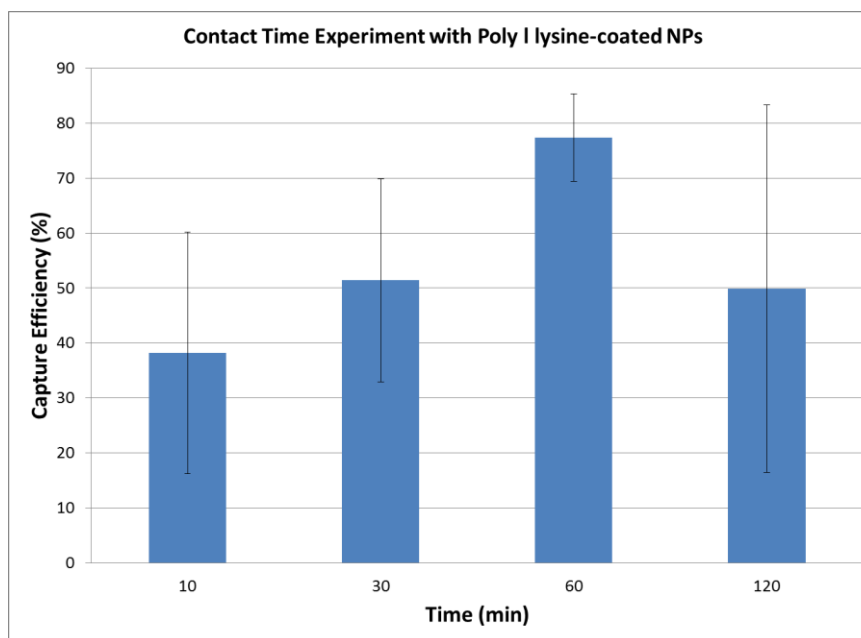
Figure 3.17 Results of contact time variation test with Poly-l-lysine-coated NPs

Several time variation tests were conducted in this fashion before deciding that the one hour duration yielded the best capture efficiency. Therefore, for all future experiments, the contact time of the nanoparticles and the bacteria on the shaker was 60 minutes.

3.2.3 Measuring Nanoparticle Concentration

In order to quantify the concentration of nanoparticles used in each experiment, a simple calculation was employed. The volume of a sphere is known as

$$V_{sphere} = \frac{4}{3}\pi r^3 \tag{3-1}$$

where r is the radius. This calculation can be used to determine the volume of one nanoparticle. The radius of the nanoparticle was determined from SEM characterization from each batch of nanoparticles. The average radius was used in this concentration estimation. Using the nanoparticles from Figure 3.5 (poly-l-lysine), the average radius was determined to be approximately 75nm. Plugging this into Equation 1 yields

$$V_{NP} = \frac{4}{3}\pi r^3 = \frac{4}{3}\pi(75 \times 10^{-9}m)^3 = 1.767 \times 10^{-21}m^3$$

Next the density can be assumed to be that of magnetite (Fe_3O_4) which is approximately 5g/cc. This can be plugged into Equation 3-2, along with the calculated volume to determine the mass of an individual nanoparticle.

$$\rho = \frac{M}{V} \qquad (3\text{-}2)$$

In Equation 2, ρ is density, M is mass, and V is volume. Plugging in the known quantities yields

$$5000000\frac{g}{m^3} = \frac{M}{1.767 \times 10^{-21}m^3}$$
$$M_{NP} = 8.836 \times 10^{-15}g$$

Therefore in 1mg, the number of nanoparticles can be estimated as

$$\frac{.001g}{8.836 \times 10^{-15}g} = 1.13 \times 10^{11} \, nanoparticles$$

To use this estimation, the nanoparticles can be weighed and dispersed in a known quantity of buffer, therefore allowing the concentration of nanoparticles to be known. To weigh the nanoparticles accurately, they must be dried. To dry the nanoparticles, they were stored in a small glass vial and placed in an oven at 60°C for approximately 20 hours. For all experiments, 10mg of nanoparticles was dispersed in 10mL of buffer. This dispersion was left in a vertical shaker for 24 hours to break up any clusters of dried nanoparticles. If large clusters remained, the dispersion was placed in a sonication bath for up to four hours.

3.2.4 Determining Bacteria-Nanoparticle Ratio

In this study it was important to determine the necessary bacteria-NP ratio to get the best possible capture efficiency. To do this, the experiment shown in Figure 3.15 was

used. The bacteria sample was diluted to 10^5CFU/mL in pH 6. Ten milliliters of this bacteria solution were placed in both the experimental tube and the control tube. Therefore, there were a total of approximately 10^6CFUs in each tube. Next, the poly-l-lysine-coated nanoparticles (corresponding to 'D' in Figure A.1 in Appendix A) were added to the experimental tube to reach a desired concentration. The nanoparticle concentrations to be tested were 10^5x the bacteria concentration, 10^4x the bacteria concentration, 10^3x the bacteria concentration, and 100x the bacteria concentration. The experimental and control tubes were placed on the shaker for one hour. Then samples were taken from each tube, diluted appropriately, and plated using the magnetic separator method seen in Figure 3.15. The results of this concentration testing can be seen in Table 3.9.

Table 3.9 Results of nanoparticle concentration testing, experiment 1

NP Concentration Compared to Bacteria Concentration	No NPs Average	No NPs σ	With NPs Average	With NPs σ	Efficiency (%)
100x	104	13.4	110	14.1	-
10^3x	99	1.4	76	1.4	23.2
10^4x	89	19.8	25	2.8	71.9
10^5x	73	17.7	6	4.2	91.8

This test showed that the greater the nanoparticle concentration, the greater the capture efficiency. However, a plateau was not reached, where all the cells are captured by the nanoparticles. Therefore, further testing was performed.

The previous experiment was repeated using nanoparticle concentrations of 10^5x the bacteria concentration, 10^6x the bacteria concentration, and 10^7x the bacteria

concentration. Samples were diluted appropriately and plated. The results of this testing can be seen in Table 3.10.

Table 3.10 Results of nanoparticle concentration testing, experiment 2

NP Concentration Compared to Bacteria Concentration	No NPs Average	No NPs σ	With NPs Average	With NPs σ	Efficiency (%)
10^5x	95	0	9	7.1	90.5
10^6x	82	3.5	6	3.5	92.7
10^7x	98	5.5	14	1.2	85.7

It appears that increasing the nanoparticle concentration does not allow full capture of bacteria. However, the capture efficiency seen from this experiment is still very impressive. Testing continued using a ratio of 10^5 nanoparticles to every bacterium.

After this experiment was completed, the experimental tube containing nanoparticles and bacteria was autoclaved, to kill the bacteria. Then a sample from this tube was viewed using a scanning electron microscope (SEM) in order to observe exactly how the nanoparticles attached to the bacterium's surface. Figure 3.18 shows the results of this SEM analysis.

GTRI 6.0mm ×7.00k SE(U) 1/24/2013 11:57   5.00um
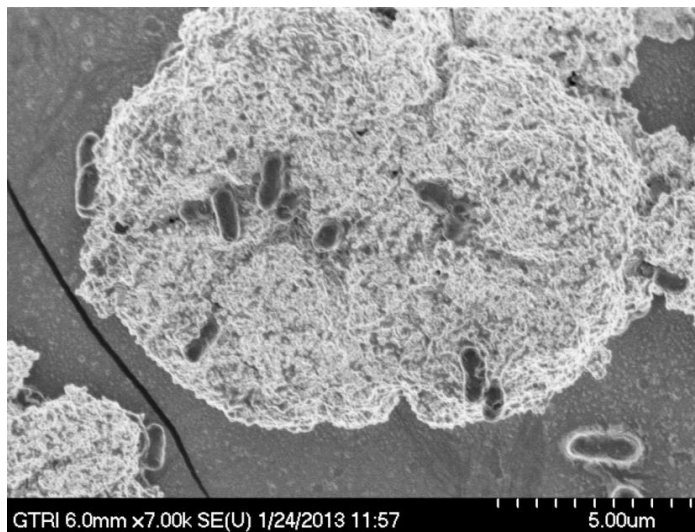
(a)
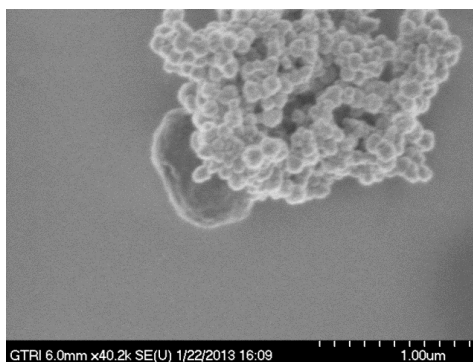
(b)
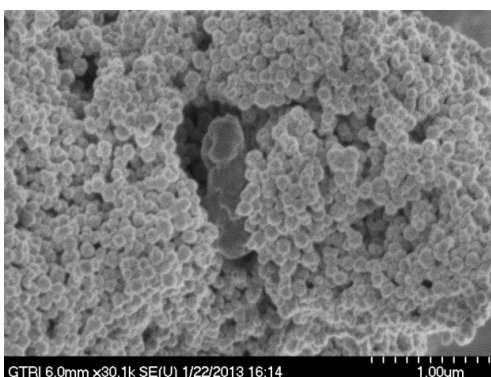
(c)

Figure 3.18 SEM images of bacteria and nanoparticles

Figure 3.18 (a) shows a very large cluster of nanoparticles with several bacteria attached on the cluster's surface. Figure 3.18 (b) shows a bacterium attached to a smaller cluster of nanoparticles, and Figure 3.18 (c) shows a bacterium that seems to be encapsulated by nanoparticles. From these images, it can be seen that the bacteria do not seem to be covered in nanoparticles, as was expected. Instead it seems as if the nanoparticles are agglomerating into large masses, and the bacteria are attracted to these clusters. However, it is possible that these clusters are a result of the autoclaving process or the SEM sample preparation process. In order to prepare a sample for the SEM, a small sample of the experimental tube is dried on a transmission electron microscope (TEM) copper grid. What is seen in Figure 3.18 is the result of this drying process.

3.2.5 Varying Buffer Ionic Strength

Thus far, all experiments have used buffers with an ionic strength of 20mM. It was decided to perform an experiment to determine what effect ionic strength had on capture efficiency. The experiment from Figure 3.15 was used. The nanoparticles corresponding to 'D' in Figure A.1 in Appendix A (poly-l-lysine coating) were used, along with a bacteria concentration of 10^5CFU/mL. The nanoparticles were placed on the shaker for one hour. Then samples were taken, diluted appropriately, and plated, using the magnetic separator method seen in Figure 3.15. The ionic strengths tested were 1mM, 10mM, 20mM, and 100mM for pH 6. The results of this testing can be seen in Table 3.11.

Table 3.11 Results of varying buffer ionic strength

Ionic Strength	No NPs Average	No NPs σ	With NPs Average	With NPs σ	Efficiency (%)
1mM	121	5.7	3	2.1	97.5
10mM	121	41.0	5	2.1	95.9
20mM	104	22.6	7	0.7	93.3
100mM	91	12.7	9	5.7	90.1

From Table 3.11, it can be seen that the lower the ionic strength, the better the capture efficiency. By altering the buffer's ionic strength, the capture efficiency of the bacteria is very close to 100%.

3.2.6 Alternative Efficiency

When determining bacteria capture efficiency for the nanoparticles, it is determined by comparing the number of bacteria plated from the control samples to the number of bacteria plated from the experimental samples. The control samples have no nanoparticles and should experience no separation when placed in the presence of a

magnetic field. Therefore the control samples plated should yield the corresponding starting concentration of bacteria in the control and experimental tubes.

However, it was decided to take samples from the experimental tube outside of the magnetic separator to serve as the 'control' samples. This was due to the fact that the control tube and experimental tube do not necessarily contain the same concentration of bacteria. There can be a variation in concentration. Therefore, taking samples from the same tube inside and outside the magnetic field will yield more information about the experiment. It will ensure that if a low concentration of bacteria is seen when in the presence of the magnetic field, it is due to the separation of the nanoparticles and not due to the fact that the tube may have held a lower concentration of bacteria. This is because when samples are taken outside the magnetic field, they should show the corresponding starting concentration of bacteria that was placed in the tube to begin with, since there is no separation phenomenon taking place. Then the sample taken in the magnetic field can be directly compared to the sample taken outside the magnetic field. This alternative method of determining capture efficiency will also ensure that the nanoparticles are not simply killing the bacteria, resulting in a lower concentration of bacteria.

3.2.7 Comparing Nanoparticle Capture Efficiencies

After determining the optimal contact time and bacteria-NP ratio, testing of each type of nanoparticle was done using the procedure in Figure 3.15. A chart of the nanoparticles tested and their capture efficiencies can be seen in Figure A.1 in Appendix A. The capture efficiency and alternative capture efficiencies can both be seen.

It appears the nanoparticles with half the normal amount of sodium acetate, double the amount of sodium acetate, and those with a pH of 8.5 yield capture efficiencies of above 90%. The poly-l-lysine coating and uncoated nanoparticles yield capture efficiencies between 80-90%. The chitosan coating and PEI coating appear to yield decent capture efficiencies, approximately 60-70%. It seems that changing the

nanoparticle recipe results in better capture efficiency than adding a polymer coating. This could indicate that the polymer coating is not attaching well to the nanoparticle surface.

3.2.8 Comparing *Salmonella* and *E. coli*

The nanoparticles were primarily tested with *Salmonella typhimurium*. However, it was decided to experiment with *E. coli* as well to see if similar results could be attained. The experiment with *Salmonella*, seen in Figure 3.15, was repeated with *E. coli* as well. The same contact time and ratio of nanoparticles to bacteria were used. The results of one of these experiments can be seen in Table 3.12. Further *E. coli* test results can be seen in the chart in Figure A.1 in Appendix A.

Table 3.12 Results of *E. coli* testing compared to *Salmonella* testing

Bacteria type	No NPs Average	No NPs σ	With NPs Average	With NPs σ	Efficiency (%)
Salmonella	53	2.1	3	1.5	94.6
E. coli	64	25	48	7.2	25

It can be seen from Table 3.12 that the capture efficiency for *Salmonella* is above 90%. However, the capture efficiency for *E. coli* is extremely low, approximately 25%. It seems that this capture method is specific to *Salmonella*.

3.2.9 Zeta Potential Measurements

To determine the surface charge of the nanoparticles as well as the bacteria, their zeta potential was measured using a Malvern Instruments Zetasizer Nano. The zeta potential is a good indicator of the degree of repulsion between similarly charged particles [40]. The zeta potential of *Salmonella* was experimentally determined to be approximately -10mV in pH 6, the buffer used for all experiments.

It was known that the nanoparticles have a negative charge when they're formed without the addition of a polymer because the sodium acetate will act as the capping material and yield a carboxyl group on the nanoparticle surface. The intention of adding the polymer coating is that it will electrostatically attach to this negative surface and produce a positively charged nanoparticle surface.

After formation, each type of nanoparticle was tested in the Zetasizer to determine its zeta potential. The results can be seen in Figure A.1 in Appendix A. Each nanoparticle's zeta potential was determined in the same buffer, pH 6. The zeta potential of each nanoparticle was measured numerous times to determine how it changed over time.

From this chart, it can be seen that all the nanoparticle's zeta potentials appear to be negative. The nanoparticles in rows 'C' and 'F' begin positive, but become negative and stay negative. This means that the method of bacteria capture cannot be electrostatic capture but some other type of attraction.

The zeta potentials of each type of nanoparticle vary each time it is taken. The nanoparticles do not appear to be very stable. For the nanoparticles with polymer coatings, this is an indication that perhaps the polymer is not attaching well to the particle. However, this is also seen by those particles with no polymer coating.

3.3 Discussion

In this chapter, several important issues arose. First of all, the nanoparticle diameter could not be increased above 200nm, even though the work the recipe was based on reported particles close to 800nm. The procedure from the literature was followed and still, the particle diameter appeared to be approximately 150nm. A possible reason for this discrepancy is the fact that the work used a metal drum with a capacity of 50mL for their mixture to be placed into the oven. In this work, only 10mL were placed in the oven at any given time. The growth of the nanoparticles is a nucleation process,

and therefore, changing the amount of available reactant materials will affect the size of the particles formed. Since the entire mixture could be placed in the oven for the nanoparticles reported in the literature, it is possible that the nucleation process continued for a longer duration, resulting in larger particles.

Even when increasing the amount of iron used in the nanoparticle mixture, no significant increase in diameter was observed. It seems that the nanoparticle size can also be attributed to the amount of sodium acetate used in the mixture because it serves as the capping material. Once the formed particle is capped by the sodium acetate, the nucleation process is halted. Therefore, a lower amount of capping material was utilized, as shown in Table 3.5. The hypothesis was that by lowering the amount of this material, the particles would be free to grow larger before the nucleation process was ended. However, as can be seen in Figure 3.8, lowering the amount of sodium acetate had a drastic effect on the surface characteristics of the formed particles, rather than on its size. The reasoning behind this is unclear, due to the fact that much of the nucleation process is complex and not well understood. However, increasing the amount of capping material may yield more information. Although the amount of sodium acetate was doubled without much change in diameter, a future experiment will be to drastically increase the amount of sodium acetate. The theory is that if there is a significantly large amount of this chemical, the nanoparticles will begin to nucleate and be capped right away, resulting in extremely small particles. This experiment will help to better explain the sodium acetate's role in particle formation.

As for the role of changing pH or water content to change the behavior and shape of the formed particles, this phenomenon has been published in the literature. The work by Cho et al. claims that by altering the water-to-ethylene glycol content, the shape and size of the nanoparticles can be changed [39]. Although only one experiment was done to change the water-to-ethylene glycol ratio in this study, the results were very obvious. The nanoparticle diameter was reduced by 50%. The work by Matijevic and Cimas states that

any small change in the process parameters, such as temperature or pH, will have extreme effects on the resulting particles [38]. This can be seen in this work, when the pH of the mixture was reduced. The resulting particles were diamond and rectangular in shape, rather than spherical. Also, when the mixture pH was increased, the resulting particles were about one-third the size of previously fabricated nanoparticles. Therefore it is obvious that any changes in process conditions will have significant effects on particle formation.

Another issue that arose in this work was the polymer attachment to the nanoparticles. The assumption was that the polymer would electrostatically attach to the nanoparticle surface. In the work by Deng et al. the surfactant, polyethylene glycol, was simply added to the mixture and placed in the oven, to coat the nanoparticles. This method was used in this work with both chitosan and poly-l-lysine. The behavior of the resulting particles with poly-l-lysine added to the mixture indicated that they were indeed coated with a polymer. The nanoparticles dispersed easily in liquid and did not adhere to the tubes in which they were kept, as the uncoated nanoparticles did. However, the zeta potential of these nanoparticles was negative, indicating that the polymer was not sufficient to change the particle surface charge. Poly-l-lysine should have a positive zeta potential at pH values below 9. It is possible that the polymer is not effectively coating the particles, or is not stable enough to remain on the nanoparticle for a long period of time. Another possibility is that other molecules may be adsorbing onto the nanoparticle after the polymer is attached, effectively changing the nanoparticle surface charge to negative once more. It also appears that the effect of the polymer, specifically poly-l-lysine, varies greatly depending on when the addition of polymer occurs. For example, according to Figure A.1 in Appendix A, the nanoparticles with poly-l-lysine added to the mixture and then placed in the oven (listed as 'poly-l-lysine before') yields a better capture efficiency than the nanoparticles that were formed with no coating and then had polymer added to them after they were formed (listed as 'poly-l-lysine after'). Perhaps

the addition of heat and pressure plays an important role in the behavior of the polymer. In the future, the nanoparticles can be characterized for their coating using Fourier transform infrared spectroscopy (FTIR). This technique measures how a sample absorbs light at different wavelengths, to determine what materials are present. By performing this analysis, it can be effectively determined if the polymer coating is present on the nanoparticles. In this study, it appears the polymers play a minimal role in the particle formation, as well as the particle-bacteria attachment. Therefore a new method of attaching the polymer to the nanoparticle may be required.

This brings up another issue encountered in this chapter, which is the bacteria-nanoparticle attachment. If the nanoparticles have a negative surface charge, then it is known that the attachment method between the nanoparticles and bacteria is not an electrostatic interaction. However, all nanoparticles tested in this study exhibited a capture efficiency of above 50%. The capture efficiency of the nanoparticles with altered sodium acetate contents showed capture efficiencies of above 90%. The impressive results of many types of nanoparticles were consistently repeated in multiple experiments. Thus, there is some type of attraction between the bacteria and nanoparticles that is not fully understood. It is certainly possible that the nanoparticles agglomerating into very large clusters are better able to attract, hold, and drag the bacteria in a magnetic field. There have been works published which detail the attachment of *Salmonella* to materials such as magnetite [41]. This work, by Stenstrom, claims that the negative charge associated with *Salmonella* plays no part in the adhesion of the cell to the particle. This interaction between the bacteria and the particles must be further researched to discern how exactly the bacteria is being pulled by these nanoparticles in the presence of the magnetic field. As of now, it appears that nanoparticles with rough surfaces, such as those seen in Figure 3.8, yield a very impressive capture efficiency. If the method behind this attachment was understood, the nanoparticle's surface characteristics could be altered as seen in Section 3.1 to cater to this interaction more favorably.

Lastly, an important concern from the experiments performed in this chapter is that these nanoparticles only appear to have a successful capture efficiency with *Salmonella*. When tested with *E. coli*, several types of nanoparticles showed an extremely low capture efficiency. This was unexpected because *E. coli* also exhibits a negative zeta potential in neutral pH's. This shows that the attachment method of the nanoparticles is very specific to *Salmonella*. Since the attachment method of the nanoparticles to *Salmonella* is not well understood, it is difficult to determine why other types of bacteria do not demonstrate such impressive results. In the work "Amine-Functionalized Magnetic Nanoparticles for Rapid Capture and Removal of Bacteria Pathogens" by Huang et al., an excellent capture efficiency for *E. coli* is presented, approximately 97% [22]. However, the capture efficiency for *Salmonella* in this work is only 55%. Therefore, it seems that the attachment process is very different for these two bacteria, no matter how similar their structure may seem. Once the attachment method can be sufficiently understood, it will be possible to alter the nanoparticles to achieve successful capture for many types of bacteria. This way, they can be more readily used in a variety of real world applications.

CHAPTER 4

PROTOTYPE DESIGN, IMPLEMENTATION, AND

CHARACTERIZATION

This chapter details the development of a continuous system for bacteria separation using the nanoparticles discussed in Chapter 3. The batch processing of water samples, as seen in Chapter 3, can become more efficient by designing a system that can continuously separate and re-suspend bacteria, rather than separate small volumes of bacteria that are already very concentrated. The experiments in Chapter 3 allowed the nanoparticles' efficiency to be characterized, as well as determined the optimal bacteria-to-nanoparticle ratio and contact time necessary to achieve the highest capture efficiency. Once these parameters were established, they could be included in the design of a prototype.

4.1 Prototype Concept

The goal of this continuous flow system is to 'clean' the water or other fluid that will pass through it, while also collecting and re-suspending the bacteria from the 'cleaned' fluid. Since this system will be employed for preconcentration purposes, it is important to be able to re-suspend these bacteria cells in very small volumes of liquid. The device will utilize the nanoparticles as the capture method of the bacteria, and therefore will require the use of a magnetic field that can be turned on and off with precision. To simplify the system, it was decided to focus on efficient separation of the bacteria, and use pre-mixed volumes of bacteria and nanoparticles. In the future, the mixing of bacteria and nanoparticles will take place within the device.

In order to continuously clean liquid as well as re-suspend the bacteria-nanoparticle aggregates that are collected using a magnetic field, it was decided to use a

three way valve. Two steps would be involved in using this system. The first valve position can be seen in Figure 4.1.
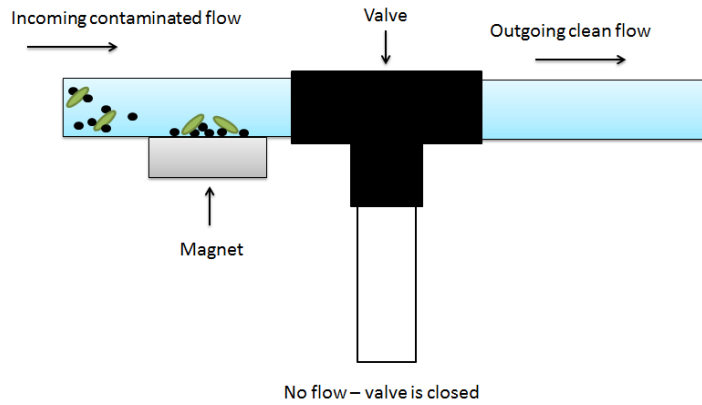
Figure 4.1 First valve position for prototype design

On the left inlet of the figure, the contaminated flow, consisting of bacteria and nanoparticles, is introduced to the system. Just before the valve, a magnetic field is produced by a permanent magnet. As the contaminated flow passes through the magnetic field, the bacteria-nanoparticle aggregates will be attracted to the magnet and thus be separated from the flow entering the valve. Therefore, the liquid passing through the valve and exiting through the outlet on the right of the figure will be cleaned.

The second step of the design will utilized the second position of the valve. This can be seen in Figure 4.2.
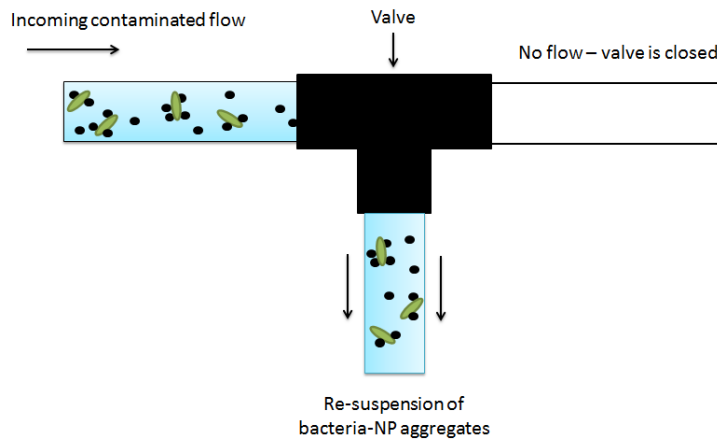
Figure 4.2 Second valve position for prototype design

The contaminated flow is seen entering the device from the left, as was seen in Figure 4.1. However, it can be seen that the magnet has been removed. Once the magnet has been removed, all previously captured bacteria will be released into the flow entering the valve. To ensure that this contaminated flow does not re-contaminate the cleaned liquid, the flow is re-directed to the second outlet of the device, as seen in Figure 4.2. This corresponds to position 2 of the valve.

This method of cleaning the fluid in the presence of the magnetic field and re-suspending the captured bacteria in the absence of the magnetic field is the basis of the proposed design. Once the desired re-suspension volume is reached, the magnetic field can be replaced and the valve can be turned back to position one, allowing liquid to be cleaned once again. This process can be repeated, allowing the system to continuously clean the liquid and re-suspend the bacteria.

To ensure that the re-suspended volume of bacteria-nanoparticle aggregates is as small as possible, it is important to ensure that the magnetic field is as close to the valve as possible. This is because when the magnetic field is removed and valve position two is in place, the re-suspension volume will be approximately the volume of the tube where the magnetic field previously was. This can be seen in Figure 4.3.
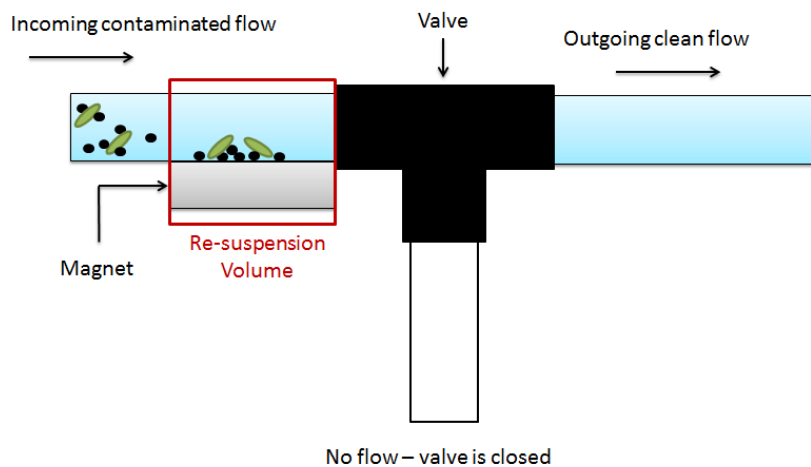
Figure 4.3 Diagram of theoretical re-suspension volume when magnet is removed

The assumption is that once the valve is turned to position two, the magnetic field will be removed, and the incoming contaminated flow will push the boxed portion of liquid in Figure 4.3 through the valve into the re-suspension volume. The magnet can then be replaced and the valve can be returned to position one, again cleaning the fluid. The re-suspended volume can either remain in place, to collect the next batch of contaminated liquid, or it can be replaced with an empty container, to ensure that the re-suspension volumes remain as small as possible.

Since the re-suspension volume depends on the volume of the tube where the magnetic field is applied, the tube diameter is an important parameter when designing this system. The tube diameter also relies on the magnet used. If the magnetic field of the magnet is not strong enough to quickly attract bacteria-nanoparticle aggregates from across the width of the tube, the system will not collect all the bacteria in the contaminated flow. These parameters must be carefully considered to ensure the prototype works efficiently and effectively.

4.2 Materials and Completed Design

To begin implementation of this design, appropriate materials and equipment had to be chosen. The first consideration was to decide what type of pump would be employed. For demonstration purposes, one liter of liquid would be separated at any given time. However, in the future, larger volumes will be separated by this device, such as tens of liters. Therefore, a syringe pump would not work. However, a peristaltic pump is simple to use, inexpensive, and can pump larger volumes, depending on the tubing diameter and pump head on the pump driver. It is important to note that this pump will not damage cells passing through it, as the cells are much too small for the peristaltic action to affect them in any significant way.

Next, materials were selected for the tubing and valve. It was important to select materials that are resistant to bleach, as this was the method to clean all surfaces after

each experiment. Therefore, chemical-resistant clear PVC tubing was selected for the prototype. The tubing will not degrade when used with bleach and is clear, offering a view of nanoparticle separation when the magnetic field is in place. PVC was also chosen as the material for the three-way valve, to allow proper cleaning of this surface as well. The tubing and valve diameters were chosen based on the flow rate the chosen pump would be able to produce. The pump head used tubing with an outside diameter of approximately 3/8 inch (0.0095m). Therefore, tubing with an inner diameter of 3/8 inch was chosen for the tubing of the rest of the prototype. This would allow the pump head tubing to fit snugly inside the prototype tubing. This tube diameter is small, but would achieve an acceptable flow rate of approximately 3.03×10^{-6} m^3/s, or approximately 1 liter in 5 minutes. In the future, a larger pump can be used, which will achieve a higher flow rate, yielding more cleaned liquid in a given amount of time.

Finally, the magnet had to be chosen. Ideally, an electromagnet would be utilized. This would allow the automation of the magnet field from the on position to the off position. For demonstration of concept purposes, a permanent bar magnet was chosen. These magnets are inexpensive and allow multiple lengths and magnetic field strengths to be tested. The magnet material used was neodymium, which is the same material that was used in the magnetic separation seen in Figure 3.1. These magnets are extremely strong, yielding a maximum field strength of approximately 1.45T, when used in pairs of two. The dimensions of this magnet were determined from calculations in Section 4.3.

The final prototype utilizing these materials can be seen in Figure 4.4.
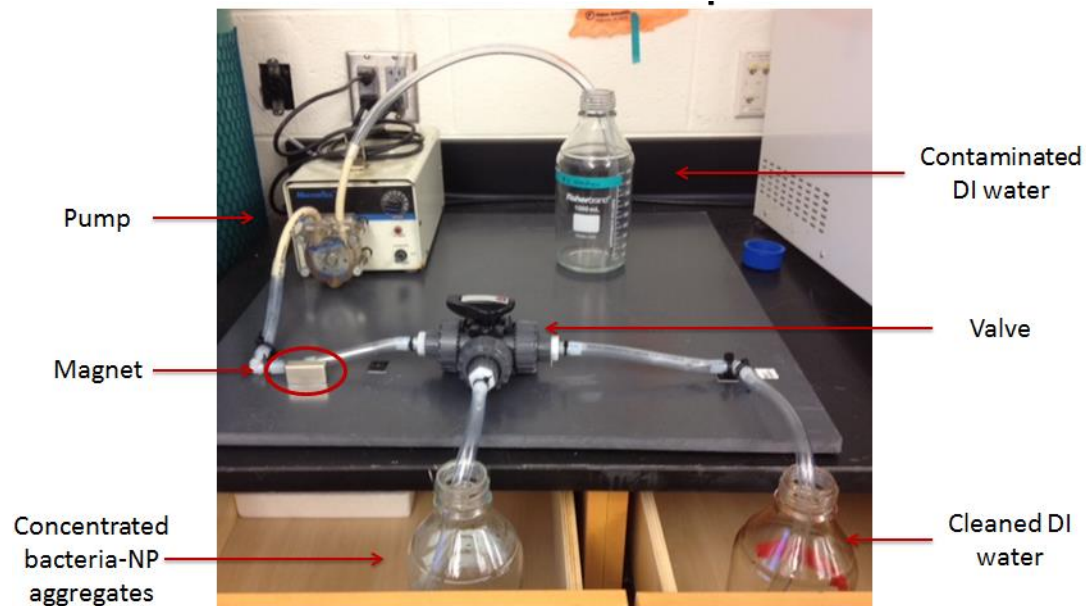
Figure 4.4 Final prototype

Glass bottles were used to hold the contaminated DI water, the re-suspension volume of bacteria-nanoparticle aggregates, and the cleaned DI water. The pre-mixed volume of bacteria and nanoparticles is labeled as the contaminated DI water. This volume is pumped through the pump head, past the magnet, and into the valve. The cleaned fluid will flow into the cleaned DI water bottle. When the valve is turned and the magnet is removed, the bacteria-nanoparticle aggregates will then flow into the contaminated bacteria-nanoparticle aggregates bottle.

Only one magnet is seen in Figure 4.4, to show the placement of the magnetic field. However, two magnets were used. The tubing is very flexible, and if the magnets were placed directly opposite to each other, the tubing would be forced closed by the magnets' attraction to each other. Therefore a redundant system was used, as seen in Figure 4.5.
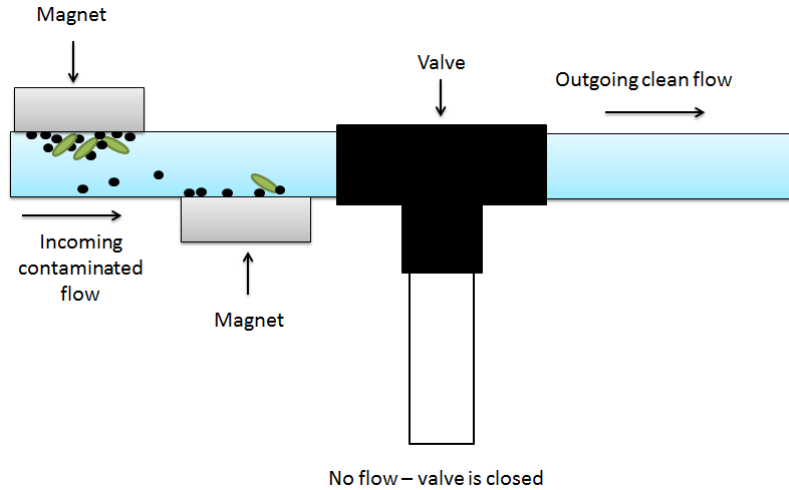
Figure 4.5 Use of two magnets in prototype

As can be seen in Figure 4.5, the magnets are placed slightly staggered. This method allows the capture of bacteria-nanoparticle aggregates that may have passed through the first magnetic field without being captured. This is possible because, as the first magnet begins to attract large amounts of bacteria-nanoparticle aggregates, its surface becomes clogged, and this lessens its pull on future nanoparticles passing through the system. Therefore, by introducing a second magnet, capture of remaining bacteria-nanoparticle aggregates is possible.

4.3 Calculations

To determine the dimensions of the magnet that would be necessary to capture the nanoparticles in a moving fluid, it was necessary to determine the time it will take for the nanoparticles to separate in the presence of the magnetic field, and the axial distance it will take for the nanoparticle to reach the wall of the tube (where the magnet is placed). This magnetic force was determined using an equation set forth by Zhang et al. [42].

$$F_{mag} = \frac{\Delta\chi V_{MNP} \nabla B \cdot B}{\mu_0} \qquad (4\text{-}1)$$

In Equation 4-1, F_{mag} is the magnetic force on the nanoparticle due to the magnetic field, $\Delta\chi$ is the difference in magnetic susceptibility between the nanoparticle

and the surrounding medium, V_{MNP} is the volume of the nanoparticle (determined in Section 3.2.3), B is the magnetic field strength, ∇B is the gradient of the magnetic field strength, and μ_0 is the magnetic permeability of free space.

From the work by Zhang et al., it is stated that the movement of a microsphere in a magnetic field due to a magnetic force is exactly opposed by a hydrodynamic drag force [42]. This drag force is given by

$$F_{drag} = 3\pi v d\eta \qquad (4\text{-}2)$$

where F_{drag} is the drag force, v is the velocity induced by the magnetic force, d is the diameter of the material of interest, and η is the viscosity of the surrounding medium (viscosity of water = 8.94×10^{-4} Pa·s). These forces can be said to equal each other because the movement of the nanoparticle in the magnetic field will be slow enough to assume Stokes flow. Stokes flow assumes that inertial forces are very small compared to viscous forces, because the Reynold's number is below 1[43]. Therefore, setting Equations 4-1 and 4-2 equal to each other and rearranging yields

$$v = \frac{dr}{dt} = \frac{\Delta \chi V_{MNP} \nabla B \cdot B}{3\pi d\eta \mu_0} \qquad (4\text{-}3)$$

This equation will be solved for a nanoparticle directly in the center of the channel. First, the magnetic susceptibility of the nanoparticles must be characterized. To calculate this, an equation from Barnes et al. was utilized [44].

$$\chi = \frac{s}{H}\rho \qquad (4\text{-}4)$$

In Equation 4-4, s is magnetic saturation, H is magnetic field and ρ is density. The magnetic saturation of the nanoparticles is given in the work by Deng et al. as 81.9emu/g [34]. The density of magnetite is 5000kg/m^3 [45]. To get H, Equation 4-5 was used.

$$B = \mu_0 H \qquad (4\text{-}5)$$

B was experimentally determined from the magnet at a distance of .25 inches (0.00635m) using a DC magnetometer. B was determined to be .14T. The magnetic permeability of

free space is known to be 1.256×10^{-6} N/A^2. Plugging these values into Equation 4-4 yields H=1.1×10^5A/m. Plugging the appropriate values into Equation 4-4 yields a magnetic susceptibility of 3.67. The magnetic susceptibility of water is known to be -9.035×10^{-6} [46].

Next, it is necessary to write B and ∇B from Equation 4-1 in terms of the radius in the tube. This is because the magnetic force will change as distance between the nanoparticle and the magnet change. To find the relationship between B and r, B was measured and plotted against corresponding distances, as seen in Figure 4.6.
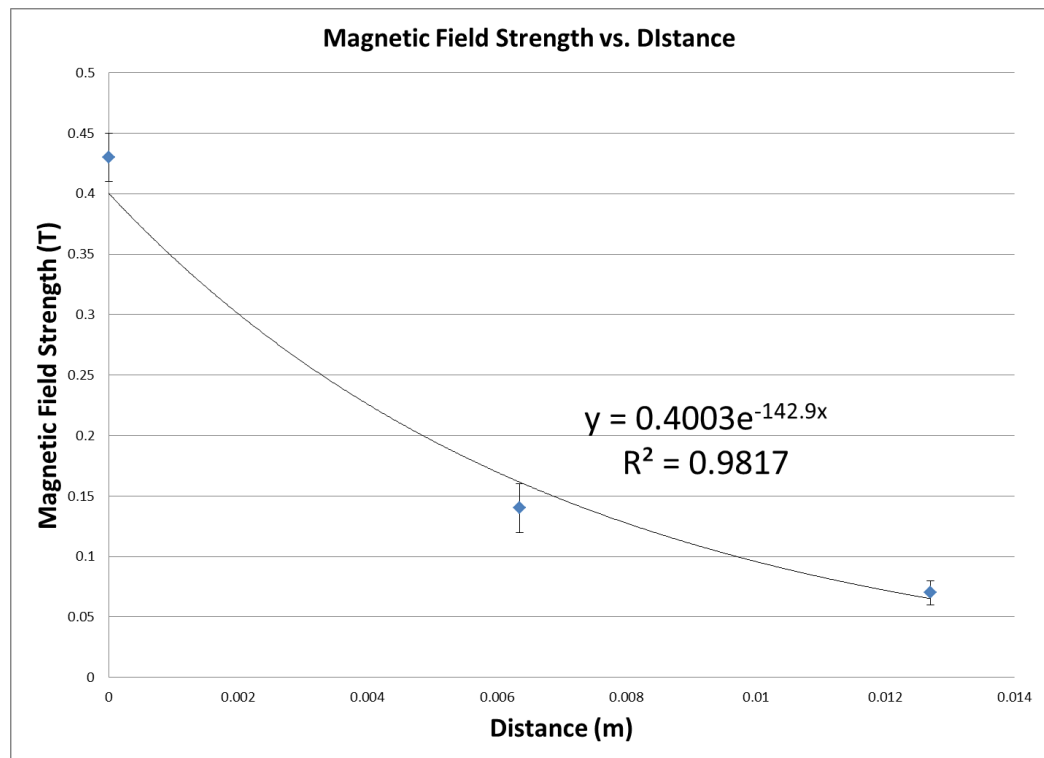
Figure 4.6 Determination of relationship between B and radius

The equation given in Figure 4.6 is an estimation of the relationship of B to r for the magnets purchased, where r is written as x in the figure. To get ∇B, the derivative of this equation can be taken. Therefore plugging appropriate values into Equation 4-3 yields

71

$$v = \frac{dr}{dt} = \frac{\left(3.67 - (-9.035 \times 10^{-6})\right)(1.767 \times 10^{-21})(.4e^{-143r})(-57.2e^{-143r})}{3\pi(75 \times 10^{-9}m)(8.94 \times 10^{-4}Pa \cdot s)(1.256 \times 10^{-6} \frac{N}{A^2})}$$

Rearranging this equation gives

$$dt = \frac{\left[3\pi(75 \times 10^{-9}m)(8.94 \times 10^{-4}Pa \cdot s)(1.256 \times 10^{-6} \frac{N}{A^2})\right] dr}{\left(3.67 - (-9.035 \times 10^{-6})\right)(1.767 \times 10^{-21})(.4e^{-143r})(-57.2e^{-143r})}$$

Therefore, to get the time it will take for the nanoparticle to separate from the center of the channel to the wall, the above equation can be integrated with respect to r, as seen below.

$$t = \int_0^{-.00635} \frac{\left[3\pi(75 \times 10^{-9}m)(8.94 \times 10^{-4}Pa \cdot s)(1.256 \times 10^{-6} \frac{N}{A^2})\right] dr}{\left(3.67 - (-9.035 \times 10^{-6})\right)\left(1.767 \times 10^{-21}\right)(.4e^{-143r})(-57.2e^{-143r})} = 15.7s$$

The limits used in the above equation are such that the center of the channel is r=0 and the wall is r=-.00635m. Therefore, it can be seen that it will take one nanoparticle approximately 15.7s to separate from the center of the channel to the wall.

To consider the time it will take for a nanoparticle to drag a bacterium in the magnetic field, this equation can be altered so that the diameter in the drag force equation represents the diameter of a bacterium, rather than a nanoparticle. This diameter can be approximated by 3μm (assuming a bacterium can be approximated as a sphere). To consider more than one nanoparticle dragging a single bacterium, the equation can be further altered, by changing the volume used in the magnetic force equation from one nanoparticle to the volume of the desired number of nanoparticles. Figure 4.7 exhibits the separation time for different numbers of nanoparticles dragging a single bacterium.
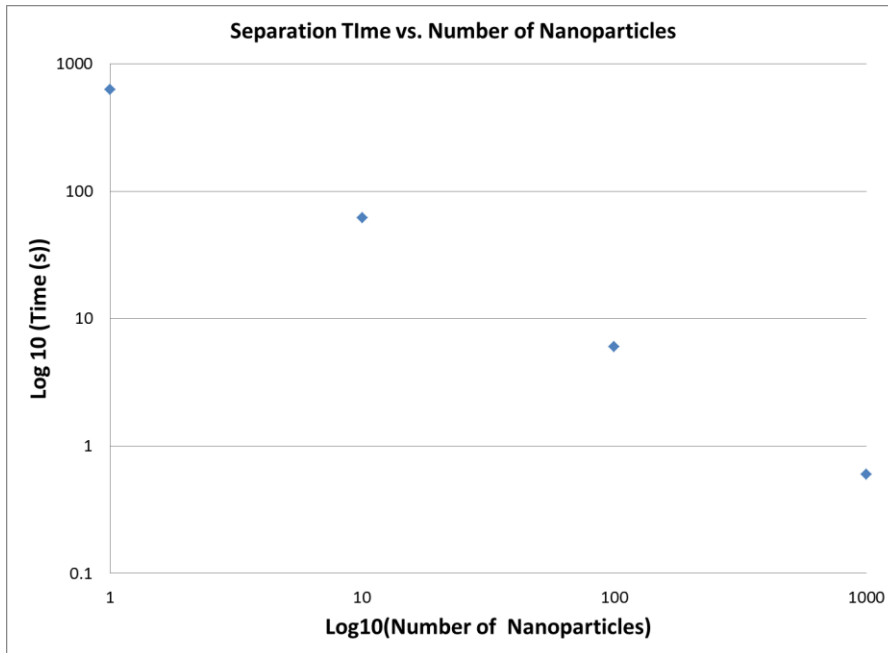
Figure 4.7 Separation time for one bacterium based on the number of nanoparticles

attached

The axial distance that the bacterium-nanoparticle aggregate will move in the tube due to the fluid flow can be calculated using the average velocity in the tube. This is an approximation because the velocity of the flow in the channel is a parabolic flow profile, meaning that the flow is fastest in the center of the channel and slowest at the walls. To find the average velocity, Equation 4-6 can be used.

$$Q = \frac{\pi}{4} d^2 v \tag{4-6}$$

In this equation, Q is the flow rate in the channel, d is the diameter of the channel, and v is the average velocity. The flow rate was determined to be $3.03 \times 10^{-6} m^3/s$ and the diameter of the channel is .0127m. Plugging these values into the channel yields v = .024m/s. Therefore, to get axial displacement, one must only multiply this velocity by the calculated separation time. Assuming at least 1000 nanoparticles are used per bacterium, the axial distance traveled by this bacteria-nanoparticle aggregate is .015m, which is about .6 inches. The magnets chosen were approximately 1.5 inches in length, to ensure

the best chances of capturing all the nanoparticles passing in the channel. Figure 4.8 shows the capture distance versus the number of nanoparticles, using the capture times in Figure 4.7 and the calculated average velocity.
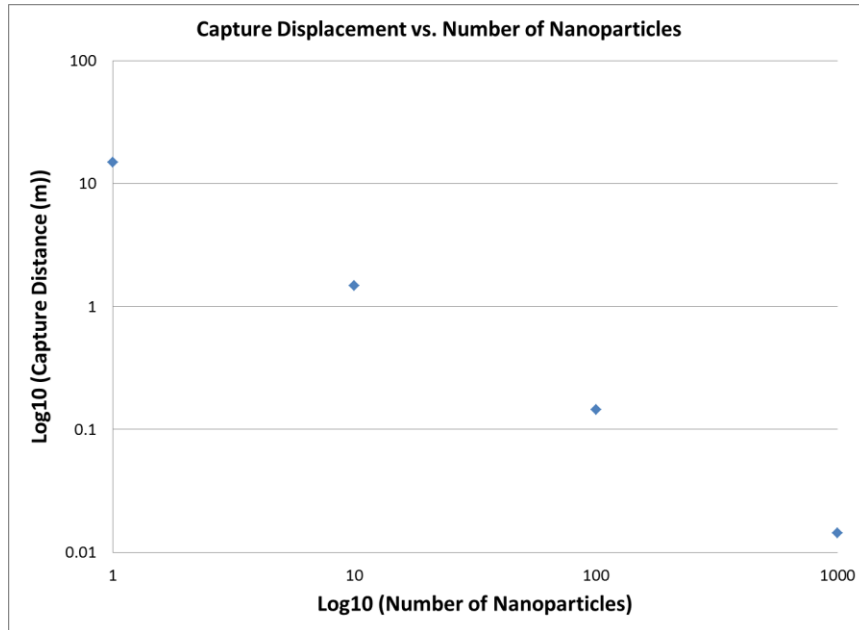
Figure 4.8 Capture distance versus the number of nanoparticles for one bacterium

4.4 Characterization

4.4.1 Preliminary Nanoparticle Experiments

After the prototype was completed, some characterization was necessary before bacteria capture experiments could be started. Preliminary experiments using only nanoparticles in the prototype revealed that some of the nanoparticles that were collected by the magnet remained adhered to the walls of the tubing when the magnet was removed. A slight residue was left by these nanoparticles on the tubing. This residue was seen when very large concentrations of nanoparticles were used, such as 10mg of nanoparticles in 500mL of DI water. It was decided to test Teflon tubing, to see if the nanoparticles would still adhere to this type of tubing as well. After conducting an experiment using Teflon tubing, it was seen that a slight nanoparticle residue remained

after the magnet was removed. Since the Teflon tubing showed the same type of nanoparticle residue, and was much more rigid than the PVC tubing, it was decided to continue testing using the PVC tubing. Further testing of the recovered nanoparticle concentration can be seen in Section 4.4.4.

4.4.2 Preliminary *Salmonella* Experiments

The main concern to be addressed was bacteria adhesion to the tubing. No surfactant was used to coat the tubing due to the fact that the system would be a continuous flow system, and this coating would need to be replaced, requiring the system to be halted periodically for this purpose. It was also decided to not use a surfactant, as it may have an effect on the nanoparticle surfaces and capture efficiency, which at this time is unknown and would have to be tested.

Therefore to determine how much bacteria could be recovered from the system, an experiment was conducted using only *Salmonella* (no nanoparticles were used in this experiment). A starting concentration of approximately 10^3CFU/mL of bacteria in 1 liter of DI water was used. Samples were taken and plated before the volume was introduced to the prototype, to verify the starting concentration of bacteria. This volume was the 'contaminated DI water' in Figure 4.4. The volume of contaminated DI water was run through the prototype, and collected in the 'concentrated bacteria-NP aggregates' bottle in Figure 4.4, even though no nanoparticles were used in this experiment. Samples from this recovered volume were taken and plated, to compare with the samples taken before the experiment. The valve was not turned at any time, because there was no separation taking place. This test was to determine how much bacteria was lost due to adhesion to the tubing. After the test, the prototype was cleaned with bleach and rinsed with DI water. The results of this testing can be seen in Table 4.1.

Table 4.1 Results of testing to determine *Salmonella* adhesion to tubing

	Average CFUs on plate	**σ**
Before Testing	168	19.6
After Testing	154	30.2

From this testing, it can be seen that almost 100% of the bacteria introduced to the prototype was recovered. Therefore, the amount of bacteria adhesion to the tubing was assumed to be negligible, and further testing could be commenced.

4.4.3 *Salmonella* **Capture Efficiency Experiments using Prototype**

To begin testing the prototype to determine its bacteria capture efficiency, a pre-mixed volume of bacteria and nanoparticles had to be attained. The mixing method used in Section 3.2.1 was utilized. Two tubes containing ten milliliters of 10^5CFU/mL of *Salmonella* were each mixed with approximately 10^{11} nanoparticles on a shaker for one hour. The nanoparticles used correspond to the nanoparticles in row D in Figure A.1 in Appendix A. These nanoparticles were used, even though they do not exhibit the highest capture efficiency, because they do not adhere to the tubes they are shaken in, as was seen with the other types of nanoparticles tested. The concentrations of nanoparticles and bacteria were chosen after the testing seen in Section 3.2.4, where the optimal bacteria-nanoparticle ratio was determined.

After one hour of shaking, each tube was diluted in 1 liter of DI water. This resulted in the desired bacteria concentration of 10^3CFU/mL in each 1 liter bottle. Samples were taken and plated before testing to verify these starting concentrations. The first of these volumes was pumped through the prototype with no magnetic field present, to determine how much bacteria could be recovered when nanoparticles are present in the test volume. Samples were taken and plated after the volume had been flowed through the prototype. The results of this testing can be seen in Table 4.2.

Table 4.2 Results of control experiment with no magnetic field present

	Average CFUs on plate	**σ**
Before Experiment	124	13.5
After Experiment	109	15.7

It can be seen that almost 100% of the bacteria was again recovered, meaning that the bacteria adhesion to the tubing is minimal. The prototype was cleaned with bleach and rinsed thoroughly with DI water. Then, the second volume of contaminated DI water was run through the prototype. The valve remained in position one until approximately 800mL of contaminated DI water had been cleaned. Then the valve was turned to position two and the magnets were removed, allowing the rest of the volume to be pumped through the prototype to be the re-suspension volume of the bacteria-nanoparticle aggregates. This was done to ensure that all collected bacteria-nanoparticle aggregates could be flowed into the re-suspension volume as opposed to being caught in the tubing or valve, once the contaminated volume became empty. The results of this testing can be seen in Table 4.3.

Table 4.3 Results of bacteria-nanoparticle experiment with magnetic field present, experiment 1

	Average CFUs on plate	**σ**
Before Experiment	116	21.7
After – Cleaned Volume	47	5.9
After - Contaminated Volume	322	18.2

The corresponding bacteria recovery can be seen in Table 4.4.

Table 4.4 Bacteria recovery from experiment 1

	Volume (mL)	Average Concentration	Total number of bacteria
Before Experiment	1000	1.16×10^3 CFU/mL	1.16×10^6 cells
Sampling before experiment	50	1.16×10^3 CFU/mL	5.8×10^4 cells
After – Cleaned Volume	800	4.70×10^2 CFU/mL	3.76×10^5 cells
After - Contaminated Volume	150	3.22×10^3 CFU/mL	4.83×10^5 cells

From Table 4.4, if the total number of bacteria from before the experiment is compared with the total bacteria from after the experiment, it can be seen that the bacteria recovery is 80%. From Table 4.3, the capture efficiency, when comparing the average number of nanoparticles from the 'after-cleaned volume' and the 'after-contaminated volume,' is approximately 85%. This means that approximately 85% of the bacteria from the starting contaminated volume (in 1 liter) was successfully re-suspended in 150mL (in the 'after-contaminated volume'). This was the expected outcome because the capture efficiency from these nanoparticles is approximately 85%, as can be seen in Figure A.1 in Appendix A.

For consistency purposes, this second experiment was repeated exactly as outlined above. The results of this testing can be seen in Table 4.5.

Table 4.5 Results of bacteria-nanoparticle experiment with magnetic field present, experiment 2

	Average CFUs on plate	σ
Before Experiment	109	10.4
After – Cleaned Volume	62	6.0
After - Contaminated Volume	322	20.8

The corresponding bacteria recovery can be seen in Table 4.6.

Table 4.6 Bacteria recovery from experiment 2

	Volume (mL)	Average Concentration	Total number of bacteria
Before Experiment	1000	1.09×10^3 CFU/mL	1.09×10^6 cells
Sampling before experiment	60	1.09×10^3 CFU/mL	6.54×10^4 cells
After – Cleaned Volume	820	6.20×10^2 CFU/mL	5.08×10^5 cells
After - Contaminated Volume	120	3.22×10^3 CFU/mL	3.86×10^5 cells

From this second experiment, it can be seen that the bacteria recovered increased to 90%. The capture efficiency was approximately 81%. Therefore, the prototype appears to be working relatively consistently in the expected manner.

4.4.4 Nanoparticle Capture Efficiency Experiments using Prototype

After the prototype proved to efficiently capture bacteria, it had to be tested to determine its capture efficiency of the nanoparticles. This testing was conducted using an inductively coupled plasma optical emission spectrometry system (ICP-OES). This tool allows detection of metals, and can determine their concentrations. Therefore it was used to determine concentrations of iron in samples from before and after use in the prototype.

First, samples from the bacteria-nanoparticle experiment in Section 4.4.3 were tested. To prepare these samples, they were autoclaved to kill the bacteria. Then they were diluted ten times in 2% HNO_3 (nitric acid) in DI water. This allows the iron to dissolve so it can be detected in the tool. Finally, the samples were filtered, to remove the bacteria. However, when the samples were tested using the ICP-OES system, it appeared that there was no iron detected in any of the samples.

Therefore, the prototype was tested again using only nanoparticles, at a much higher concentration. To begin testing, 5mg of nanoparticles, corresponding to D in Figure A.1 in Appendix A, was diluted in 1 liter of DI water. Samples were taken before introduction to the prototype as well as after. These samples were diluted ten times in 2%

HNO$_3$ to allow the iron to dissolve before testing them in the ICP-OES. This test was performed to observe the capture efficiency of the magnetic field when only nanoparticles are present. The results of this testing can be seen in Table 4.7.

Table 4.7 Results of ICP-OES iron testing, experiment 1

	Volume (mL)	Total amount of iron (mg)
Before experiment	1000	.51
After experiment – cleaned volume	800	.144
After experiment – contaminated volume	400	.204

It can be seen that the 'after experiment- contaminated volume' is very large, and the two 'after' volumes add up to more than the starting volume. This is because when the magnet was removed to re-suspend the collected nanoparticles in the contaminated volume, it was observed that the nanoparticles settled to the bottom of the channel and did not flow with the incoming liquid. Therefore, more DI water was added in an attempt to collect these settled nanoparticles. However, it appears some of these nanoparticles became trapped in the valve because the recovery of the nanoparticles is approximately 73%. It also appears that approximately 28% of the nanoparticles were found in the 'cleaned' volume, meaning that some of the nanoparticles are bypassing the magnets. One very important note is that the expected starting concentration of this volume was 5ppm, since 5mg of nanoparticles were dispersed in 1 liter of DI water (ppm = mg/L). However, it appears this is off by an order of magnitude. This will be discussed in Section 4.5.

To verify these results, the prototype was tested again. However, instead of using the valve, the tubing with incoming flow was manually moved from the cleaned flow container to the contaminated flow container. This would determine if the nanoparticles were getting caught in the valve. Five mg of the nanoparticles listed in row D in Figure A.1 in Appendix A were dispersed in 500mL of DI water. This volume was run through the prototype. The results of this testing can be seen in Table 4.8.

Table 4.8 Results of ICP-OES iron testing, experiment 2

	Volume (mL)	Total amount of iron (mg)
Before experiment	500	1.26
After experiment – cleaned volume	360	.233
After experiment – contaminated volume	100	.711

Here, the total amount of iron in the 'before experiment' volume was 5 mg. However, it was determined that the total amount of iron in this volume was approximately 1.26mg, yielding a concentration of .63ppm, or .63mg/L. This is consistent with the previous experiment, where the starting concentration of nanoparticles was approximately 10x lower than what was expected. Approximately 83% of the nanoparticles were recovered and it was found that approximately 30% of the nanoparticles were found in the 'cleaned' volume. These results are also consistent with the previous experiment, meaning that the valve is not trapping a significant amount of nanoparticles.

4.5 Discussion

It is important to note that the concentration of nanoparticles calculated in Section 3.2.3 is a rough estimation of the number of nanoparticles in 1mg. This is due to the fact that the nanoparticles varied in diameter from approximately 100nm to 150nm. For the calculations in Section 3.2.3, the radius used was 75nm, assuming all the nanoparticles shared the same size. Therefore, the calculation could have drastically underestimated the concentration of nanoparticles in 1mg, since many of the nanoparticles are actually smaller than 150nm. In the future, the distribution function of the magnetic nanoparticles' size can be measured to yield a more accurate estimation of the concentration of nanoparticles in a given volume.

For the calculations describing the movement of nanoparticles and bacteria in the prototype (Section 4.3), several important assumptions were made. Firstly, it was

assumed that the magnetic force only depends on the distance from the magnet. It was assumed that the magnetic force is constant in the z direction. Secondly, the relationship between B and r was determined experimentally, meaning there is room for error in the equation that was obtained. Therefore, the resulting time that can be calculated from this relationship is an estimation based on measured values. Thirdly, the time calculation was altered to take into account a bacterium being dragged by a nanoparticle by changing the drag force portion of the equation. The drag force includes the diameter of the material of interest. Therefore a sphere of diameter 3µm was used to represent a bacterium. The diameter of the nanoparticles was not included here because it was assumed that the bacterium is so much larger than the nanoparticles that their addition to this diameter is negligible. Fourthly, it was assumed that, to increase the number of nanoparticles dragging a bacterium in the magnetic force, the volume in the magnetic force equation could be increased to include the total volume of the selected number of nanoparticles. Finally, to determine axial displacement, the average velocity in the channel was utilized, rather than integrating over the channel radius to vary the axial velocity based on a parabolic flow profile. Several assumptions were made to estimate the separation time of the bacteria-nanoparticle aggregates. It was assumed that nanoparticles attach to the bacterium's surface and drag it in the magnetic field. However, as can be seen in Figure 3.18, the nanoparticles appear to agglomerate into clusters measuring several microns in diameter. Attached to these clusters are bacteria cells. If this is the method of capture, the approach used to determine separation time may not be appropriate. It will be very difficult to accurately estimate the separation time if these clusters are to be modeled, since it is unknown how large the clusters grow. It is also unknown how many bacteria cells typically attach to each cluster. Until more is known about the method of capture, the method set forth in Section 4.3 represents a good estimation for separation time as well as axial distance traveled before capture.

It appears from Section 4.4.3 that the prototype is working very efficiently, with a bacteria capture efficiency of 80% or higher for the experiments performed thus far. This capture efficiency could possibly be higher if nanoparticles with higher capture efficiencies were used. However, the nanoparticle capture efficiency must be increased, due to the fact that currently, almost a third of the nanoparticles are contaminating the clean water volume. This could be a reason why bacteria cells are found in the clean water volume. Since some of the nanoparticles are not being collected by the magnets, they are passing into the clean water volume, and if they are attached to a bacterium, it will pass directly into the clean water volume as well. Since the bacteria capture efficiency is relatively high, it is possible that the nanoparticles that are passing into the clean water volume are unattached to bacteria cells. It is possible that these nanoparticles remained unattached to each other or bacteria. As seen from the calculation in Section 4.3, a single nanoparticle will take approximately 15.7 seconds to separate. This corresponds to an axial distance of approximately 37cm, meaning that the magnetic field is not long enough to successfully capture these nanoparticles. This can be rectified by using stronger magnets (to increase the force on each individual nanoparticle) or using lower flow rates (which will allow less axial distance to be traveled before the nanoparticle is captured). However, as long as the bacteria concentration is being effectively captured, the prototype is deemed successful. If necessary, the system could compensate for this poor capture of nanoparticles by flowing the cleaned volume of water through another set of magnets to collect any remaining nanoparticles before the water is considered 'clean.'

This setup can be altered in many ways to change the capture efficiency. The flow rate of the prototype can be changed. By increasing the flow rate, and utilizing the same diameter tubing as was specified in Section 4.2, the velocity in the tubing will increase based on Equation 4-6, meaning the bacteria-nanoparticle aggregates will be exposed to the magnetic field for less time. This may decrease the capture efficiency that was seen in

Section 4.4, where approximately 30% of the nanoparticles were not captured. If the flow rate is increased, it can be speculated that even less nanoparticles would be captured. However, more liquid could be processed in a given amount of time.

By decreasing the flow rate (and maintaining the same tube diameter used in Section 4.2), less liquid would be processed in a given period of time. However, it can be inferred that the capture efficiency would increase, because the bacteria-nanoparticle aggregates would be subjected to the magnetic field for a greater amount of time, since the axial velocity would be decreased.

If the tubing diameter was increased, without changing the flow rate of the pump, the velocity in the channel will decrease, based on Equation 4-6. This would allow the bacteria-nanoparticle aggregates more time in the magnetic field to separate to the walls of the tubing, because the axial velocity in the channel will be lessened. However, the tradeoff to this change is that the tubing diameter will be larger, and therefore the bacteria-nanoparticle aggregates will have to cover more distance in the radial direction to separate to the walls of the channel once they are in the presence of the magnetic field.

If the tubing diameter was decreased, the axial flow velocity will be increased, meaning that the bacteria-nanoparticle aggregates will be subjected to the magnetic field for less time. However, since the tube diameter has decreased, the bacteria-nanoparticle aggregates will be closer to the magnets in the magnetic field. This may allow a better capture efficiency than using larger tubing diameters, as these aggregates will experience a stronger force and they will not have to travel as far in the radial direction to reach the wall of the channel.

Magnet size can also have an effect on the capture efficiency. By increasing the magnet length, there is more distance available for the bacteria-nanoparticle aggregates to be captured. However, this will also increase the re-suspension volume. This may be a reasonable tradeoff because the main goal of the prototype is to separate as much bacteria as possible from the incoming contaminated liquid.

By changing parameters in the prototype, the capture efficiency can be altered. The parameters must be changed in an appropriate manner to maintain excellent capture efficiency as well as ensure large volumes can be processed in a reasonable amount of time.

The recovery of bacteria appears to be between 80-90%, while the recovery of nanoparticles appears to be approximately 70%. It is possible that the loss of some of the nanoparticles is due to the fact that they are adhering to the tubing and not being re-suspended when the magnetic field is removed. These particles seem to make up the residue that was discussed in Section 4.4.1. Since some of these nanoparticles may have bacteria attached, this could explain why some of the bacteria concentration is not being recovered.

One important concern revealed in this chapter is the fact that the nanoparticle concentration measured by the ICP-OES was much lower than what was expected. There could be error associated with weighing the nanoparticles, as well as re-dispersing them in water for testing. When the nanoparticles are re-dispersed in water, they are placed in a vertical shaker to break up dried clusters of nanoparticles. Many nanoparticles adhere to the tube walls while this re-dispersion is taking place. However this does not account for a concentration of nanoparticles 10x lower than what is expected. It is important to allow the nanoparticles to dissolve in HNO_3 so their concentrations can be determined by the ICP-OES. Since the measured concentrations appear very low compared to what was expected, it is possible that not all of the nanoparticles have dissolved fully. It may be necessary to let the nanoparticles digest in HNO_3 for a longer period of time to ensure they dissolve fully. It is important to note that the nanoparticles are not only composed of iron, but oxygen as well as any residual polymer that may be on the nanoparticle surface. Therefore, the measured iron content will be lower than what is expected. Further testing will need to be performed to determine what the actual iron content is for each

nanoparticle. In the future, concentrations of nanoparticles can be verified using ICP-OES analysis before testing.

The fact that the expected iron content seems to be very different than what is measured by the ICP-OES could be an explanation for why no iron was found in the bacteria-nanoparticle samples tested in Section 4.4.4. The iron concentration was expected to be 1ppm. However, if the realistic nanoparticle concentration is 10x less than what was expected, as was determined in the nanoparticle experiments in Section 4.4.4, the actual concentration may have been closer to .1ppm. The calibration that was performed to determine nanoparticle concentrations used .1ppm as the lowest calibration standard. Therefore, if the actual nanoparticle concentration was very near to this, it is possible that it was not distinguishable, and thus measured 0ppm. The lower limit of the calibration can be reduced to .01ppm to account for this in future testing.

Finally, if this prototype can be successfully adapted to a large-scale setting, it may be possible to use this mechanism for bacteria preconcentration, and then use the preconcentrated bacteria in a device similar to that seen in Figure 2.7. Then, not only will the bacteria be separated from the bulk liquid that was processed, but it can then be analyzed to determine its viability. As was stated in Section 2.5, it is necessary to determine if bacteria that is separated from large sample volumes is viable or nonviable. Viable bacteria cells pose a threat to public safety if they are in drinking water or on foods. However, if nonviable cells are found in these settings, they pose no threat to people, as they will not cause illness. Therefore, it is important to determine the viability of separated cells in order to deduce if public health is at risk. By joining these two techniques, preconcentration using nanoparticles and viability determination using chemotaxis, this can be effectively achieved.

CHAPTER 5

INTERVENTION OF *SALMONELLA*

This chapter focuses on the discovery and exploration of iron (III) as a method for intervention of *Salmonella typhimurium*, as well as other bacteria.

5.1 Pure Culture Experiments

During chemotaxis experimentation with repellents, it became obvious that *Salmonella* growth was being inhibited by chemicals containing Fe (III). The first experiment that this became obvious utilized the capillary tube setup referenced in Section 2.4. Iron (III) nitrate nonahydrate was employed to determine if it efficiently repelled *Salmonella* from entering the capillary tubes in this setup. Concentrations of 0.5M, 0.05M, and 0.005M were prepared in DI water and tested. DI water was used as the negative control. A sample of *Salmonella* was grown at 37°C for approximately 18 hours in TSB. The concentration of Salmonella in the wells was a 10^4 dilution of this original culture. This concentration should be on the order of 10^4-10^5 CFU/mL. Two capillary tubes for each concentration were used. After ten minutes, the capillary tubes (with an approximate volume of 5μL) were emptied onto agar plates and incubated at 37°C overnight. The results of this testing can be seen in Table 5.1.

Table 5.1 Results of initial test with Fe $(NO_3)_3$

	Average	σ
0M	44	10.6
0.005M	0	0
0.05M	0	0
0.5M	0	0

It can be determined from Table 5.1 that the concentration in the capillary tubes with 0M (DI water) of the chemical matches the concentration in the wells, approximately 10^4 CFU/mL. All other agar plates yielded no bacteria growth, meaning that either no bacteria migrated into the tube or the chemical was killing bacteria. This prompted further testing of this chemical for its inhibition efficiency.

To confirm that Fe $(NO_3)_3$ was killing *Salmonella*, a second test was conducted without using the capillary tube setup. Fe $(NO_3)_3$ was added to 1 milliliter of *Salmonella* diluted 10^4 times (yielding an approximate bacteria concentration of 10^4 CFU/mL) to achieve a concentration of 0.5M. A sample of 10μL was plated after 10 minutes and 30 minutes. A 10μL sample of *Salmonella* diluted 10^4 x was plated as well as a control. The results can be seen in Table 5.2.

Table 5.2 Results of 0.5M Fe $(NO_3)_3$ testing

	After 10 minutes	After 30 minutes
0.5M Fe $(NO_3)_3$	0	0
10^4 x dilution of *Salmonella*	235	290

The control sample was used to provide the background concentration of *Salmonella.* The samples with 0.5M of chemical again show no bacteria growth, confirming previous test results. It was postulated that perhaps the concentration of 0.5M was too high, so this test was repeated using 0.005M Fe $(NO_3)_3$. These results can be seen in Table 5.3.

Table 5.3 Results of 0.005M Fe $(NO_3)_3$ testing

	After 10 minutes	After 30 minutes
0.005M Fe $(NO_3)_3$	0	0
10^4 x dilution of *Salmonella*	373	330

Even using a lower concentration of chemical, no growth was seen on the agar plates. The control plates, however, show an order of magnitude corresponding to the starting concentration of bacteria. The use of this chemical yields consistent results, as can be seen by the reproducibility of the experiments performed.

5.1.1 Testing with Different Bacteria

Since the killing effects of $Fe(NO_3)_3$ were seen with *Salmonella*, testing continued using *Staphylococcus aureus*, *Pseudomonas aeruginosa*, and *Escherichia coli (E.coli)*. Each bacteria type was grown in TSB at 37°C for approximately 18 hours. After 18 hours, each bacteria type, including *Salmonella*, was diluted 100 times from the grown sample concentration. $Fe(NO_3)_3$ was then added to 1 milliliter of each sample to achieve a concentration of .005M. The test continued for 10 minutes and then 10μL samples were plated. Each bacteria type was diluted 10^4 times from the grown sample concentration and plated as a control sample. No chemical was added to these samples. These control samples could then be used to calculate the starting concentration of each bacteria type. The results of this testing can be seen in Tables 5.4, 5.5 and 5.6.

Table 5.4 Results of samples exposed to 0.005M $Fe(NO_3)_3$. Dilution: 100x from grown sample

	Average	σ
Salmonella typhimurium	4	7.3
Staphylococcus aureus	1	2.0
Pseudomonas aeruginosa	1	1.5
Escherichia coli	388	62.9

Table 5.5 Results of control samples (not exposed to chemical) Dilution: 10^4 x from grown sample

	Average	**σ**
Salmonella typhimurium	410	14.1
Staphylococcus aureus	171	2.8
Pseudomonas aeruginosa	285	49.5
Escherichia coli	465	21.2

Table 5.6 Reduction results of 0.005M Fe $(NO_3)_3$ testing based on starting concentrations obtained from control samples

	Average concentration from chemical samples (CFU/mL)	**Starting concentration from control samples (CFU/mL)**	**Reduction**
Salmonella typhimurium	$4.0x10^2$	$4.10x10^6$	4 orders of magnitude
Staphylococcus aureus	$1.0x10^2$	$1.71x10^6$	4 orders of magnitude
Pseudomonas aeruginosa	$1.0x10^2$	$2.85x10^6$	4 orders of magnitude
Escherichia coli	$3.88x10^4$	$4.65x10^6$	2 orders of magnitude

Based on the results from Table 5.6, it can be seen that *E. coli* exhibits some resilience when in the presence of Fe $(NO_3)_3$. However, a noticeable reduction in *E. coli* concentration was still observed. All other bacteria strains tested demonstrated the same killing effects as was seen by previous *Salmonella* testing.

5.1.2 Testing with Different Chemicals

To isolate which chemical was responsible for these excellent killing results (either iron (II), iron (III), or nitrate), several chemicals were tested in the presence of

pure cultures of *Salmonella*. The chemicals to be tested were iron (III) chloride, iron (II) chloride, iron (III) nitrate, and sodium nitrate. To begin the experiments, *Salmonella* was grown at 37°C in TSB for approximately 18 hours. *Salmonella* was then diluted 100x and 10^4x in PBS from the grown culture, respectively. The starting concentration of *Salmonella* was determined to be approximately $7.0x10^8$ CFU/mL by series dilution testing. The experiment required that 1mL of each dilution of bacteria be mixed with each chemical to achieve a chemical concentration of approximately 0.005M of the testing ions. Sodium nitrate, however, was mixed with the bacteria to achieve a chemical concentration of approximately .015M. This is due to the fact in Fe $(NO_3)_3$, there are 3 nitrate ions (NO_3) for every iron ion. Thus, the concentration of nitrate must be three times the concentration of iron used. After the chemical was introduced to the bacteria sample for ten minutes, 1 mL of 0.02M sodium thiosulfate in DI water was added to the sample to quench the killing reaction. Sodium thiosulfate is a powerful reducing agent, and will stop the oxidizing reaction that is killing the bacteria in the experiment. Finally, two 100 μL samples were plated for quantification. The results of this testing can be seen in Table 5.7.

Table 5.7 Results of different chemical testing

Chemical	Bacteria Dilution	Average	σ
Fe (III) Nitrate	100x	205	15.6
	10^4 x	0	0
Fe (III) Chloride	100x	80	28.3
	10^4 x	1	0.7
Fe (II) Chloride	100x	Thousands	-
	10^4 x	Thousands	-
Sodium Nitrate	100x	Thousands	-
	10^4 x	Thousands	-

From Table 5.7, it can be seen that iron (III) appears to be the chemical responsible for the killing of *Salmonella*. Both iron (III) nitrate and iron (III) chloride demonstrate excellent bacteria reduction, while iron (II) chloride and sodium nitrate appear to have no effect on bacteria growth. A comparison of the iron (III) nitrate and iron (III) chloride results can be seen in Table 5.8.

Table 5.8 Comparison of iron (III) nitrate and iron (III) chloride killing results

Chemical	Dilution	Average concentration (CFU/mL)	Expected Concentration (CFU/mL)	Reduction
Fe (III) Nitrate	100x	2.05×10^3	7.0×10^6	3 orders of magnitude
	10^4x	0	7.0×10^4	4 orders of magnitude
Fe (III) Chloride	100x	8.0×10^2	7.0×10^6	4 orders of magnitude
	10^4 x	1.0×10^1	7.0×10^4	3 orders of magnitude

Both iron (III) nitrate and iron (III) chloride exhibit excellent killing abilities and appear to be killing at very similar rates.

5.1.3 Testing Iron (III) at Lower Concentrations

After confirming that iron (III) was inhibiting bacteria growth, testing was performed to determine the lowest concentration that could be used with significant killing results. At this point, testing had only been performed using 0.005M. Therefore, experiments using iron (III) nitrate continued with concentrations of 5×10^{-5} M, 1×10^{-4} M, 5×10^{-4} M, and 1×10^{-3} M. The starting concentration of *Salmonella* was verified during each experiment by plating samples of the diluted bacteria before it was exposed to any chemical. To start the experiment, *Salmonella* was grown at 37°C in TSB for approximately 18 hours. The bacteria was diluted 10^6 x from the grown culture in PBS.

Ferric nitrate was then added to 1 mL of this dilution to achieve the desired chemical concentrations. After ten minutes, the killing reaction was quenched using 1 mL of 0.02M sodium thiosulfate in DI water. 100μL samples were plated for quantification. This testing was performed twice. The results of this testing can be seen in Tables 5.9 and 5.10. The determined starting concentration for experiment 1 was approximately 1.85×10^9 CFU/mL and the determined starting concentration for experiment 2 was approximately 1.15×10^9 CFU/mL.

Table 5.9 Results of low chemical concentration testing, experiment 1

Chemical Concentration	Average	σ	Average Concentration (CFU/mL)	Expected Concentration (CFU/mL)	Reduction (order of magnitude)
5×10^{-5} M	55	5.8	5.5×10^2	1.85×10^3	1
1×10^{-4} M	41	4.9	4.1×10^2	1.85×10^3	1
5×10^{-4} M	56	15.5	5.6×10^2	1.85×10^3	1
1×10^{-3} M	41	12.7	4.1×10^2	1.85×10^3	1

Table 5.10 Results of low chemical concentration testing, experiment 2

Chemical Concentration	Average	σ	Average Concentration (CFU/mL)	Expected Concentration (CFU/mL)	Reduction (order of magnitude)
5×10^{-5} M	114	91.2	1.14×10^3	1.15×10^3	0
1×10^{-4} M	81	15.5	8.1×10^2	1.15×10^3	1
5×10^{-4} M	110	78.7	1.1×10^3	1.15×10^3	0
1×10^{-3} M	76	50.4	7.6×10^2	1.15×10^3	1
5×10^{-3} M	2	1.8	2.0×10^1	1.15×10^3	2

Experiment 2 included the concentration of 0.005M to ensure consistency with previous test results. It can be seen from Tables 5.9 and 5.10 that lower concentrations of iron (III) nitrate have very little to no effect on bacteria growth. It is also interesting to note that as the concentration of chemical increases, there is no significant increase in killing until the concentration of 0.005M is reached. It appears this is the lowest concentration of chemical that can be used to ensure reasonable killing efficiency. Therefore, this is the concentration that was used for all further testing.

5.2 Testing with Chicken

Since such impressive results were seen when testing iron (III) nitrate with pure culture samples, the next step was to test the chemical in the presence of food, such as raw chicken. A sample of *Salmonella* was grown at 37°C in TSB for approximately 18 hours. The original concentration of the bacteria was verified by doing a series dilution of the grown sample and plating it. The results indicated that the starting bacteria concentration was approximately 9.5×10^8 CFU/mL.

Six samples of raw chicken were cut and placed in plastic bags, each weighing approximately 600g to 800g. Two of these samples were not spiked with bacteria and served as control samples. The other four samples were spiked with 2 mL of *Salmonella* at a concentration of 10^7 CFU/mL. The meat was massaged briefly to allow the bacteria to adhere to it. All six samples were then placed in a refrigerator at approximately 4°C for several hours to allow the bacteria to become attached to the meat.

After the samples were removed from the refrigerator, the chemical testing could begin. First, the control chicken samples were submerged in 500 mL of DI water for ten minutes. 100µL samples were taken and plated after 10 minutes. This test would be the background number of bacteria that was on the chicken when it was purchased. The next two chicken samples, which were spiked with *Salmonella*, were submerged in 500 mL of 0.005M Fe $(NO_3)_3$ in DI water for 10 minutes. 100µL samples were taken and plated.

Finally, the last two chicken samples, which were spiked with *Salmonella*, were submerged in 500 mL of DI water, to serve as a comparison to the chicken submerged in Fe $(NO_3)_3$. There should be no killing exhibited by these samples, and therefore, they served as verification of the *Salmonella* concentration that the chicken was spiked with for testing. 500mL of 0.02M sodium thiosulfate was added to all samples to quench the reaction. The control chicken samples (no spike) and chicken samples with iron (spiked) were not diluted before plating. However, the spiked samples with no chemical introduced were diluted 100x for quantification purposes. A diagram of this process can be seen in Figure 5.1.
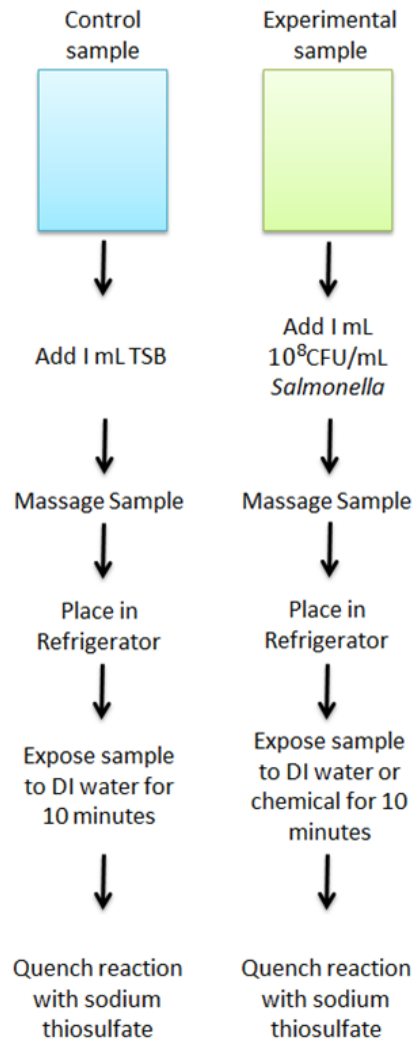
Figure 5.1 Process flow of iron (III) testing

The results of this testing can be seen in Tables 5.11.1, 5.11.2, and 5.11.3. Control samples were labeled as C1 NS1, meaning Chicken 1, No Spike, Sample 1, etc. Spiked samples with no chemical introduced were labeled as C1S NI1, meaning Chicken 1, Spiked, No Iron, Sample 1, etc. Spiked samples with iron introduced were labeled as C1S I1, meaning Chicken 1, Spiked, Iron, Sample 1, etc.

Table 5.11.1 Results of control chicken testing

	Average	σ
C1 NS1	7	0.7
C1 NS2	9	3.5
C2 NS1	3	0
C2 NS2	3	0.7

Table 5.11.2 Results of chicken spiked with *Salmonella*. Samples diluted 100x and plated

	Average	σ
C1S NI1	1000	70.7
C1S NI2	900	70.7
C2S NI1	1000	70.7
C2S NI2	900	70.7

Table 5.11.3 Results of chicken spiked with *Salmonella* and introduced to 0.005M $Fe(NO_3)_3$

	Average	σ
C1S I1	30	8.5
C1S I2	42	7.1
C2S I1	1	1.4
C2S I2	0	0

It is known that the starting bacteria concentration was approximately 9.5×10^8 CFU/mL. The bacteria was diluted 10x and then 2 mL were massaged onto the

chicken. All samples were submerged in 500 mL of liquid. Therefore the concentration of bacteria in the testing bags was expected to be 3.8×10^5 CFU/mL. Based on this expected concentration, the results of the spiked samples with no chemical introduced show no bacteria reduction throughout the experiment. However, the spiked samples with 0.005M Fe $(NO_3)_3$ show a significant bacteria reduction when compared to the expected concentration. This can be seen in Tables 5.12 and 5.13.

Table 5.12 Reduction results for spiked chicken samples with no chemical. Since the samples taken from these testing bags were diluted 100x, the expected concentration was adjusted from 3.8×10^5 CFU/mL to 3.8×10^3 CFU/mL

	Average Concentration (CFU/mL)	Expected Concentration	Reduction
C1S NI1	10×10^3	3.8×10^3 CFU/mL	0 orders of magnitude
C1S NI2	9.0×10^3	3.8×10^3 CFU/mL	0 orders of magnitude
C2S NI1	10×10^3	3.8×10^3 CFU/mL	0 orders of magnitude
C2S NI2	9.0×10^3	3.8×10^3 CFU/mL	0 orders of magnitude

Table 5.13 Reduction results for spiked chicken samples with 0.005M Fe $(NO_3)_3$

	Average Concentration (CFU/mL)	Expected Concentration	Reduction
C1S I1	3.0×10^2	3.8×10^5 CFU/mL	3 orders of magnitude
C1S I2	4.2×10^2	3.8×10^5 CFU/mL	3 orders of magnitude
C2S I1	1.0×10^1	3.8×10^5 CFU/mL	4 orders of magnitude
C2S I2	0	3.8×10^5 CFU/mL	5 orders of magnitude

Pictures were taken of the agar plates after approximately 18 hours incubating at 37°C. A comparison between the spiked chicken sample with no chemical and the spiked chicken sample with 0.005M Fe $(NO_3)_3$ can be seen in Figure 5.2.
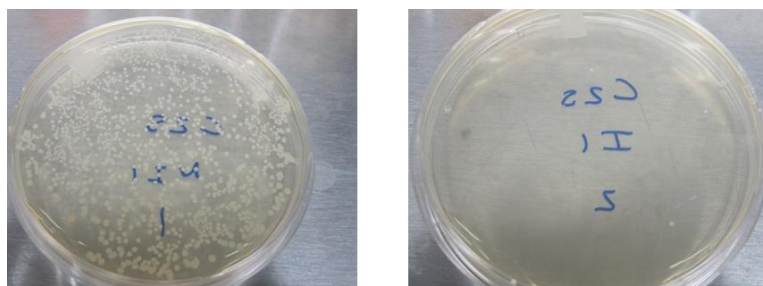
Figure 5.2 Left: 100x diluted sample of spiked chicken with no chemical and Right: Undiluted sample of spiked chicken with .005M Fe $(NO_3)_3$

5.2.1 Comparing Iron (III) and Chlorine Effects

Since chlorine is the standard for bacteria killing in chillers at poultry plants, it became necessary to compare the killing effects of iron (III) versus chlorine. Therefore, raw chicken was procured for testing purposes. A sample of *Salmonella* was grown at 37°C for approximately 18 hours.

The experiment followed the process flow in Figure 5.1. Eight samples were placed in plastic bags, each weighing approximately 75g. Two chicken samples were spiked with 1 mL of TSB. These would serve as control samples and be used to obtain the background amount of bacteria on the chicken. The other six samples, the experimental samples, were spiked with 1 mL of *Salmonella* in TSB at a concentration of 10^8 CFU/mL. The chicken samples were massaged briefly to allow the bacteria to evenly cover the chicken and to attach to the meat. All eight samples were placed in a refrigerator at approximately 4°C for 1 hour and 15 minutes.

While the samples were in the refrigerator, a solution of chlorine in pH 6 buffer was prepared at a concentration of 4ppm and confirmed by DPD method [47]. Using pH 6 buffer ensured that chlorine exhibited optimal killing characteristics [48]. It was necessary to prepare the chlorine solution right before use to ensure that it would not decompose before testing.

After the samples were kept in the refrigerator for 1 hour and 15 minutes, chemical testing could begin. Table 5.14 describes the chemical each sample was submerged in. After ten minutes, 100 mL of 0.02M sodium thiosulfate was added to each sample to stop any killing reactions. 100μL samples were taken and plated at appropriate dilutions.

Table 5.14 Chemicals for iron (III) vs. chlorine experiment with chicken, experiment 1

Bags:	Submerged in 100mL of:
1, 2 (no spike)	DI water
3, 4 (spike with10^8 CFU *Salmonella*)	DI water
5, 7 (spike with 10^8 CFU *Salmonella*)	4 ppm Chlorine
6, 8 (spike with 10^8 CFU *Salmonella*)	0.005M FeCl$_3$

Samples 1 and 2 yielded the background of bacteria that was on the chicken when it was purchased. Samples 3 and 4 served as comparison for the iron (III) and chlorine tests. There should be no killing associated with these samples. These samples would also allow the concentration of bacteria spiked on the chicken to be determined.

The results of this testing can be seen in Table 5.15.

Table 5.15 Results of iron (III) vs. chlorine with chicken, experiment 1

	Spike	Chemical	10x Dilution Average	σ	100x Dilution Average	σ	1000x Dilution Average	σ
Bag 1	No	DI water	0	0				
Bag 2	No	DI water	0	0				
Bag 3	Yes	DI water			386	19.8	37	1.4
Bag 4	Yes	DI water			356	34.6	20	0.7
Bag 5	Yes	Chlorine			470	14.1		
Bag 6	Yes	Fe (III)	144	43.8	33	11.3		
Bag 7	Yes	Chlorine			425	35.4		
Bag 8	Yes	Fe (III)	186	105.3	24	4.2		

As can be seen in Table 5.15, no bacteria growth was seen on agar plates from the unspiked chicken samples. The spiked samples that were submerged in DI water yielded results corresponding to a starting concentration on the chicken of approximately 2.9×10^5 CFU/mL. This starting concentration is slightly lower than what was expected to be seen. The chicken was spiked with approximately 10^8 CFUs, and then 200mL of liquid was introduced to each sample, diluting this concentration to approximately 10^6 CFU/mL. However, this concentration is very close to the expected concentration, and therefore it is possible that the grown sample had a slightly lower starting concentration than was expected.

Although both iron (III) and chlorine displayed bacteria killing, it can be seen that the iron (III) killing results were an order of magnitude better than the chlorine killing results. It is important to note that 0.005M of $FeCl_3$ is equivalent to approximately 280 ppm of ferric cation. This fact is discussed further in Section 5.4.

This experiment was repeated using a higher concentration of chlorine. Instead of using 4 ppm of chlorine in pH 6, a concentration of 45 ppm was used. In addition, another test was added. It was hypothesized that combining .005M Fe (III) with 45 ppm of chlorine would produce an even better killing response. Therefore, ten chicken samples were placed in plastic bags, each weighing approximately 75g. Two samples were spiked with 1 mL TSB and would serve as the control samples in the experiment. The other eight samples were spiked with 1 mL of 10^8 CFU/mL *Salmonella*. The meat was placed in a refrigerator at 4°C for 1 hour. A solution of 45 ppm fresh free chlorine was prepared as well as a solution of 45 ppm free chlorine in 0.005M Fe (III). Table 5.16 describes the tests performed for this second set of experiments. 100μL samples were taken and plated at appropriate dilutions.

Table 5.16 Chemicals for iron (III) vs. chlorine experiment with chicken, experiment 2

Bags:	Submerged in 100 mL of:
1, 2 (no spike)	DI water
3, 8 (spike with 10^8 CFU *Salmonella*)	DI water
4, 9 (spike with 10^8 CFU *Salmonella*)	0.005M $FeCl_3$
5, 10 (spike with 10^8 CFU *Salmonella*)	45ppm Chlorine in 0.005M $FeCl_3$
6, 7 (spike with 10^8 CFU *Salmonella*)	45 ppm Chlorine

Samples 1 and 2 yielded the background of bacteria that was on the chicken when it was purchased. Samples 3 and 8 served as comparison for the iron (III) and chlorine tests. There should be no killing associated with these samples. These samples would also allow the concentration of bacteria spiked on the chicken to be determined.

Due to the fact that the previous test involving chlorine did not produce effective killing results, it was important to test whether there was any free chlorine left in the sample after ten minutes, before the sodium thiosulfate was added. It was questioned whether all the free chlorine was being consumed by the organic materials in the sample, and thus not allowing proper killing of the bacteria for the duration of the test. To assess this, the chlorine solution was tested before the experiment to verify the starting concentration using DPD method. After the experiment, 10mL of the chlorine solution in each sample bag (Samples 5, 6, 7, and 10) were collected and tested. It was found that, in all sample bags, all the free chlorine had been consumed during the experiment. Therefore, it was not surprising that such poor killing results had been seen in the previous test using 4 ppm of free chlorine. Even using a chlorine solution 10x stronger, all chlorine was consumed during testing.

The results of this second set of testing can be seen in Table 5.17.

Table 5.17 Results of iron (III) vs. chlorine with chicken, experiment 2

	Spike	Chemical	No Dilution Average	σ	10x Dilution Average	σ	100x Dilution Average	σ
Bag 1	No	DI water	17	2.8	5	2.1		
Bag 2	No	DI water	28	4.9	13	0.7		
Bag 4	Yes	Fe (III)			450	70.7	89	21.9
Bag 5	Yes	Chlorine + Fe (III)					168	31.1
Bag 6	Yes	Chlorine					600	70.7
Bag 7	Yes	Chlorine					600	70.7
Bag 9	Yes	Fe (III)			238	97.6	31	5.7
Bag 10	Yes	Chlorine + Fe (III)					128	19.1

There was some growth on the control sample plates, which were from samples not spiked with bacteria. The agar plates used are not selective to *Salmonella*, and therefore this could be any type of bacteria that is common to uncooked meat in grocery stores. This bacteria growth may not even be pathogenic. Samples from bags 3 and 8, which were spiked with *Salmonella* and submerged in DI water for comparison purposes, had to be diluted 10^4x instead of 1000x in order to be quantified. These results can be seen in Table 5.18.

Table 5.18 Results of spiked chicken samples with no chemical introduced, experiment 2

	Spike	Chemical	10^4 x Dilution Average	σ
Bag 3	Yes	DI water	104	24.0
Bag 8	Yes	DI water	159	24.0

Based on the results from Table 5.18, the starting concentration of bacteria spiked on the chicken was approximately 1.28×10^7 CFU/mL. The fact that these samples had to

be diluted 10x more than in experiment 1 is explained by the fact that this concentration is slightly higher than what was expected.

The results in Table 5.17 indicate that iron (III) exhibits the best killing power of the three types of chemical solutions tested. Iron (III) paired with chlorine shows similar killing power, and chlorine by itself shows the least killing power. Although all three solutions demonstrate some type of bacteria inhibition, it is clear that iron (III) is the most effective.

5.3 Testing with Lettuce

Iron testing was also conducted on lettuce to see the killing effect in a food matrix with less organic matters.

The experiment began by weighing 6 samples of store-bought lettuce and placing them in 50mL centrifuge tubes. Each sample weighed approximately 5g. Two of these samples acted as control samples. One milliliter of DI water was introduced to these tubes. The other four samples were spiked with 1 mL of 10^8 CFU/mL *Salmonella*. The samples were shaken, to allow the lettuce to be evenly coated with the DI water or bacteria. All six samples were placed in a refrigerator at approximately 4°C for two hours. This allowed the bacteria enough time to attach to the lettuce.

After two hours, two of the spiked samples were removed from the refrigerator. The two samples were submerged in 20 mL of 0.005M $FeCl_3$ for ten minutes. Then 20 mL of 0.02M sodium thiosulfate were added to stop all killing in the sample. 100 μL samples were plated immediately after testing. 100 μL samples were also taken and diluted 10x and 100x for quantification purposes.

The next two spiked samples were removed from the refrigerator and submerged in 20 mL of DI water. After ten minutes, 20 mL of 0.02M sodium thiosulfate were added to the samples, to keep the experiment consistent with the iron test samples. However, there should be no reactions taking place in these samples. These samples were used to

compare the killing efficiency of the iron (III) chloride and to verify the bacteria concentration that was originally spiked on the lettuce. 100 µL samples were taken and plated immediately. 100 µL samples were also taken and diluted 10x, 100x, and 1000x for quantification.

Lastly, the two control samples, with no bacteria spike, were submerged in 20 mL of DI water for ten minutes. Then 20mL of .02M sodium thiosulfate were added. Again, no killing should be exhibited in these samples. These samples were used to determine the background concentration of bacteria on the lettuce when it was purchased. 100 µL samples were plated immediately after testing. 100 µL samples were also taken and diluted 10x for quantification.

The results of this testing can be seen in Figures 5.3, 5.4, and 5.5 and in Table 5.19.
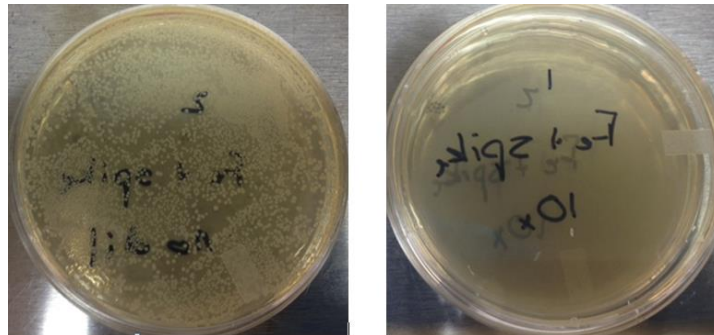
Figure 5.3 Results of spiked lettuce with iron introduced. Left: No dilution. Right: 10x dilution
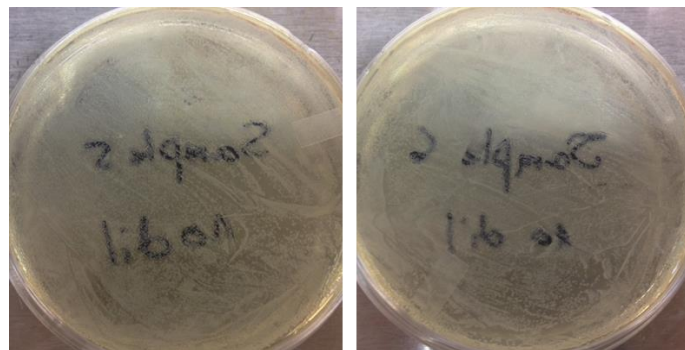
Figure 5.4 Results of spiked lettuce with no iron introduced. Samples are undiluted.
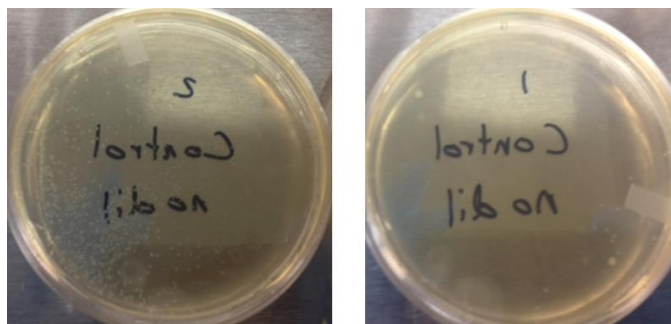
Figure 5.5 Results of lettuce samples with no spike and no chemical. Samples are undiluted

Table 5.19 Results of 1000x dilution of spiked lettuce samples

	Average	**σ**
Spike Only	200	31.2

As can be seen in Figure 5.3, the undiluted sample containing iron still shows bacteria growth covering the plate. However, the 10x dilution of that sample shows almost no growth on the plate. It was hypothesized that since the undiluted sample was plated immediately and the 10x diluted sample was plated some time later, perhaps the iron required a longer amount of time to kill the bacteria sample. This also suggested that perhaps the sodium thiosulfate was not quenching the reaction, and that killing continued, even after it was added.

Even though the spiked sample with iron (III) chloride appears to have inconsistent dilution results, it still appears to show some killing. When comparing the undiluted spiked samples with no chemical in Figure 5.4 with the undiluted spiked samples with iron (III) chloride in Figure 5.3, it can be noted that there is an obvious reduction in bacteria. The spiked samples with no iron appear to have so much bacteria growth that the colonies have grown very little overnight. They still appear extremely small in size, and that is due to the fact that there is not enough room for them to grow larger. These colonies cannot be differentiated, so it almost appears as if the bacteria growth is smeared on the plate. In Figure 5.3 left, there is a dramatic decrease in the

105

number of colonies that have grown, and therefore, they can grow larger and be differentiated.

5.3.1 Comparing Iron (III) and Chlorine Effects

Lettuce testing was continued by comparing the killing power of iron (III) with chlorine. These chlorine experiments follow the process flow in Figure 5.1.

To begin the experiment, eight samples of lettuce were placed in plastic bags, each weighing approximately 75g. Two samples acted as control samples and were spiked with 1 mL of TSB. The other six samples were spiked with 1 mL of *Salmonella* at a concentration of 10^8 CFU/mL. All eight samples were then placed in a refrigerator at 4°C for two hours to allow the bacteria to properly attach to the lettuce.

While the samples were in the refrigerator, a chlorine solution with a concentration of approximately 30 ppm was prepared in pH 6 buffer.

After the samples were kept in the refrigerator for 2 hours, chemical testing could begin. Table 5.20 describes the chemicals each sample was submerged in for testing.

Table 5.20 Chemicals for iron (III) vs. chlorine experiment with lettuce

Bags:	Submerged in 200mL of:
1, 2 (no spike)	DI water
3, 5 (spike with 10^8 CFU *Salmonella*)	DI water
4, 8 (spike with 10^8 CFU *Salmonella*)	30 ppm Chlorine
6, 7 (spike with 10^8 CFU *Salmonella*)	0.005M FeCl$_3$

200 mL was needed to ensure all the lettuce in each sample was entirely submerged during the experiment. After ten minutes, 200 mL of 0.02M sodium thiosulfate were introduced to the samples to stop the killing reaction.

Samples 1 and 2 yielded the background of bacteria that was on the lettuce when it was purchased. Samples 3 and 5 served as comparison for the iron (III) and chlorine

tests. There should be no killing associated with these samples. These samples would also allow the concentration of bacteria spiked on the lettuce to be determined.

The concentration of chlorine was verified before and after testing, as was done for the chicken experiments. After testing and before the sodium thiosulfate was added to the sample, 20 mL of the chlorine solution were collected and measured for chlorine content. After ten minutes, the chlorine concentration had decreased from 30 ppm to approximately 0.1ppm. Although this is a drastic decrease, it shows that not all the chlorine was consumed during the experiment.

The results of this testing can be seen in Table 5.21.

Table 5.21 Results of iron (III) vs. chlorine with lettuce

	Spike	Chemical	10x Dilution Average	σ	100x Dilution Average	σ	1000x Dilution Average	σ
Bag 1	No	DI water	2	0				
Bag 2	No	DI water	105	7.1				
Bag 3	Yes	DI water					340	56.6
Bag 4	Yes	Chlorine	175	35.4	47	4.2		
Bag 5	Yes	DI water					360	28.3
Bag 6	Yes	Fe (III)	0	0	0	0		
Bag 7	Yes	Fe (III)	0	0	0	0		
Bag 8	Yes	Chlorine	160	14.1	60	28.3		

As can be seen by Table 5.21, there was some bacteria growth on the control agar plates from the samples that were not spiked with bacteria. This bacteria growth was very small in size, when compared to typical *Salmonella* growth, and therefore could be any number of nonpathogenic bacteria found on lettuce at grocery stores. Based on the results of the spiked samples with no chemical added (only DI water), the concentration of bacteria spiked on the lettuce was approximately 3.5×10^8CFU/mL, which was the expected concentration.

It is important to note that there was no bacteria growth on the 10x and 100x dilution plates for the Fe (III) tests. However, there was growth on the undiluted sample that was taken and plated immediately after the test was completed. These results can be seen in Table 5.22.

Table 5.22 Results of undiluted Fe (III) test samples, experiment 1

	Spike	Chemical	No dilution Average	σ
Bag 6	Yes	Fe (III)	800	106.1
Bag 7	Yes	Fe (III)	800	106.1

Based on the results in Table 5.22, there should be bacteria growth on the 10x and 100x dilution plates. One consideration was that the undiluted samples were taken and plated immediately after testing. The 10x and 100x diluted samples were plated after all tests were completed. Therefore, it was proposed that perhaps the sodium thiosulfate was not stopping the killing reaction, and killing continued while the samples were waiting to be plated. This type of result was also seen in the previous lettuce experiment. To confirm this, samples from Bags 6 and 7 were taken approximately 20 hours after the experiment was performed and plated. These bags were kept in a freezer after testing was completed. If this hypothesis was correct, the results of this plating should show no bacteria growth. The results of this re-plating can be seen in Table 5.23.

Table 5.23 Results of re-plated samples from Fe (III) tests

	Spike	Chemical	No dilution Average	σ	10x Dilution Average	σ	100x Dilution Average	σ
Bag 6	Yes	Fe (III)	291	118.1	14	4.2	2	0.7
Bag 7	Yes	Fe (III)	189	42.4	25	7.8	4	2.8

After re-plating samples from Bags 6 and 7, it can be seen that there is still bacteria growth. However, the averages from the undiluted samples are much lower than

averages from the original undiluted samples taken at the time of the experiment. Therefore, it is possible that killing continued after the sodium thiosulfate was added and stopped several hours later.

Based on the results in Table 5.21 and 5.22, it can be seen that Fe (III) exhibits better killing efficiency than chlorine by one order of magnitude.

During this experiment, it was observed that the 0.005M concentration of $FeCl_3$ underwent a dramatic color change within several hours of preparation. When the solution was first prepared, it was pale yellow in color. However, within several hours, it began to change to a dark yellow/orange color. The pH of the solution when it was first prepared was determined to be approximately 2.3. It was determined that the solution was hydrolyzing with time, and this could be decreasing the killing efficiency of the solution. To prevent this from happening, the solution's pH could be reduced to below 2 by adding acetic acid.

To verify this, two fresh solutions of 0.005M $FeCl_3$ were prepared. Acetic acid was added to one of these solutions until a pH of approximately 1.97 was reached. A picture of the two solutions on day 1 can be seen in Figure 5.6.
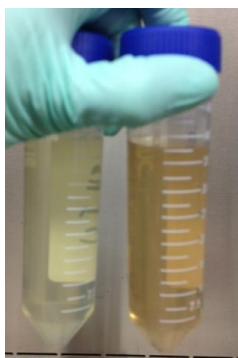
Figure 5.6 $FeCl_3$ solutions on Day 1. Left: 0.005M $FeCl_3$ Right: 0.005M $FeCl_3$ with acetic acid

After 24 hours, another picture of the solutions was taken. This can be seen in Figure 5.7.

Figure 5.7 FeCl$_3$ solutions on Day 2. Left: 0.005M FeCl$_3$ Right: 0.005M FeCl$_3$ with acetic acid

As can be seen from Figure 5.7, the solution without acetic acid dramatically changes color. However, the solution with acetic acid does not change in color or pH. It was decided to compare the killing power of freshly made FeCl$_3$ (before the color change due to hydrolysis) with FeCl$_3$ after acetic acid has been added.

This experiment followed the process flow in Figure 5.1. Eight samples of lettuce were placed in plastic bags, each weighing approximately 75g. Two samples acted as control samples and were spiked with 1 mL of TSB. The other six samples were spiked with 1 mL of *Salmonella* at a concentration of 10^8 CFU/mL. All eight samples were then placed in a refrigerator at 4°C for two hours to allow the bacteria to properly attach to the lettuce.

After the samples were kept in the refrigerator for 2 hours, chemical testing could begin. Table 5.24 describes the chemicals each sample was submerged in for testing.

Table 5.24 Chemicals for iron (III) vs. iron (III) with acetic acid experiment with lettuce

Bags:	Submerged in 100mL of:
1, 2 (no spike)	DI water
3, 8 (spike with 10^8 CFU *Salmonella*)	DI water
5, 7 (spike with 10^8 CFU *Salmonella*)	0. 005M FeCl$_3$ (pH 2.3)
4, 6 (spike with 10^8 CFU *Salmonella*)	0.005M FeCl$_3$ with acetic acid (pH 1.93)

The results of this testing can be seen in Table 5.25.

Table 5.25 Results of iron (III) vs. iron (III) with acetic acid experiment with

lettuce

	Spike	Chemical	No dilution Average	σ	10x Dilution Average	σ	100x Dilution Average	σ
Bag 1	No	DI water			200	0		
Bag 2	No	DI water			192	44.5		
Bag 4	Yes	Fe (III) with acetic acid	303	95.5	5	6.4	0	0
Bag 5	Yes	Fe (III)	390	28.3	25	11.3	1	0.7
Bag 6	Yes	Fe (III) with acetic acid	192	18.4	6	2.8	0	0
Bag 7	Yes	Fe (III)	520	14.8	24	5.7	5	4.2

The results of the spiked lettuce with no chemical added (only DI water) can be seen in Table 5.26.

Table 5.26 Results of spiked lettuce with no chemical added in iron (III) vs. iron (III) with acetic acid experiment

	Spike	Chemical	1000x Dilution Average	σ
Bag 3	Yes	DI water	295	7.1
Bag 8	Yes	DI water	290	28.3

According to the results in Table 5.26, the starting concentration of bacteria on the lettuce was approximately 2.925×10^8 CFU/mL, which was the expected concentration.

From the results in Table 5.25, it can be seen that the iron (III) with acetic acid was more effective at inhibiting bacteria growth than the freshly made iron (III) solution with no acetic acid added.

5.4 Discussion

The killing effects of Fe (III) have been previously published by the Washington School of Medicine [49] [50]. In the published works by this institution, it is claimed that Fe (III) disrupts the outer membrane of Gram-negative bacteria, thus making the bacterium susceptible to normally non-toxic materials.

Essentially, it seems that damaging this outer membrane does not only render the bacterium vulnerable, but also seems to be killing the cell. It is also possible that an excess amount of this chemical could be aiding in the killing of bacteria. Experiments in this work used relatively high levels of Fe (III) (approximately 280ppm) to produce impressive killing results. Another theory is that since Fe (III) is an oxidizing agent, it could be oxidizing the cell, resulting in its death. Although the exact mechanism of its antibacterial capabilities is still unknown, it has been proven to be a very effective killing agent.

In the pure culture experiments, it appeared that the killing strength of Fe (III) varied from experiment to experiment. The order of magnitude of the bacteria reduction varied between experiments. This may be due to the fact that preliminary experiments used ferric nitrate, and this was changed to ferric chloride. From further testing it was observed that the killing strength seemed to vary depending on bacteria concentration, as can be seen in the Fe (III) Killing Strength tables in Appendix A. It appears the killing strength is greater when there is a higher concentration of bacteria present.

It was seen during testing that when a solution of $FeCl_3$ was prepared in DI water, the color of the solution would change over time, as seen in Figure 5.6. It was determined that the Fe (III) was hydrolyzing. Essentially, $FeCl_3$ ionizes to Fe and chloride ions, while the water ionizes to hydrogen and hydroxyl ions [51]. The hydroxide ions combine partially with iron. However, ferric hydroxide is not very soluble and can be seen as a precipitate. This was observed when the $FeCl_3$ solution was untouched for several days. The solution became cloudy. The solution now has an excess of hydrogen ions, and the

solution becomes increasingly acidic [51]. It was considered that, since some of the solution was precipitating, it would not kill as effectively as if the ferric ions were still in the solution. Therefore, to prevent this hydrolysis, acetic acid was added to the $FeCl_3$ solution to lower the pH below 2. As can be seen in Figure 5.5 and 5.6, the solution with acetic acid does not change color and remains stable. It was noted that the killing power of this Fe (III) solution with acetic acid was superior to that of the original Fe (III) solution. Therefore it seems the iron precipitates do render the $FeCl_3$ solution weaker.

It appears, from the testing performed in this chapter, that the killing efficiency of Fe (III) is significantly better than that of chlorine. Chlorine is currently the standard for disinfection of poultry chillers and water treatment facilities, and therefore it was very important to compare Fe (III) killing to chlorine killing. It is important to note that when the effects of Fe (III) were being tested in comparison to the effects of chlorine, the concentrations of the two chemicals were very different. The highest concentration of chlorine tested was approximately 40ppm, while the concentration of Fe (III) was approximately 280ppm. It was found in Section 5.1.3 that the lowest concentration of Fe (III) that resulted in effective bacteria killing was $5x10^{-3}$M, which is equivalent to approximately 280ppm. Therefore the concentration of Fe (III) was not lowered from this concentration. However, the chlorine concentration was not increased to match this concentration either. This is due to the fact that chlorine concentration in drinking water applications as well as poultry chillers is limited to below 5ppm [52]. Testing began by using 4ppm, and when results were poor for this concentration, the concentration was increased to 40ppm. However, this exaggerated concentration is not used for commercial disinfection purposes.

The effects of .005M Fe (III) used in conjunction with 45 ppm of chlorine were also tested, to determine if the concentrations of these chemicals could be lessened if they are used simultaneously. It was found, however, that the effects of Fe (III) by itself still proved to have a better killing strength than Fe (III) with chlorine, as can be seen in the

Fe (III) Killing Strength tables in Appendix A. Further testing of the use of these chemicals in combination is needed to ensure the accuracy of this test.

There are harmful effects to both people and foods that are exposed to high levels of chlorine [52]. In particular, foods can be bleached from chlorine and have a poor taste. There are some disadvantages to the use of Fe (III) as well, such as color and taste. For drinking water applications, iron content must be less than 200ppb after processing [53]. Therefore, finding a method to remove iron after its antibacterial activity has been completed is necessary.

CHAPTER 6

CONCLUSION

6.1 Chemotaxis Studies

Several methods of bacteria separation were outlined in this work. Chemotaxis studies involved testing chemical attractants and repellents in multiple configurations independently as well as in conjunction with each other to determine their effects on bacteria movement. It appears from testing in Section 2.1.1 that high attractant concentrations, such as 10% chemical attractant in DI water, yielded much larger numbers of bacteria in the capillary tubes than smaller concentrations. The best results were seen when all three chemical attractants tested were used together in the 'all solution.' It seems that these high concentrations produce a larger chemical gradient in the bacteria solution that the bacteria can sense more easily than when low concentrations are used.

Chemotaxis experiments utilizing repellent chemicals revealed that these chemicals, such as nickel chloride, may be negatively affecting the swimming patterns of the bacteria, resulting in very low bacteria mobility. Therefore, strong chemical repellents may lessen the effectiveness of using chemicals to direction bacteria movement. It was also discovered that chemicals containing Fe (III) do not repel bacteria, but rather kill the cells.

Future work for the study of chemotaxis includes further testing of the device seen in Figure 2.7. Currently, it appears attractant chemicals seem to diffuse to the bacteria side of the channel, resulting in less bacteria migration to the attractant side. It is also apparent that this device relies solely on the motility of the bacteria that is used in the device. If the bacteria cells are not motile, they will not swim to the attractant side. However, if they are very motile, the bacteria cells can be swimming back and forth

between the bacteria side of the channel and attractant side of the channel. Therefore, it may be necessary to introduce a weak chemical repellent to the bacteria side, to persuade the bacteria to swim toward the preferable environment. However, the chemical repellent will have to be chosen carefully, so as not to disturb normal bacteria swimming patterns.

6.2 Nanoparticle Fabrication and Experimentation

Many types of magnetic nanoparticles were successfully fabricated and tested with *Salmonella* to determine their bacteria capture efficiency. It appears that altering the recipe set forth by Deng et al. had the most effect on the produced nanoparticles [34]. By lowering the sodium acetate in the recipe, nanoparticles with very rough surfaces were produced. These nanoparticles surprisingly had one of the highest capture efficiencies of all the nanoparticles tested, approximately 94%, which could suggest that this morphology might be aiding in bacteria capture. By doubling the amount of sodium acetate used in the nanoparticle recipe, a capture efficiency of 90% was seen. Also, by changing the pH of the original mixture to 8.5, the nanoparticles produced were much smaller and yielded a capture efficiency over 90%.

When adding polymer coatings to the nanoparticles, it seems very little effect was seen on their formation and zeta potential. It was expected that the polymer coatings would yield positive zeta potentials. However, all zeta potential measurements appeared to be negative, meaning that the polymers may not be sufficiently attached to the nanoparticles or that other material from the buffer environment is adsorbing onto the nanoparticles, causing a negative surface charge. This was further confirmed after noting that uncoated nanoparticles have a very similar capture efficiency to the nanoparticles 'coated' with poly-l-lysine, approximately 80%.

Since the nanoparticles appear to have a negative zeta potential, it is evident that the attraction between the particles and the bacteria is not an electrostatic interaction. However, many of the nanoparticles tested have capture efficiencies higher than 80%,

with some as high as 94%. Therefore this nanoparticle separation method seems to be very effective, although the exact mechanism of attachment is unknown.

In the future, a method of effectively attaching the polymer coating to the nanoparticle surface must be determined. This will yield a positive zeta potential on the nanoparticles, and may increase their capture efficiency. Ensuring proper polymer attachment to the nanoparticle surface will then allow experimentation with different polymers. If it can be determined that the polymer is successfully attached to the nanoparticles but other materials from the buffer are adsorbing onto the polymer and causing a negative surface charge, this will have to be accounted for and rectified for further testing. By producing a positive zeta potential on the surface of the nanoparticles, it may yield better capture efficiencies for other types of bacteria. As of now, *E.coli* was the only type of bacteria to be tested other than *Salmonella*, and resulted in capture efficiencies of approximately 25%. However, it is hoped that by properly coating the nanoparticles with a positive surface charge, they may be able to be utilized for capture of many types of bacteria. Finally, a method of producing nanoparticles with larger diameters is desired, to test the capture efficiency of larger nanoparticles, as well as to determine the optimal bacteria-nanoparticle ratio necessary for effective capture. It is believed that, by employing larger nanoparticles, they will have a greater force in the magnetic field, and thus be more capable of dragging a bacterium cell toward the tube walls. This will result in a lower concentration of nanoparticles necessary for effective bacteria capture. However, testing must be performed to determine if larger nanoparticles will result in a magnetic force strong enough to dislodge the bacterium from the nanoparticle's surface, which would lessen the capture efficiency. It is also possible that larger nanoparticles will precipitate out of solution, and therefore, further experimentation is required.

6.3 Prototype Characterization and Experimentation

A prototype allowing continuous cleaning of water, as well as re-suspension of bacteria-nanoparticle aggregates, was assembled and characterized. The prototype was tested to ensure that bacterial adhesion to the tubing was minimal. When testing the prototype with contaminated DI water, above 80% of the bacteria was captured and re-suspended in approximately a tenth of the original volume in 5 minutes. This capture efficiency matches the typical capture efficiency of the nanoparticles used in the experiment, as can be seen by row D in Figure A.1 in Appendix A. Approximately 80-90% of the bacteria cells were recovered from the experiments performed. The capture efficiency of the nanoparticles appeared to be approximately 70%.

There are several improvements that can be made to the prototype to improve its performance. Firstly, it is important to ensure capture of all nanoparticles so they do not contaminate the cleaned volume of water. This can be done by using more magnets in conjunction with each other, or by using stronger magnets. By increasing the length of tube that the magnetic field is applied (by using more magnets), the nanoparticle will have a greater chance of separating from the moving fluid. However, this length could be extensive, and therefore it may be preferable to use a stronger magnetic field instead. By using rigid tubing, the magnets can be placed directly across from each other on the sides of the tubing, producing a very strong magnetic field between them. Pairs of magnets can be used in conjunction with each other to ensure capture of all nanoparticles, as can be seen in Figure 6.1.
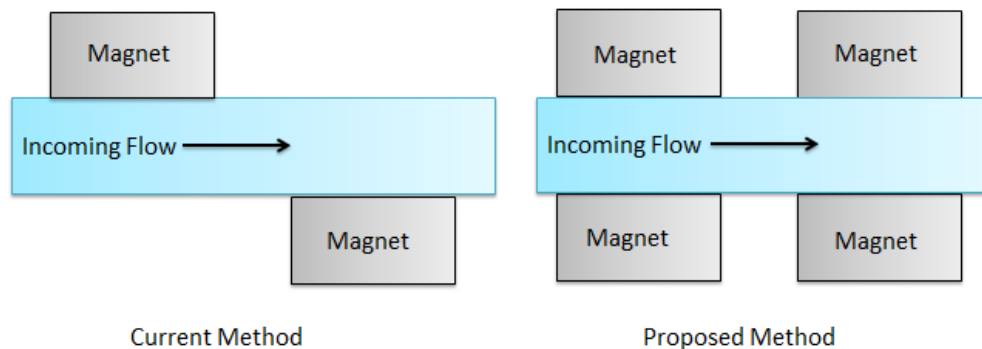
Figure 6.1 Current method of placing magnets versus proposed method of placing
magnets for optimal nanoparticle capture

By ensuring that all nanoparticles are captured, this may increase the bacteria capture efficiency, as some of the nanoparticles passing into the cleaned water volume may have bacteria cells attached to them. Also, by using nanoparticles from Figure A.1 in Appendix A that have a higher capture efficiency, it may be possible to increase the bacteria capture efficiency to almost 95%.

It is also important to determine why the concentration of nanoparticles measured by the ICP-OES was significantly less than what was expected. It is known that the nanoparticles are not only composed of iron, but also contain oxygen as well as any of the polymer coating that was retained on the nanoparticle surface. Therefore, the expected concentration of iron in any given sample is a drastic overestimation of the actual concentration of iron. It is necessary to determine the content of iron in one nanoparticle in order to estimate how much iron can be expected in an estimated concentration of nanoparticles. The number of nanoparticles in a given weight can only be estimated since the nanoparticles have varying diameters. Therefore, for the calculations in this work, the average diameter was used to calculate an estimated concentration of nanoparticles.

In the future, the prototype will be tested with faster flow rates (using a larger pump). This will allow larger volumes of contaminated fluid to be cleaned in a reasonable amount of time. Therefore, these flow rates must be taken into consideration

when determining the magnetic field strength necessary to capture the nanoparticles, now that they will be flowing past the magnets at a higher velocity.

If this system were to be used on a larger scale for applications such as water treatment, it would be necessary to automate this system. An electromagnet or multiple electromagnets could be used, so the magnetic field could simply be turned on and off. However, large currents may be required to produce large magnetic fields. Therefore, motorizing permanents magnets might be an easier solution. This would allow the magnetic field to be removed and re-introduced, without requiring large currents. The valve would also be automated. Therefore when the permanent magnets are removed, the valve could be turned at the precise moment to ensure there is no contamination of the clean water.

By optimizing this system, it could be a viable and simple method of capturing bacteria from large volumes of water, and allowing these cells to be further studied in a microfluidic system, such as the device seen in Figure 2.7. By using these two devices together, not only will bacteria separation be achieved, but the viability of the bacteria can also be determined.

6.4 Intervention of Bacteria using Iron (III)

Experiments in this study revealed the antibacterial characteristics of Fe (III). It appears that bacteria growth can be reduced by several orders of magnitude using .005M Fe (III). This was proven using pure cultures, as well as food matrices, such as chicken and lettuce. This impressive bacteria killing was observed after only ten minutes of Fe (III) exposure to the samples. The effects of this chemical were also compared to the effects of chlorine, the commercial method of disinfection. Since the allowable chlorine content in commercial settings is extremely low, it is not surprising that Fe (III) achieved better killing results when the two chemicals were compared. It appears that Fe (III) results in a killing strength one order of magnitude better than chlorine, as seen in the Fe

(III) Killing Strength tables in Appendix A. The two chemicals were used together to determine if this would achieve superior killing to when they are used independently. As seen in Section 5.2.1, it was observed that the two chemicals together produced better killing than chlorine by itself. However, Fe (III) by itself still produced the best killing results. This can be seen in the Fe (III) Killing Strength tables in Appendix A.

To continue Fe (III) testing, live chickens will be infected with *Salmonella*. During post-processing of these chickens, they will be sprayed with a solution of Fe (III) at specific concentrations for specific periods of time to determine if effective disinfection can be achieved. If so, this Fe (III) spraying process may become a normal and necessary part of processing chickens at poultry plants.

Further testing must be performed to determine the allowable amount of Fe (III) that can be used to safely disinfect without having harmful effects on people or the environment. However, Fe (III) appears to be a promising method for disinfection of food and water that is comparable and perhaps more effective than chlorine.

6.5 Concluding Remarks

This work has detailed effective methods of bacteria separation and intervention that show promise for the future. Chemotaxis studies can allow bacteria separation on a small scale, as well as allow the study of bacteria movement in the presence of different chemical repellents and attractants. Nanoparticles allow separation of bacteria on a large scale, when effectively implemented in a model, as was seen in Chapter 4. By separating bacteria from large amounts of liquid, it not only cleans the liquid, but allows further analysis of the captured bacteria cells. By combining this prototype with a microfluidic device (such as that seen in Figure 2.7), the separated bacteria's viability can be determined through chemotaxis to protect public health. Finally, bacteria intervention studies were also conducted. If disinfection is desired, rather than collecting bacteria for future characterization, it is important to have an effective antibacterial chemical. Fe (III)

demonstrates very effective bacteria killing in as little as ten minutes with high concentrations of bacteria. This chemical has even been proven more effective than chlorine, which is the current standard for disinfection in water treatment facilities and poultry plants.

By continuing research in the proposed methods of bacteria separation and intervention, these techniques could be optimized for use in commercial settings, taking the place of expensive and less efficient approaches.

APPENDIX A

SUPPLEMENTARY DATA

Fe (III) Killing Strength Tables

Table A.1 Killing strength results of chicken testing 1

	Ending Concentration (CFU/mL)	Expected Concentration (CFU/mL)	Killing Power
Spike only	3.80×10^5	2.90×10^5	-
Spike only	2.00×10^5	2.90×10^5	-
Chlorine (4ppm)	4.7×10^5	2.90×10^5	-
Chlorine (4ppm)	4.25×10^5	2.90×10^5	-
Fe III (.005 M)	3.3×10^4	2.90×10^5	8.8
Fe III (.005 M)	2.4×10^4	2.90×10^5	12.1

Table A.2 Killing strength results of chicken testing 2

	Ending Concentration (CFU/mL)	Expected Concentration (CFU/mL)	Killing Power
Spike only	1.04×10^7	1.32×10^7	-
Spike Only	1.59×10^7	1.32×10^7	-
Chlorine (45 ppm)	6.0×10^5	1.32×10^7	21.8
Chlorine (45 ppm)	6.0×10^5	1.32×10^7	21.8
Fe III (.005 M)	8.9×10^4	1.32×10^7	147
Fe III (.005 M)	3.1×10^4	1.32×10^7	422.6
Fe III+ Chlorine (30 ppm)	1.68×10^5	1.32×10^7	77.97
Fe III + Chlorine (30 ppm)	1.28×10^5	1.32×10^7	102

Table A.3 Killing strength results of lettuce testing 1

	Ending Concentration (CFU/mL)	Expected Concentration (CFU/mL)	Killing Power
Spike only	3.4×10^6	3.5×10^6	-
Spike only	3.6×10^6	3.5×10^6	-
Chlorine (30 ppm)	4.7×10^4	3.5×10^6	72
Chlorine (30 ppm)	6.0×10^4	3.5×10^6	56.7
Fe III (.005 M)	$\sim8.0\times10^3$	3.5×10^6	425
Fe III (.005 M)	$\sim8.0\times10^3$	3.5×10^6	425

Table A.4 Killing strength results of lettuce testing 2

	Ending Concentration (CFU/mL)	Expected Concentration (CFU/mL)	Killing Power
Spike only	2.90×10^6	2.925×10^6	-
Spike only	2.95×10^6	2.925×10^6	-
Fe III (pH 2.3)	3.90×10^3	2.925×10^6	750
Fe III (pH 2.3)	5.20×10^3	2.925×10^6	562.5
Fe III w/acetic (pH 1.9)	3.03×10^3	2.925×10^6	965

	Coating	Size	ZP 1	ZP 2	ZP 3	Efficiency (Salm)	Efficiency ALTERNATIVE	Results (E.coli)
A	1g chit	~150 nm	-2.11	-7.99	-9.82	51.3/54.5		
B	PEI	120-150nm		-5.57	-6.24	74.8		
C	Polylysine after	120-150nm	21.6	-6.85	-9.64	78.3/88.2		
D	polylysine before	100-150nm	-34.6	-18	-13.6	72.9/77.1	87.9/86.1	
E	uncoated	120-150nm	-40	-10.2	-5.13	82/ 83.7/82.1/83.3	85.8/86.3/80.2	21.4
F	polylysine after	120-150nm	21.6	-9.12	-1.51	68.8/74.5		36.6
G	0.5 acetate	~150nm		-22.5	-22.1	94.3		25
H	2x acetate	100-130nm	-21.6	-38.4	-19.8	90	95	
I	50% water	50-80nm	-33.3	-22.5	-18.2			
J	pH8.5	30-40nm	-22.5	-20.7	-32.4	90.7	94.9	
K	0.5 g chit	120-150nm		-13.4	-26.4	62	67.6	
L	2 g chit	120-150nm		-6.2	-8.3	63	33	
M	1 g chit (3 days)	120-150nm		-14.3	-5.46	69	62	
N	polylysine before	100-150nm		NA	-13.4	91.8/90.5/93.2/(81.5)	83.6	

Figure A.1 Nanoparticle comparison chart

REFERENCES

[1] K. Todar, "Bacterial Endotoxin," 2008-2012. [Online]. Available: http://textbookofbacteriology.net/endotoxin.html.

[2] S. Gould, "How to eat your host: Pathways for nutrition in Salmonella," 6 May 2013. [Online]. Available: http://blogs.scientificamerican.com/lab-rat/2013/05/06/how-to-eat-your-host-pathways-for-nutrition-in-salmonella/. [Accessed May 2013].

[3] K. Soni, A. Balasubramanian, A.Beskok and S. Pillai, "Zeta Potential of Selected Bacteria in Drinking Water When Dead, Starved, or Exposed to Minimal and Rich Culture Media," *Current Microbiology,* pp. 93-97, 2007.

[4] L. McCarter, "Multiple Modes of Motility: a Second Flagellar System in Escherichia coli," *Journal of Bacteriology,* vol. 187, no. 4, pp. 1207-1209, 2005.

[5] "Salmonellosis," Centers for Disease Control and Prevention, [Online]. Available: http://www.cdc.gov/nczved/divisions/dfbmd/diseases/salmonellosis/.

[6] "Salmonella," Centers for Disease Control and Prevention, [Online]. Available: http://www.cdc.gov/salmonella/general/technical.html.

[7] "Definition of Preconcentration," [Online]. Available: http://www.lexic.us/definition-of/preconcentration.

[8] R. Noble and S. Weisberg, "A review of technologies for rapid detection of bacteria in recreational waters," *Journal of Water and Health,* pp. 381-392, 2005.

[9] "CONVENTIONAL WATER TREATMENT: COAGULATION AND FILTRATION," Safe Drinking Water Foundation, [Online]. Available: http://www.safewater.org/PDFS/knowthefacts/conventionalwaterfiltration.pdf.

[10] "ULTRAFILTRATION, NANOFILTRATION AND REVERSE," Safe Drinking Water Foundation, [Online]. Available: http://www.safewater.org/PDFS/knowthefacts/Ultrafiltration_Nano_ReverseOsm.pdf

. [Accessed May 2013].

[11] A. Bren and M. Eisenbach, "How Signals Are Heard during Bacterial Chemotaxis: Protein-Protein Interactions in Sensory Signal Propagation," *Journal of Bacteriology,* vol. 182, no. 24, pp. 6865-6873, 2000.

[12] "Bacterial Chemotaxis," Carnegie Mellon University, [Online]. Available: https://www.bio.cmu.edu/courses/03441/TermPapers/99TermPapers/TwoCom/chemo taxis.html. [Accessed May 2013].

[13] Biotweet, [Online]. Available: http://2011.igem.org/wiki/index.php?title=Team:WITS-CSIR_SA/Project/Concept&oldid=257284. [Accessed May 2013].

[14] E. Schwarz-Weig, "Life and Work of Wilhelm Pfeffer (1845-1920)," German Botanical Society, [Online]. Available: http://www.deutsche-botanische-gesellschaft.de/html/043PfefferCV.html. [Accessed May 2013].

[15] J. Adler, "A Method for Measuring Chemotaxis and Use of the Method to Determine Optimum Conditions for Chemotaxis by Escherichia coli," *Journal of General Microbiology,* pp. 77-91, 1972.

[16] W. Jong and P. Borm, "Drug delivery and nanoparticles: Applications and hazards," *International Journal of Nanomedicine,* pp. 133-149, 2008.

[17] A. Mandal, "Antibody-What is an Antibody'," News-Medical, [Online]. Available: http://www.news-medical.net/health/Antibody-What-is-an-Antibody.aspx. [Accessed May 2013].

[18] "Immunotherapy," Cancer Information and Support Network, [Online]. Available: http://cisncancer.org/research/new_treatments/immunotherapy/index.html. [Accessed May 2013].

[19] M. Saleh, H. Soliman, O. Haenen and M. El-Matbouli, "Antibody-coated gold nanoparticles immunoassay for direct detection of Aeromonas salmonicida in fish tissues.," *Journal of Fish Disease,* vol. 34, no. 11, pp. 845-852, 2011.

[20] M. Varshney, L. Yang, X. Su and Y. Li, "Magnetic nanoparticle-antibody conjugates for the separation of Escherichia coli O157:H7 in ground beef.," *Journal of Food Protection,* vol. 68, no. 9, pp. 1804-1811, 2005.

[21] A. Kell, G. Stewart, S. Ryan, R. Peytavi, M. Boissinot, A. Huletsky, M. Bergeron and B. Simard, "Vancomycin-Modified Nanoparticles forEfficient Targeting and Preconcentration of Gram-Positve and Gram-Negative Bacteria," *ACS Nano,* vol. 2, no. 9, pp. 1777-1788, 2008.

[22] Y.-F. Huang, Y.-F. Wang and X.-P. Yan, "Amine-Functionalized Magnetic Nanoparticles for Rapid Capture and Removal of Bacterial Pathogens," *Environmental Science and Technology,* vol. 44, no. 20, pp. 7908-7913, 2010.

[23] "Technical Update SAS Process Water Acidifier," Jones-Hamilton Co., [Online]. Available: http://www.joneshamiltonag.com/jh/wp-content/uploads/2011/10/SAS-Technical-Update.pdf.

[24] "Disinfectants," Lenntech Water Treatment Solutions , [Online]. Available: http://www.lenntech.com/processes/disinfection/chemical/disinfectants-chlorine.htm. [Accessed May 2013].

[25] "Ozone Treatment of Drinking Water Supplies," Rhode Island Department of Health, [Online]. Available: http://www.uri.edu/ce/wq/has/PDFs/Ozone.pdf. [Accessed May 2013].

[26] "Drinking Water Treament with Ferric Chloride," California Water Technologies LLC, [Online]. Available: http://www.californiawatertechnologies.com/pdf/PotableBulletin.pdf. [Accessed May 2013].

[27] "Microbial Growth and Metabolism," Phoenix College, [Online]. Available: http://www.pc.maricopa.edu/Biology/rcotter/BIO%20205/LessonBuilders/Chapter%207%20LB/Chapter7and8LessonBuilder_print.html. [Accessed May 2013].

[28] K. Todar, "Growth of Bacterial Populations," University of Wisconsin-Madison, [Online]. Available: http://textbookofbacteriology.net/themicrobialworld/growth.html. [Accessed May

2013].

[29] D. Blair, "How Bacteria Sense and Swim," *Annual Review of Microbiology,* pp. 489-522, 1995.

[30] L. Tisa and J. Adler, "Cytoplasmic free-Ca2+ level rises with repellents and falls with attractants in Escherichia coli chemotaxis," *Proceedings of the National Academy of Sciences,* vol. 92, pp. 10777-10781, 1995.

[31] W.-W. Tso and J. Adler, "Negative Chemotaxis in Escherichia coli," *Journal of Bacteriology,* vol. 118, no. 2, pp. 560-576, 1974.

[32] J. Adler, G. Hazelbauer and M. Dahl, "Chemotaxis Toward Sugars in Escherichia coli," *Journal of Bacteriology,* vol. 115, no. 3, pp. 824-847, 1973.

[33] E. Kung, "Speed of a Bacterium," The Physics Factbook, 2000. [Online]. Available: http://hypertextbook.com/facts/2000/ElaineKung.shtml. [Accessed May 2013].

[34] H. Deng, X. Li, Q. Peng, X. Wang, J. Chen and Y. Li, "Monodisperse Magnetic Single-Crystal Ferrite Microspheres," *Angewandte Chemie International Edition,* pp. 2782-2785, 2005.

[35] I. Aranaz, M. Mengíbar, R. Harris, I. Paños, B. Miralles, N. Acosta, G. Galed and A. Heras, "Functional Characterization of Chitin and Chitosan," *Current Chemical Biology,* pp. 203-230, 2009.

[36] "Magnets for Molecular and Cell Separation Applications," Life Technologies, [Online]. Available: http://www.invitrogen.com/site/us/en/home/brands/Product-Brand/Dynal/Magnets.html. [Accessed August 2012].

[37] "Poly-Lysine," Sigma-Aldrich, [Online]. Available: http://www.sigmaaldrich.com/technical-documents/articles/biofiles/poly-lysine.html. [Accessed November 2012].

[38] E. Matijevic and S. Cimas, "Formation of Uniform Colloidal Iron (III) Oxides in

Ethylene Glycol-Water Solutions," *Colloid and Polymer Science,* pp. 155-163, 1987.

[39] S.-B. Cho, J.-S. Noh, S.-J. Park, D.-Y. Lim and S.-H. Choi, "Morphological control of Fe3O4 particles via glycothermal process," *Journal of Material Science,* pp. 4877-4886, 2007.

[40] "ZETA POTENTIAL OF BOVINE SERUM ALBUMIN (BSA) PROTEIN," Horiba, 2009. [Online]. Available: http://www.horiba.com/fileadmin/uploads/Scientific/Documents/PSA/AN184_app.pdf. [Accessed May 2013].

[41] T.-A. Stenstrom and S. Kjelleberg, "Fimbriae mediated nonspecific adhesion of Salmonella typhimurium to mineral particles," *Archives of Microbiology,* pp. 6-10, 1985.

[42] H. Zhang, L. Moore, M. Zborowski, P. Williams, S. Margel and J. Chalmers, "Establishment and implications of a characterization method for magnetic nanoparticle using cell tracking velocimetry and magnetic susceptibility modified solutions," *The Royal Society of Chemistry,* pp. 514-527, 2005.

[43] S. Childress, "An Introduction to Theoretical Fluid Dynamics," 12 February 2008. [Online]. Available: http://www.math.nyu.edu/faculty/childres/. [Accessed May 2013].

[44] A. Barnes, R. Wassel, F. Mondalek, K. Chen, K. Dormer and R. Kopke, "Magnetic Characterization of superparamagnetic nanoparticles pulled through model membranes," *BioMagnetic Research and Technology,* 2007.

[45] J. Ralph and I. Chau, "Magnetite," [Online]. Available: http://www.mindat.org/min-2538.html. [Accessed November 2012].

[46] G. Arrighini, M. Maestro and R. Moccia, "Magnetic Properties of Polyatomic Molecules. I. Magnetic Susceptibility of H2O, NH3, CH4, H2O2," *The Journal of Chemical Physics,* vol. 49, no. 2, 1967.

[47] ThermoScientific, "FREE CHLORINE DPD METHOD," 7 July 2002. [Online]. Available: http://fscimage.fishersci.com/cmsassets/downloads/segment/Scientific/pdf/WaterAna

lysis/Method_Free_Chlorine_Drinking_Water_Orion_AC4P71_Powder_EPA_TFS.p
df. [Accessed March 2013].

[48] M. Herrera, "MANUAL FOR CHLORINE TREATMENT OF DRIP IRRIGATION
SYSTEMS," [Online]. Available:
http://www.nm.nrcs.usda.gov/technical/handbooks/iwm/NM_IWM_Field_Manual/Se
ction21/21q-Chlorination_Procedure.pdf. [Accessed May 2013].

[49] S. Chamnongpol, W. Dodson, M. J. Cromie, Z. L. Harris and E. A. Groisman,
"Fe(III)-mediated cellular toxicity," *Molecular Microbiology,* vol. 45, no. 3, pp. 711-
719, 2002.

[50] K. Nishino, F.-F. Hsu, J. Turk, M. J. Cromie, M. M. S. M. Wösten and E. A.
Groisman, "Identification of the lipopolysaccharide modifications controlled by the
Salmonella PmrA/PmrB system mediating resistance to Fe(III) and Al(III),"
Molecular Microbiology, vol. 61, no. 3, pp. 645-654, 2006.

[51] S. Hoskins and R. Pearce, "The chemistry of ferric chloride," [Online]. Available:
http://www.artmondo.net/printworks/articles/ferric.htm. [Accessed May 2013].

[52] S. Barbut, Poultry Products Processing: An Industrial Guide, Boca Raton: CRC Press
LLC, 2002.

[53] "Iron (Fe) and water," Lenntech Water Treatment Solutions, [Online]. Available:
http://www.lenntech.com/periodic/water/iron/iron-and-water.htm. [Accessed May
2013].